Reinforcement Alternatives for Timber–Concrete-Composite Floor Slabs

Structural evaluation and Sustainability Perspectives

T.H. Visser

Delft University of Technology

TU Delft

ARUP

Reinforcement Alternatives for Timber–Concrete-Composite Floor Slabs

Structural evaluation and Sustainability Perspectives

by

Tesla Visser

A thesis presented to obtain the degree of Master of Science
Faculty of Civil Engineering
Delft University of Technology

Student number:	5067588
Project Duration:	February 10th, 2025 - July, 2025
Thesis committee:	Dr. F. Zhang (Chair) - TU Delft - Concrete structures
	Dr. F. Messali - TU Delft - Materials and Environment
	Ir. E.B. van Helmond (Daily Supervisor) - ARUP
	Prof.dr.ir. H.M. Jonkers - TU Delft - Materials and environment

Cover: Picture from ARUP of DPG TCC floors (2022)

TU Delft

Preface

This thesis marks the conclusion of my time at TU Delft and reflects the culmination of everything I've learned throughout my academic journey. Working on Timber–Concrete Composite systems and exploring sustainable reinforcement solutions allowed me to combine my interest in structural engineering with my passion for sustainability. It was both challenging and rewarding to dive into a topic that bridges technical innovation and environmental responsibility.

I'm grateful to have had the opportunity to work with and learn from a group of inspiring experts. Fengqiao Zhang, thank you for your guidance and support throughout the process, and for helping me stay focused on the bigger picture. Francesco Messali, your insights into finite element modelling were invaluable and helped me deepen my understanding of structural behavior. Henk Jonkers, I truly appreciated your perspective on sustainability and the thesis process—it added a meaningful dimension to this research. Emily van Helmond, thank you for your support from the industry side and for helping me connect academic work with practical relevance. To all the experts I reached out to during this thesis—thank you for your time, your feedback, and your willingness to share your knowledge. This project has been a journey of curiosity, growth, and collaboration, and I'm proud of what it has become.

T.H. Visser
Delft, November 2025

Abstract

Timber–Concrete Composite (TCC) floor systems offer a sustainable and structurally efficient solution by combining the tension capacity of timber with the compressive strength of concrete. Despite their advantages, the environmental impact of concrete and conventional steel reinforcement remains a concern. This thesis explores the use of alternative reinforcement methods and materials, focusing on loose basalt fibres, to evaluate their mechanical and environmental performance in TCC slabs.

The central research question is: *"What are the mechanical and environmental implications of using a suitable alternative reinforcement method and material in timber-concrete-composite (TCC) floor systems, assessed against a case study?"*

A standard floor element from the DPG Media building was selected as the case study. Eight reinforcement alternatives were evaluated through a multi-criteria analysis (MCA), considering parameters such as strength, ductility, sustainability, and buildability. The most promising option, loose basalt fibre reinforcement, was selected for further comparison against the original steel mesh-reinforced design.

In the MCA, each reinforcement alternative was scored from 0.0 to 100.0 per criterion, with scores linearly interpolated between the best and worst performers. To reflect the priorities of this study, environmental impact was weighted twice as heavily as performance capability, which itself was weighted four times more heavy than buildability and cost. The final weights assigned were: sustainability (0.5), performance capability (1.0), and buildability and cost (each 0.125). Performance capability included two equally weighted sub-criteria, ensuring it did not disproportionately influence the overall outcome. The total score for each alternative was calculated by multiplying the criterion weights with the respective scores and summing the results.

To test the robustness of the MCA outcome, a sensitivity analysis was performed on both the weighting scheme and scoring method. This confirmed that the selection of basalt fibre reinforcement remained consistently high across variations, reinforcing confidence in the methodology and its conclusions.

Numerical modelling was conducted to assess crack formation due to shrinkage (using LS-DYNA) and structural capacity under horizontal wind loading (using GSA Oasys) for the selected reinforcement alternative. LS-DYNA models were developed for three scenarios: non-reinforced, steel mesh-reinforced, and basalt fibre-reinforced slabs. A smeared cracking approach was used to estimate crack widths under expected shrinkage. The slab was supported with pinned edges and discrete spring elements representing the stiffness of notched connections with dowels. The steel mesh model was validated against the Eurocode analytical method, yielding a crack width of 0.19 mm, which complies with the Eurocode's Serviceability Limit State (SLS) requirements of 0.40 mm. These limits are primarily based on corrosion prevention. For basalt fibre, which is corrosion-resistant, a maximum crack width of 0.70 mm was adopted based on aesthetic considerations found in literature. The model results exceeded both analytical predictions and crack width limits:

- Non-reinforced slab: 0.95 mm
- Basalt fibre-reinforced slab: 0.96 mm
- Steel mesh-reinforced slab: 1.35 mm

A separate GSA model was developed to assess stress distribution in the top concrete layer of the TCC slab under horizontal loading, comparing standard steel mesh and basalt fibre reinforcement. For extra validation, the values are also compared to the values from the SCIA-model from the documentation of the original design. The unity check for steel mesh was 0.55 in the GSA model and 1.0 in the SCIA model. For basalt fibre, an additional safety factor was applied due to its brittle nature, resulting in unity checks of 0.31 (GSA) and 0.43 (SCIA). These results demonstrate the superior mechanical performance of basalt fibre, supporting the MCA-based material selection.

Environmental impact was assessed using a cradle-to-gate Global Warming Potential (GWP) analysis for life-cycle-stages A1-A3, based on available Environmental Product Declarations (EPDs). Fibre-based reinforcements showed significant reductions in carbon footprint when considering only the reinforcement material. However, for a fair comparison, both concrete and reinforcement must be considered. Since fibre-reinforced concrete typically requires a higher cement content per m^3 of concrete than steel-reinforced concrete. GWP values per square meter of TCC floor (reinforcement only):

- Steel mesh: 4.05 $kg\ CO_2\ eq/m^2$
- Basalt fibre: 0.45 $kg\ CO_2\ eq/m^2$

GWP values for combined concrete and reinforcement:

- Steel mesh: 16.93 $kg\ CO_2\ eq/m^2$
- Basalt fibre: 17.40 $kg\ CO_2\ eq/m^2$

Comparison of results for the GWP of only reinforcement and combination of reinforcement and concrete matrix emphasizes the importance of evaluating the entire concrete-reinforcement system. To refocus on the reinforcement material, a concrete mix using eco$_2$cem, a lower GWP cement alternative, was studied. The adjusted GWP values are:

- Steel mesh with eco$_2$cem: 11.26 $kg\ CO_2\ eq/m^2$
- Basalt fibre with eco$_2$cem: 11.43 $kg\ CO_2\ eq/m^2$

The analysis revealed that fibre reinforcement, when applied with the same cross-sectional height as steel mesh, results in higher GWP values. However, using low-GWP concrete and considering potential design optimizations—such as reduced cross-sectional height due to the elimination of corrosion-sensitive steel and the associated need for concrete cover—could make basalt fibre a more attractive alternative. An additional finding was the high GWP contribution of dowels, measured at 12.97 $kg\ CO_2\ eq/m^2$. The high GWP value for the dowels is most likely due to the high-level of detail and intervention during the manufacturing, leading to a more energy intensive process.

The findings indicate that the mechanical behaviour and the sustainability of a TCC floor system are strongly interconnected, primarily through the concrete mixture rather than the reinforcement alone. Basalt fibre reinforcement relies on its bond with concrete for structural efficiency, while the environmental impact in terms of GWP is largely determined by cement content. Using conventional fibre quantities from literature led to an overdesigned structure with a GWP exceeding that of the reference DPG TCC floor. This demonstrates that optimizing the concrete mixture is essential for achieving both structural adequacy and sustainability, even when reinforcement selection is the primary focus.

This research demonstrates that basalt fibres can meet structural performance requirements and improve the sustainability of TCC floor systems, particularly when focusing on the reinforcement material. It also underscores the necessity of evaluating all components of the system together. The developed MCA offers a framework for assessing novel reinforcement strategies in terms of both mechanical behaviour and environmental impact.

Recommendations for future research include:

- Expanding data on bio-based fibre-reinforced concrete.
- Experimental validation of fibre-reinforced concrete behaviour.
- Development of design codes for fibre reinforcement
- More comprehensive EPDs to support life cycle assessments of emerging materials

Contents

1 Introduction

1.1. Background

The global population continues to grow, driving an increasing demand for buildings and infrastructure [1, 2]. However, the materials commonly used in construction—especially concrete—have a significant environmental impact. The processes involved in sourcing, transporting, and producing these materials release large amounts of greenhouse gases and other pollutants [3]. Among the various components of a building, floor systems contribute the highest share of embodied carbon, making them a critical focus for sustainable innovation [4, 5]. Concrete is one of the most widely used materials in the construction industry, with an average global consumption of one ton per capita annually [6]. Concrete's environmental burden stems largely from cement, a key ingredient, which is responsible for 5–7% of global CO_2 emissions [7]. These emissions accelerate global warming and intensify extreme weather events, while also posing health risks through air and water pollution during production and construction activities [8]. To address these challenges, composite floor systems have emerged as a promising alternative. These systems typically consist of a concrete layer combined with a tensile material that replaces traditional steel reinforcement. This approach reduces the volume of concrete required and lowers the overall weight of the floor system. However, despite these improvements, composite structures still rely on emission-intensive materials such as steel reinforcement meshes [9]. Timber presents a renewable and well-documented alternative for sustainable construction. Timber offers favourable structural properties and a lower environmental footprint. Nevertheless, timber floor systems face limitations, including sensitivity to vibrations, span restrictions, deflection concerns, and cost. Timber-Concrete Composite (TCC) systems aim to overcome these challenges by combining timbers tensile strength and sustainability with concretes compressive capacity, resulting in hybrid structures that leverage the advantages of both materials [10].

While TCC systems offer improved mechanical performance and partial environmental benefits, the inclusion of concrete remains a significant contributor to their overall carbon footprint. Recent research has focused on mitigating this impact by reducing concrete thickness, incorporating recycled aggregates, and developing low-emission concrete mixtures [11–13]. Additionally, advancements in shear connector design have enhanced the composite action between timber and concrete, further improving structural efficiency [14–18]. Despite these efforts, most studies address either mechanical performance or environmental impact in isolation, lacking an integrated approach. A particularly underexplored aspect is the reinforcement within the concrete layer. Steel remains the standard choice, yet its production accounts for approximately 9% of global CO_2 emissions from industrial and energy processes [19]. This makes steel reinforcement a major contributor to the environmental footprint of the industry and possibly TCC floor systems. To achieve truly sustainable hybrid floor solutions, it is essential to investigate alternative reinforcement techniques that reduce embodied carbon without compromising structural integrity.

1.2. Research scope

There are many alternatives to the current standard reinforcement methods. This research will focus on fibre reinforcement as an alternative to steel reinforcement meshes. Within TCC-floor-systems, there are many configurations possible, with different factors influencing the reinforcement quantity and lay-out. This study will focus on one configuration, following a case study. Loading cases in the assessment will stay limited to static analysis and the performance of the TCC-floor-systems will be based on those of standard TCC-slabs, according to the Eurocode and eventual extra information from international codes will be used for these criteria, based on similar projects within Europe. Building materials and structures have several life cycle phases, all contributing to the total environmental impact of a structure. In this thesis the life cycle phases A1-A3 (production stage) of the TCC-floor-systems will be studied quantitatively, whereas the other life cycle stages will be studied qualitatively.

1.3. Research questions

This study investigates alternative reinforcement materials for TCC floor systems by examining their mechanical and environmental performance through a case study approach, forming the basis for the following research questions. The main research question of this research summarizes this objective and is as follows:
"What are the mechanical and environmental implications of using a suitable alternative reinforcement method and material in timber-concrete-composite (TCC) floor systems, assessed against a case study"

To answer this question, the following sub questions are proposed.
1. "Based on the functional roles and requirements for reinforcement in TCC floor systems, which alternative reinforcement method and material is most suitable for application using a multi-criteria analysis?"
2. "How does the most suitable alternative reinforcement method and material compare to an existing case study design based on their individual mechanical and environmental performances?"
3. "To what extent do the mechanical and environmental performances influence each other with the implementation of the most suitable reinforcement method and material?"

1.4. Research objective and methodology

In this research the focus lies on identifying sustainable alternatives to conventional steel meshes, examining their influence on structural behaviour and environmental impact. A Multi-Criteria Analysis (MCA) will be applied to integrate mechanical and environmental performance indicators, identifying the most promising reinforcement option for further detailed analysis. To achieve this, the study combines theoretical understanding with practical tools, integrating numerical simulations and environmental assessments. The methodology includes a functional analysis, safety and liability checks based on mechanical behaviour, and a carbon footprint evaluation. The scope is limited to one TCC-floor-system configuration under static loading conditions, with performance criteria based on Eurocode standards and relevant international codes. Environmental impact is assessed quantitatively for life cycle stages A1–A3 (production phase), while other stages are evaluated qualitatively. The research is structured in three key methodological components.

1.4.1. Assessment of reinforcement alternatives (multi-criteria analysis)

A set of evaluation criteria will be developed and weighted according to their relevance. Reinforcement alternatives will be scored on a scale from 0.0 to 100.0 using linear interpolation. The total score for each alternative will be calculated as the weighted sum of individual criteria scores, allowing for a ranked comparison. This MCA will identify suitable reinforcement options for modelling, based on literature data, without physical testing. Preliminary environmental impact estimates will also be included in this phase.

1.4.2. Modelling of the alternatively Reinforced Structure

Finite element (FE) model simulations will be used to model the mechanical behaviour of the TCC floor slab reinforced with selected alternatives. The modelling will focus on:

- **Cracking:** Simulating serviceability limit state-induced stresses and predicting concrete cracking and its interaction with timber.
- **Shear Capacity:** Evaluating load transfer mechanisms and the influence of reinforcement type on shear strength, particularly under wind-induced tensile stresses.

FE model tools such as LS-Dyna (for crack width modelling) and GSA (for wind-load stress distribution) will be used. The models will be calibrated using existing data and designed to be adaptable for future updates with field or lab data.

1.4.3. Carbon footprint comparison

A detailed environmental assessment will be conducted to compare the carbon footprint of the original steel mesh reinforcement with the selected alternative. While the MCA includes preliminary estimates, this phase will provide a more in-depth analysis using Environmental Product Declarations (EPDs) and supplementary literature data. The comparison will focus on the global warming potential (GWP) for life cycle stages A1–A3, quantifying the environmental impact of both individual materials and the complete TCC slab system. By integrating these findings into a holistic framework for TCC optimisation, the study aims to bridge the gap between theoretical modelling and practical application, contributing to sustainable construction through evidence-based strategies that reduce carbon footprint without compromising structural integrity.

1.5. Thesis outline

This thesis is structured in alignment with the methodological approach, presenting each phase of the evaluation in a dedicated chapter. Chapter 2 presents a literature study covering reinforcement fundamentals, alternative materials, TCC system behaviour, and sustainability aspects. Chapter 3 introduces the case study of the DPG Media office building, outlining the original floor structure and proposed design adaptations for fibre reinforcement. In Chapter 4, a Multi-Criteria Decision Analysis (MCDA) evaluates reinforcement alternatives based on mechanical performance, environmental impact, buildability, and cost, identifying the most promising options. These selected alternatives are assessed in two stages. Chapter 5 investigates the serviceability limit state (SLS) behaviour of the TCC floor slab, comparing crack width predictions from Eurocode-based calculations with results from a FE model in LS-DYNA. Chapter 6 examines the ultimate limit state (ULS) performance using two FE models in GSA Oasys, comparing stress distribution and tensile capacity across different reinforcement materials. Chapter 7 builds on the MCDA by comparing the carbon footprint of the original steel mesh reinforcement with selected alternatives using Environmental Product Declarations (EPDs), quantitatively for life cycle stages A1–A3 and qualitatively for later stages. Chapter 8 gives a reflection on the research and its limitations. Chapter 9 concludes the research by summarizing findings, and offering recommendations for future work. Supporting figures, criteria, and calculation examples are included in the appendices.

2

Literature Study

This literature review establishes the foundation for the research by first introducing timber–concrete-composite (TCC) systems, outlining their structural composition, historical development, applications, and mechanical behaviour. It then examines sustainability in the context of TCC floors, with a focus on assessment methods such as life cycle assessment (LCA) and multi-criteria analysis (MCA). Finally, the review examines both conventional and alternative reinforcement types, emphasizing their structural performance and environmental impact. Throughout these discussions, it consolidates existing knowledge, synthesizes insights from prior research, and identifies gaps in the literature. This provides the foundation and rationale for the current study, while also presenting potential reinforcement options for comparison in the MCA outlined in Chapter 4.

2.1. TCC systems

TCC floor systems combine the favourable properties of timber and concrete to create structural elements that are both strong and efficient. This section provides an overview of their structural composition and function, traces their historical development and applications, examines their cross-sectional behaviour, and summarises current research trends in the field.

2.1.1. Structural composition and cross-sectional behaviour

TCC floor systems combine a timber element and a concrete element to create a composite cross-section that exploits the strengths of each material. The timber forms the bottom layer, resisting tensile stresses, while the concrete forms the top layer, resisting compressive stresses under loading. Most TCC floors are designed as one-way spanning, simply supported elements subjected to vertical loading, which results in positive bending moments and corresponding tensile stresses at the bottom and compressive stresses at the top [20].

The two layers are connected by connectors, which prevent horizontal slip and enable shear transfer between the timber and concrete. The stiffness of this connection governs the degree of composite action, influencing both the shear transfer and the resulting normal stress distribution in the cross-section. In turn, this affects the element's overall stiffness, bearing capacity, and deflection [20]. Connections can be classified into three types [20]:

- **Perfectly rigid connections:** No horizontal slip occurs, enabling full shear transfer and full composite action. This results in the highest bearing capacity and the lowest normal stresses. While true rigid connections are rare, glued connections can approach this behaviour.
- **No connection:** The timber and concrete layers act independently, with no shear transfer and no composite action. This leads to the highest normal stresses and deflections.
- **Semi-rigid connections:** The most common in practice, providing partial composite action. Their stiffness depends on the connector type and configuration, resulting in intermediate values of bearing capacity, stresses, and deflections.

Connector types include dowel-type fasteners, notched joints, glued joints, nail-plate connectors, and friction-based connections. Each type offers different stiffness and ductility characteristics, influencing both structural performance and failure mode. Failure is defined as the moment when any of the individual components - timber, concrete, or connectors - fail, with the failure mode dependent on the connection type [20].

The timber layer can be either solid timber or a composite product such as glue-laminated timber (Glulam), laminated veneer lumber (LVL), or cross-laminated timber (CLT). It may be used as a continuous slab or arranged as individual beams, with a thin timber layer serving as formwork that remains permanently embedded in the floor slab. The concrete top layer typically contains reinforcement that meets minimum code requirements; this reinforcement is positioned in the compression zone, where it does not contribute to bending resistance, but instead controls crack widths and can provide diaphragm action in floor slabs [20].

2.1.2. History and application

TCC structures have recently gained popularity due to various characteristics that make them beneficial compared to both full timber and concrete floor systems. However, the origin of TCC systems is one out of necessity. After the First and Second World Wars, in Europe a shortage of steel forced engineers to develop alternatives. In 1922, Muller designed a system of steel braces and nails that could act as a connector between timber beams and concrete slabs. Whereas in 1939 Schaub filed a patent for a different connection system, made up of I- and Z-profiles [21]. These older designs fail to meet the sound insulation and fire resistance requirements of current design codes and do not comply with modern legislation [22].
To understand the evolution of TCC systems and their growing application, it is important to consider the structural elements that define their behaviour and composite action. Modern TCC-floor systems are composed of several key components, each with distinct functions and impacts. These include the concrete compressive layer on the top, often incorporating a reinforcement mesh to mitigate shrinkage cracks; shear connectors such as notches and dowels to facilitate effective load transfer; and an engineered timber layer at the bottom designed to resist tensile forces. Together, these elements contribute to the unique performance characteristics of TCC slabs, balancing strength, durability, and material efficiency [10, 20].
The application and research of TCC systems got an increase in interest in the 1990's, ranging from retrofitting existing timber floors, to applications as bridge slabs and as floors in new building projects. Using nails spaced throughout the beam for the connection between timber and concrete has been a widely used system and was first used in Bratislava in a historical building in 1960. It gained popularity as this renovation technique resulted in less than half of the costs for a new floor system [21].

Despite their sensitivity to vibrations and limited spans, TCC floor decks have also been used in bridges. Since the 1970's bridges of TCC have been built in New Zealand [23]. A great example of a TCC bridge, constructed in 1999, is the Vihantasalmi bridge in Finland. The 11 meter wide highway road accompanied by a 3 meter broad sidewalk, bridge spans 168 meters [24]. Early TCC bridge projects were crucial in the development of codes and guiding the research of TCC systems. Another of these early age TCC bridges was the first major composite system in Australia, mid-1950's, was a highway bridge over the Maria River. Applications continued throughout the 21st Century, with slight innovations. In 2023, a 70-meter-long pedestrian and biking bridge, was realised in Stuttgart, using a carbon fibre mat instead of the standard reinforcement mesh [25].
Since the start of the 21st century, TCC systems have found increasing popularity as an alternative to concrete floor systems, in both residential, industrial and commercial buildings, where sustainability is a key focus. These systems are particularly suited for low-carbon designs, as by minimizing concrete volumes and enhancing material reuse [10, 13]. TCC floor systems have a reduced structural weight and faster construction times, as well as enhanced acoustic and thermal performance compared to more conventional systems, such as concrete slabs and steel composite concrete slabs [10, 26, 27].
In North-America, an increase in utilization of timber constructions has been seen since 2012. In the same year, TCC systems got its first large scale project application. The five-story Earth Science Building (ESB) at the University of British Columbia established an innovative precedent for the use of wood in building structures, with the first of its kind free-floating cantilevered solid timber staircase[28]. As with the ESB, other applications of TCC floor systems, applications have been limited to a select few

renowned projects across the globe. In Australia the Dr. Chau Chak Wing Building located at the University of Technology Sydney, a 12 story Building designed by Frank Gehry made use of TCC floor slabs in some of its classroom floors [29]. In Europe, the tallest building using TCC floor was finished in 2019 and is located in Vienna being 84 meters tall, HoHo is a mixed use building that makes use of the XC® ceiling panels. The floor slabs are prefabricated as opposed to other common TCC application where the concrete is cast in-situ [30]. In the Netherlands there are two building recently constructed using TCC floors, HAUT and the new DPG office, both located in the metropolitan area of Amsterdam. The HAUT building is the tallest building using TCC floors in the Netherlands, consisting of 21 floors at 73-meters in height. HAUT also used energy-generating façades and made use of triple glazing and recycled materials where possible [31]. These elements highlight the current shift towards sustainability in the building sector. Arup was involved as consulting engineering firm. DPG will be used as a case study for this thesis and more information will be provided in section 3.

2.2. Sustainability of TCC floors

Sustainability is a key driver in modern construction, pushing the industry toward solutions that balance environmental, economic, and structural performance. TCC systems offer a promising approach, combining the strengths of timber and concrete to reduce material use and enhance efficiency. Assessing the sustainability of TCC systems requires a comprehensive evaluation of their environmental footprint across their life cycle, from material extraction and manufacturing to construction, use, and end-of-life (EOL) scenarios. Since January 1, 2013, environmental impact calculations have been mandatory for office and residential buildings, following guidelines that require data from the National Environmental Database and consideration of at least eleven environmental impact categories. Recently these have been expanded to 19 environmental impact categories, their implementation will start in 2025 [32].
This section explores how sustainability is assessed in TCC systems, focusing on key metrics such as carbon footprint, embodied energy, and resource efficiency. Particular attention will be given to the integration of LCA methodologies and their application in quantifying the environmental benefits of TCC systems compared to traditional construction methods.
Furthermore, the potential role of TCC systems in advancing a circular economy will be examined. Their hybrid nature presents unique opportunities for reuse, recycling, and resource recovery, aligning with circular economy principles of minimizing waste and maximizing material value. Challenges such as the compatibility of timber and concrete for recycling, the feasibility of disassembly, and the durability of composite materials will also be addressed. By evaluating these aspects, this section aims to provide a holistic understanding of how TCC systems can contribute to sustainable construction practices and support the transition to a circular economy.

2.2.1. General analysis methods

Two terms have been used interchangeably to describe the environmental impact of buildings, green buildings and sustainable buildings. There is a big difference between these terms, green buildings have been described as creating spaces that are healthy, functional, and efficient while promoting architecture that harmonizes with nature, minimizes resource use (energy, land, water, materials), protects the environment. Sustainable buildings have been described as the results of interpersonal processes, such as communication and co-operation, resulting in information and systems of rules governing the interaction of members of a society. Sustainability is a multifaceted and interdisciplinary concept, leading to various interpretations and applications [33].
The first green building label and one of the main green building labels in Europe is BREEAM, its certifications dominate 80% of the European market for sustainable building certifications. While BREEAM has the capacity to evaluate all pillars of sustainability, its primary focus remains on environmental factors, assessed through eight key categories: Management, Energy, Transport, Water, Materials, Waste, Land Use & Ecology, and Pollution [33]. It assesses most of the mentioned categories based on checklists, sometimes using a specific number. For example, X percentage of light sources should be of Y capacity, while other requirements can be performing one specific action on the checklist [34]. This mix of specified numbers in combination with relatively open to interpretation checklists allows for a flexible grading but can be difficult to quantify. A lot of countries have their own requirements on the area of sustainability that the BREEAM and other green building labels adapt to [35].
Green building labels and local regulations typically measure environmental impact through LCA.

However, while green labels take a broad approach, LCA studies often fail to examine the integration of environmental, economic, and social aspects. Instead, these aspects are usually evaluated separately and independently, without offering solutions that combine them. A significant challenge in integrating these three dimensions lies in their reliance on different measurement units. Two possible methods for addressing this issue include disregarding the measurement units or converting them into financial terms (monetization). Due to the qualitative nature of many social impact indicators, monetizing social impacts is often subjective and speculative, making the option of ignoring measurement units more suitable for developing an integrated, life-cycle-based framework to assess building sustainability [35]. In 2008 Klöpffer wrote an article highlighting that this integration of the three pillars of sustainability: environment, economy and social aspects, as an assessment method for materials is not a new methodology. Yet, this integration of multiple aspects influencing sustainability is often overlooked [36]. A rising method, dubbed the Finnish method, evaluates emissions across the building's life cycle, covering material production, construction, replacements, operational energy, and EOL, typically over a 50-year period. It uses predefined emission factors that account for future reductions based on national commitments. Uniquely, the method also allows for calculating a "carbon handprint," capturing positive impacts such as recycling benefits, concrete carbonation, bio-based carbon storage, and renewable energy surplus. Manufacturers can report product-specific impacts via Environmental Product Declarations (EPDs) in line with EN 15804, commonly published through Finland's RTS system, ensuring standardized and market-recognized data. [37]

2.2.2. Assessment of sustainability of TCC floors

In 2021 Siddika et al. assessed the sustainability of TCC slabs by looking at the embodied energy, kilograms of equivalent CO_2 emissions, up to the EOL stage per m^2 floor slab, but not going into a detailed analysis. Research into TCC floor systems assessing the sustainability of these systems often make use of LCA. LCAs have become a critical tool in evaluating the sustainability of TCC systems. LCA is an internationally standardized method for assessing environmental consequences of products and processes [38]. The lifecycles that can be studied in an LCA are defined in the EN 15978 and shown in Figure 2.1 [39].

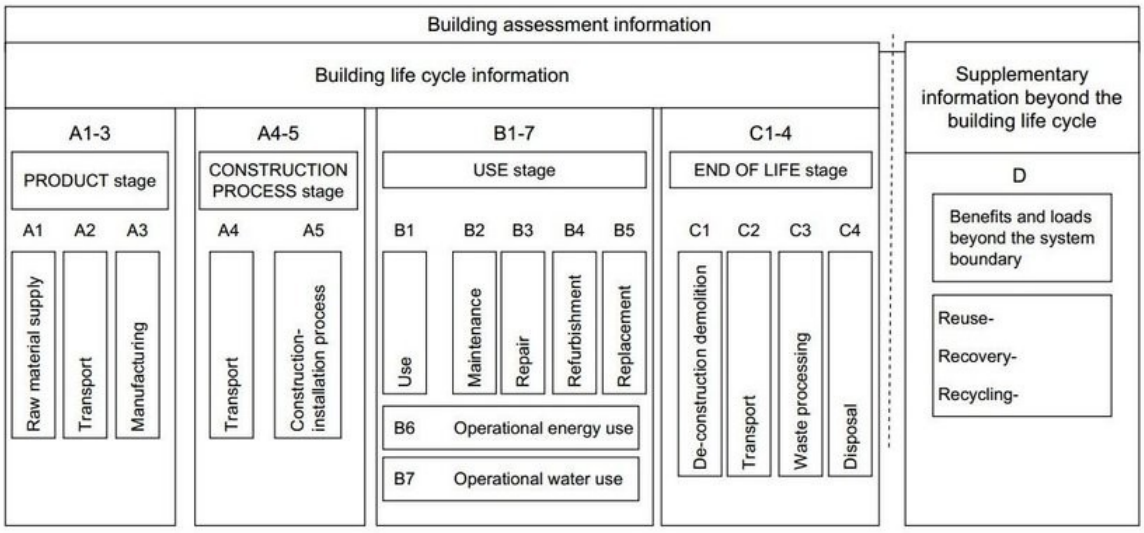

Figure 2.1: Life cycle stages [39]

The Global Warming Potential (GWP) is a commonly used as a way to showcase the environmental impact of a construction in kg CO_2 eq./m^2, together with Primary Energy (PE), for some or all of the life cycle stages of a designed product. GWP quantifies the total global warming impact of a substance over a specific time, comparing its cumulative radiative forcing to that of CO_2 emissions. PE refers to energy extracted from natural sources for electricity, heat, or other uses, encompassing both renewable

sources (e.g., wind, solar, hydro, geothermal) and non-renewable sources (e.g., coal, oil, natural gas). Assessments are often carried out by looking at cradle-to-grave, cradle-to-cradle, or cradle-to-gate, focusing on different life-cycle stages. Cradle-to-grave is a comprehensive life cycle assessment that spans from resource extraction ("cradle") through the use phase to the final disposal stage ("grave"). Cradle-to-cradle is a specialized form of cradle-to-grave assessment in which the product's EOL stage involves recycling rather than disposal. This approach seeks to reduce environmental impact by adopting sustainable practices throughout production, operation, and disposal, while also aiming to integrate social responsibility into the product development process. Cradle-to-gate refers to an assessment of a product's partial life cycle, covering the stages from resource extraction (cradle) up to the factory gate, prior to its transportation to the consumer (A1-A3) and is always included in environmental product declarations (EPD) [40].

Dalbiso and Baghban (2025) recently reviewed LCA studies on TCC systems, highlighting that GWP is the most frequently used indicator. Other common metrics include Ozone Depletion Potential (ODP), Acidification Potential (AP), Eutrophication Potential (EP), Photochemical Oxidation (POCP), and Abiotic Depletion (ADP). The majority of studies concentrated on the product stage (A1-A3), reflecting the greater availability of data for this phase compared to others. The most detailed analyses covered a broader range of modules, including A1-3, B4, C1-4, and D [41].

In 2021, Kromoser and Holzhaider conducted a comparative LCA of six different floor types, beginning with an analysis of material requirements for concrete and timber. The environmental impacts were then evaluated across six characterisation categories: GWP, total use of non-renewable primary energy resources (PENRT), total use of renewable primary energy resources (PERT), ODP, AP, and EP. To address uncertainty and ensure comparability in EOL assumptions, the study used sector-average environmental product declarations (EPDs) rather than manufacturer-specific data, covering the full life-cycle stages A1-D in accordance with EN 15804. This included the reuse, recovery, and recycling potential in stage D as represented in the EPD datasets.
Qualitative design and performance attributes (e.g., floor type, cross-section shape, presence of cavities) were converted into quantitative environmental impacts by calculating exact material quantities for each system and linking them to the averaged EPD impact factors for all six categories [12].
Corti et al. delved into the different recycling scenarios (life cycle stage D) by performing an LCA, assessing the GWP of several scenarios. The LCA was studied from cradle to cradle, focusing on stages A, C and D. It analysed multiple EOL scenarios for timber, including landfill, incineration with energy recovery, recycling, and reuse, while emphasizing the role of sustainably sourced timber in reducing CO_2 emissions through biogenic carbon content. They explored four main EOL scenarios for timber: landfill, incineration with energy recovery, recycling, and reuse. To provide a comprehensive assessment, the study examined multiple slab configurations, varying in thickness of timber and concrete layers, and spanning different lengths. Reuse and recycling scenarios showed better performance than landfill, with pure timber slabs generally having the lowest GWP impact in these scenarios [13]. The inclusion of carbon capture for concrete further improved the environmental performance, especially in reuse-oriented scenarios.

Similarly, Lecours et al. optimized composite floors for sustainability and efficiency. Their paper evaluates sustainability primarily through embodied carbon emissions and LCA, focusing on the environmental impacts of construction materials. It uses cradle-to-gate analysis, assessing impacts from raw material extraction to the factory gate, and incorporates scenarios with and without carbon storage in timber. Data from Gestimat software and the ecoinvent 3.1 database inform greenhouse gas emission estimates for materials like Cross Laminated Timber (CLT) and various types of concrete: Non-reinforced concrete, Fibre reinforced Concrete (FRC), High Performance Fibre Reinforced Concrete (HPFRC) and Ultra High Performance Fibre Reinforced Concrete (HPFRC). The study compares emissions across materials, reporting metrics in $kgCO_2eq/m^2$ or $kgCO_2eq/m^3$, and highlights UHPFRC's potential to reduce timber use by 20%, emphasizing resource efficiency. While it briefly considers material costs, the focus remains on environmental sustainability. Future work is proposed to include cradle-to-grave LCA with EOL scenarios for a more comprehensive assessment [14].

It should be mentioned that a proper and comprehensive exploitation of low environmental im-

pact of timber is ensured in case an additional focus on LCA stages C and D is considered. When an engineer is designing and gets values for an EPD, the EOL stage often includes the incineration of the timber part of the elements. However, by designing for a different end-of life scenarios, the environmental impact of TCC floor could be different.
In 2023, Eslami studied the impact of different EOL scenarios of TCC floor slabs on the GWP and PE. The analysis compared a concrete floor slab, a steel-concrete composite slab, and a TCC slab of the same dimensions in a cradle-to-grave LCA. In this first comparison, the TCC slab had the smallest impact for both GWP and PE [42].
A second, cradle-to-cradle LCA was then performed, calculating the potential GWP and PE associated with stage D for each slab to assess the benefits of reuse, recycling, or recovery. Here, the TCC slab again proved considerably more advantageous than the other two slabs [42].
For the TCC slab, three EoL scenarios were modelled to address uncertainty:

1. **Full energy recovery** - assumes complete incineration of timber to produce steam, heat, or electricity.
2. **Typical European average** - based on literature data: 37% landfill, 33% recycling, and the remainder used for energy recovery.
3. **Full reuse** - assumes design for deconstruction, with a shear connection allowing the CLT panel to be removed and reused, as targeted by the ECON4SD building prototype.

These qualitative strategies were translated into quantitative LCA results by assigning specific material flows and applying impact factors for each route. Scenario 3 was shown to have the lowest GWP and PE, as well as the highest potential benefit in stage D, demonstrating that, for this case, a demountable and reusable TCC slab is the most sustainable option [42].

2.2.3. The role of TCC in a circular economy

The transition from a linear to a circular economy is gaining momentum, particularly in the construction sector. In a linear economy, resources are extracted, used to produce products, and ultimately disposed of at the end of their lifecycle. Conversely, a circular economy prioritizes the reuse of products, extending their lifecycle and minimizing waste. One key strategy to foster a circular economy in construction is adopting circular design methods, where buildings, systems, and components are designed for disassembly and reuse. This approach reduces the consumption of raw materials and curtails harmful emissions.
TCC systems play a pivotal role in advancing the circular economy by enabling the recovery and reuse of materials like timber and concrete. By extending the lifecycle of these materials, TCC systems reduce waste generated during construction and demolition processes [16, 43]. Designing TCC floors for reuse marks a significant departure from traditional TCC design, which typically focuses on immediate structural needs and employs permanent connections, not designed for re-use. In contrast, design for re-use emphasizes deconstructable connection systems, easy material separation, and adaptability for future use.
Traditional TCC designs, while structurally efficient, often overlook EOL scenarios, leading to significant waste when materials cannot be separated or repurposed. As a composite system, TCC floors combine materials with distinct life cycles, making their separation and reuse critical for reducing environmental impact. Implementing design-for-deconstruction practices can unlock the full potential of these materials at the end of a building's life. For example, Derikvand et al. categorized TCC connection systems into key construction methods: Dry-Dry Systems, Wet-Dry Systems and Hybrid Solutions [16].
Dry-Dry Systems involve prefabricating the concrete slab separately and connecting it to the timber using components like steel tubes, coach screws, or bolts with additional elements made of steel, wood, or plastic. Wet-Dry Systems involve mounting connectors on the timber before casting concrete. Examples include notches with threaded steel bars glued with epoxy, rectangular notches with self-tapping screws (deconstructable even after high loads), and round notches that avoid screws altogether. Hybrid Solutions such as the FT connector, which works for both dry-dry and wet-dry systems, feature an inclined plastic tube, a steel washer, and a screw, offering flexibility across various floor configurations [16]. These connection systems simplify assembly, disassembly, and material reuse, aligning with circular economy principles and fostering sustainable construction practices. While the initial costs of designing for reuse may be higher, the long-term benefits include material recovery, waste reduction,

and compliance with circular economy goals.
In addition to enabling reuse, circular design closes the material lifecycle loop, transforming the use of resources from a linear process to a cyclical one. For reinforcement in TCC systems, renewable fibres, such as waste fibres, natural fibres, and recycled fibres (discussed in Section 2.3), present promising yet underutilized options. By integrating these practices, TCC systems can further enhance their contribution to a sustainable and circular construction industry.

2.2.4. Limitations of TCC systems and sustainability assessment

The assessment of sustainability TCC systems faces several limitations and challenges, particularly when attempting to fully evaluate their environmental impact across all stages of the life cycle. While an LCA provides valuable insights, it is often restricted to certain life cycle phases such as the product stage (A1-A3) or sometimes the cradle-to-grave approach. This partial focus can result in gaps, especially in the post-use stages like disassembly, reuse, or recycling. For instance, many studies on TCC systems tend to emphasize the initial stages of production, such as material extraction and processing, but may overlook or fail to provide detailed analysis on the environmental impacts during the EOL phase, which can significantly influence the overall sustainability of a system.
Additionally, the complexity of evaluating a composite material like TCC, made up of both timber and concrete, presents its own set of challenges. Timber and concrete have different life cycles, and their integration in a single system complicates their separation for recycling or reuse. Timber, for example, is biodegradable and can be reused or recycled, but concrete typically requires more intensive processing. This divergence creates difficulties when trying to design systems that facilitate material recovery or ensure long-term environmental benefits. The challenge is further exacerbated by the fact that most TCC systems, unless explicitly designed for disassembly, include non-deconstructable connections, making the separation of materials more challenging and costly.
Moreover, integrating environmental, economic, and social aspects into a unified sustainability framework remains a significant hurdle. LCA often isolates these dimensions, which can lead to oversimplified conclusions. The monetization of social impacts, for example, is highly subjective and often speculative, leading to uncertainty in assessments. Without a standardized approach that addresses these three pillars holistically, achieving a truly sustainable building design using TCC systems remains a complex task.
In the context of the circular economy, the potential for TCC systems to contribute is clear, but the realisation of this potential is uncertain without additional research into the reusability of components, especially at the EOL stage. The current lack of detailed analysis on material recovery processes limits the ability to fully exploit the environmental benefits of TCC systems. Furthermore, while designing for disassembly can significantly reduce environmental impact, the initial investment and design complexity are higher, posing economic challenges for widespread adoption. There are also concerns regarding the standardization of such designs and their integration into current construction practices. Therefore, a more detailed and holistic approach to LCA, alongside innovation in material separation and recovery, will be necessary to fully realize the sustainable potential of TCC systems.

2.3. Reinforcement

Reinforcement is a fundamental component of both concrete and concrete–composite structures, serving to enhance tensile capacity and prevent brittle failure. To evaluate the implications of replacing conventional reinforcement, it is necessary to first understand its structural role in both reinforced concrete (RC) systems and composite configurations. This section reviews conventional steel reinforcement and examines alternative options, considering their mechanical behaviour, applicability, and potential influence on the properties and performance requirements of the surrounding concrete.

2.3.1. Background of reinforcement

Concrete is inherently strong in compression but weak in tension, which makes reinforcement essential for preventing brittle failure. The reinforcement material itself must therefore exhibit ductile behaviour to avoid sudden collapse. Steel has long fulfilled this role, with its use in reinforced concrete dating back more than a century. The first specifications for reinforcement steel appeared in the 1910s [44], while in the Netherlands, quality guidelines have existed since 1968 and are now covered

by NEN-EN 10080 [45, 46]. Structural design rules for reinforced concrete are provided in Eurocode 2 [47].

Steel reinforcement is widely available due to the extensive global steel industry. In 2019, around 950 million tonnes of steel were used for reinforcement applications [48], and in 2023 global crude steel production reached 1.892 megatonnes. In the Netherlands, approximately 88% of steel companies specialise in producing braided concrete reinforcement, underlining its significance within the national steel sector and its ease of procurement [49–51].

However, steel production is highly energy-intensive, requiring high processing temperatures and multiple production stages. Although reinforcement steel is typically recycled at the end of a building's life, its initial production has a substantial environmental footprint. Globally, steel production accounts for roughly 9% of CO_2 emissions from energy use and industrial processes [19].

2.3.2. Alternative reinforcement types

While steel remains the default choice in most current design practices, its environmental impact has motivated research into alternative reinforcement types. These alternatives differ in material composition, reinforcement method, and compatibility with concrete, and some may also influence the concrete's mix design or structural detailing requirements. This subsection provides an overview of potential alternatives, such as fibre reinforcement, non-ferrous metal reinforcement, and composite materials, highlighting their properties, benefits, limitations, and current barriers to widespread adoption.

In table 2.1 the pro's and con's for the reinforcement methods are listed, with a more detailed explanation of the reinforcement methods following in the paragraphs in this section.

Table 2.1: Overview of pros and cons of alternative reinforcement methods

Reinforcement method	Pros	Cons
FRC	- Improves crack control, ductility, and post-cracking toughness. - Can reduce or replace conventional rebar in certain applications. - Enables slender, lightweight, and prefabricated elements. - Well-suited for seismic-resistant structures.	- Reduced workability and challenges in fibre dispersion. - Performance depends strongly on fibre type, dosage, and matrix quality. - Limited or evolving design codes for structural applications. - Higher initial costs and limited recyclability.
FRP	- Improves crack control and durability. - Corrosion-resistant, reducing maintenance needs. - Can reduce or replace conventional rebar in certain applications. - Enables slender, lightweight, and prefabricated elements.	- Linear-elastic behaviour until sudden brittle failure. - Performance depends strongly on fibre type, dosage, and matrix quality. - Limited or evolving design codes and standardised testing methods. - Higher initial costs and limited recyclability.

FRC

FRC incorporates discrete fibres into the concrete matrix to enhance its mechanical performance and durability. The use of fibres as reinforcement for brittle matrix materials has existed for thousands of years, with modern applications in concrete employing materials such as asbestos, cellulose, polypropylene, glass, and steel [52]. Depending on their properties, fibres can be broadly categorised into high-modulus types, capable of partially or fully replacing conventional reinforcement in structural applications, and low-modulus types, which are generally used in smaller quantities to control shrinkage cracking and improve fire resistance [53]. At low volumes (typically below 0.4% by volume), fibres mainly influence the post-cracking behaviour of the concrete, while higher volumes can also enhance

TRC	- High tensile strength. - Corrosion-resistant, reducing maintenance needs. - Can reduce or replace conventional rebar in certain applications. - Enables slender, lightweight, and prefabricated elements.	- Linear-elastic behaviour until sudden brittle failure. - Poor performance in compression and shear compared to steel. - Higher initial costs and limited recyclability. - Limited or evolving design codes and standardised testing methods.

pre-cracking load capacity. Fibres are often added to: (a) improve rheology or plastic cracking resistance in fresh concrete; (b) increase tensile or flexural strength; (c) enhance impact resistance and toughness; (d) control cracking and improve post-cracking ductility; and (e) increase durability [53].

The performance of FRC depends primarily on fibre volume, the physical and mechanical properties of the fibres and matrix, and the bond between them [52]. As concrete typically fails in tension before fibres reach their ultimate strain capacity, the principal benefits of fibres occur in the post-cracking stage. Here, fibres bridge cracks, improving ductility, toughness, and energy absorption [54]. This bridging effect also enhances seismic performance by preventing brittle failure under cyclic loading [54]. However, the inclusion of fibres can reduce workability, and achieving uniform fibre distribution, especially in dense mixes, often requires highly flowable self-compacting concrete [52].

FRC offers potential benefits in reducing the need for conventional reinforcement, lowering the labour and cost associated with steel rebar placement, and enabling thinner or lighter structural elements, such as tunnel linings and pavements [53]. In some cases, fibre inclusion can reduce the weight of concrete elements by one-third to one-half while maintaining equivalent load-bearing capacity [52]. Optimal fibre content is necessary to balance improvements in strength and ductility with acceptable workability [53].

Despite its advantages, the structural use of FRC remains limited. Much of the research into the structural response of FRC elements has emerged in the past fifteen years, and the absence of widely adopted international building codes for FRC design continues to hinder its uptake [54]. While design guidelines exist, practitioners often hesitate to apply them in the absence of clear, standardised code provisions, preferring to rely on established materials with codified design rules [54].

Fibre reinforced polymer (FRP) bars

FRP bars are composite materials consisting of high-strength fibres, such as glass, carbon, aramid, or basalt, embedded in a polymer matrix, typically epoxy, polyester, or vinyl ester resins. While fibres provide tensile strength and stiffness, the matrix ensures stress transfer and environmental protection [55, 56]. Surface treatments such as sand coatings or wound textures are often applied to improve the bond with concrete [57].

The mechanical behaviour of FRP rebars differs fundamentally from that of steel reinforcement. FRPs are anisotropic, linear-elastic until brittle failure, and exhibit high tensile strength in the fibre direction but reduced performance in compression and shear [58]. As a result, FRP-reinforced concrete members often display larger deflections and wider cracking prior to sudden failure [59]. Their properties are influenced by fibre orientation, fibre-to-matrix ratio, curing conditions, and manufacturing quality control [56, 60].

Global standardisation efforts have accompanied the introduction of FRPs in construction. The first design recommendations were published by the Japan Society of Civil Engineering (JSCE) in 1997, followed by codes in Europe, North America, and elsewhere [61, 62]. In particular, ACI Committee 440 established widely used guidelines for the design and testing of FRP-reinforced concrete [62]. These

documents aim to reduce design uncertainty by providing standardised test methods for mechanical and durability performance.

The main driver for FRP adoption is corrosion resistance, making it especially suitable for marine environments, bridges exposed to de-icing salts, and other aggressive conditions. Although FRPs involve higher initial costs and embodied emissions than steel, they can extend service life and reduce overall life-cycle costs [55]. Their non-magnetic and non-conductive properties also enable specialised applications, such as in MRI facilities, railway systems, or "soft-eye" tunnel boring operations where temporary reinforcement must be cut away [63].

Despite these advantages, FRPs face limitations due to their brittle failure modes, lack of ductility, and reduced compressive capacity compared to steel. However, ongoing advances in materials and design standards continue to expand their role in sustainable and durable concrete construction [56, 58].

Textile-Reinforced Concrete (TRC)
TRC replaces conventional steel reinforcement with non-metallic textile meshes made from high-tensile fibres such as carbon or alkali-resistant (AR) glass. The absence of steel removes the need for a concrete cover, allowing the design of slender, lightweight members. TRC has been applied both in new elements (e.g., façades, shells, balcony slabs) and in the strengthening of existing structures, where its corrosion resistance, flexibility, and fire performance provide advantages over FRP [64, 65].

The performance of TRC depends on fibre type, mesh geometry, and bond characteristics with the surrounding cementitious matrix. The fine mesh requires mortar mixes with small aggregate sizes ($\leq$2 mm), often combined with pozzolanic additives or mineral admixtures to improve compatibility, strength, and durability [65]. While TRC enhances tensile strength and crack control compared to plain concrete, its brittle fibre behaviour can limit ductility under extreme loading. Research into engineered cementitious materials, multi-layer textile configurations, and varied fibre orientations aims to address these challenges [64].

Bond-slip behaviour is critical for load transfer and overall composite action. Pull-out tests indicate that greater embedment length increases strength and deformation capacity, though failure typically occurs by fibre rupture. While analytical bond-slip models have been proposed, the absence of standardised testing procedures continues to hinder broader implementation [64].

TRC offers clear durability benefits, including reduced cracking, freeze–thaw resistance, chemical resistance in some fibre types, and immunity to corrosion. Its lightweight nature also supports prefabrication and ease of handling. However, its bending capacity is generally lower than conventional steel-reinforced concrete, limiting its use to secondary or non-structural applications. Although pilot projects such as pedestrian bridges in Germany highlight its potential, the lack of unified codes and manufacturing standards currently confines TRC to niche applications and research contexts [64, 65].

2.3.3. Alternative reinforcement materials

The materials used in alternative reinforcements have been briefly mentioned in the previous section, in this section a more detailed overview of materials used and the benefits are highlighted.

Most materials mentioned in literature are non-metallic materials. This brings a few benefits primarily based on eliminating the corrosion sensitivity of the reinforcement. Using a material that is not corrosion sensitive removes the need for most of the cover requirements. As these requirements are based on bonding requirements and to keep the steel reinforcement save from chloride intrusion and carbonation of the concrete. Changing the material for the reinforcement thus removed the need for the cover thickness, but also makes these reinforcement alternatives suitable for aggressive environments. In these aggressive environments, concrete structures often suffer structurally from carbonation and/or chloride ingression.

The most common materials for reinforcement are mentioned below, with their pros and cons listed.

Table 2.2: Advantages and disadvantages of common fibre materials used in concrete composites (based on [52–55, 64, 65])

Material	Advantages	Disadvantages
Steel	- High tensile strength and ductility [52] - Established design codes and standards [54] - Widely available and easily recycled [52]	- High self-weight [52] - Prone to corrosion in aggressive environments [55] - High embodied energy and CO_2 emissions [53]
Polypropylene (PP)	- Lightweight and low cost [53] - Chemical and corrosion resistant [65] - Reduces shrinkage cracking and improves fire resistance [53]	- Low tensile strength and stiffness [53] - Limited structural contribution [54] - Poor high-temperature resistance (melting) [65]
Glass (GFRP / AR-glass)	- High tensile strength [55] - Corrosion resistant [55] - Cost-effective compared to carbon fibres [64]	- Lower stiffness than steel or carbon [55] - Susceptible to alkaline attack (unless AR type) [65] - Brittle failure mode and low ductility [54]
Carbon	- Very high tensile strength and stiffness [64] - Corrosion resistant and durable [55] - Lightweight [65]	- High cost [64] - Brittle failure mode [54] - Energy-intensive production [55]
Basalt	- High tensile strength [55] - Corrosion and chemical resistant [55] - More sustainable (natural origin) [55] - Cost between glass and carbon [55]	- Limited design codes and field data [55] - Brittle failure mode [54] - Lower stiffness than carbon [55]
Cellulose / natural fibres	- Renewable and biodegradable [52] - Low cost and widely available [52] - Improves sustainability profile [53]	- Low tensile strength and stiffness [52] - Sensitive to moisture and biological degradation [53] - Limited structural applications [54]

2.3.4. Alternative reinforcements and their sustainability implications

The use of alternative reinforcement materials introduces distinct sustainability implications compared to conventional steel reinforcement. These differences arise partly from the specific environmental impact of the reinforcement material itself, and partly from indirect effects on the design and performance of the surrounding concrete system. The latter can be considered in two main areas: (a) changes in mix design and material use during production, and (b) implications for the EOL phase of the structural element.

Influence on concrete mix design

Studies on fibre-based reinforcement systems, such as FRC and TRC, highlight that the workability of the fresh mix and the allowable aggregate size often govern the performance of the hardened concrete [52, 64]. In FRC, achieving uniform fibre distribution typically requires the addition of water-reducing agents and, in many cases, an increase in cement content to compensate for the reduction in larger aggregates [53, 54]. Similarly, TRC generally demands a fine-grained matrix with a maximum aggregate size of 2 mm, often enhanced with mineral admixtures to ensure adequate bonding with the textile mesh [65].

From a sustainability perspective, these mix modifications can increase the environmental burden, particularly due to the higher cement content compared to mixes used for conventional steel-reinforced concrete. Since cement production is a major contributor to global warming potential, this adjustment can offset some of the benefits of reducing steel reinforcement. The use of supplementary cementitious materials (SCMs), such as fly ash or slag, offers a pathway to mitigate this impact and allow more equitable comparisons between reinforcement methods.

Implications for EOL
While many environmental assessments of alternative reinforcement materials are limited to cradle-to-gate analyses, some studies also evaluate EOL impacts by modelling different scenarios [55, 64]. For composite systems, however, separation of reinforcement and matrix is often energy-intensive, complicating recycling compared to steel, which benefits from a well-established recycling infrastructure. Research on TCC demonstrates that modelling EOL scenarios (reuse, recycling, energy recovery, or landfill) can significantly alter the life cycle outcomes, underlining the importance of realistic assumptions for novel systems [12, 42].

Consequently, when assessing the sustainability of alternative reinforcements, particular attention must be given to whether proposed recycling or reuse scenarios are practically achievable. Unlike steel, where established recycling chains ensure high recovery rates, the EOL pathways for composites remain less developed and therefore present significant challenges [50, 66].

2.3.5. Reinforcement in TCC

Reinforcement in TCC floor systems plays a vital role in enhancing structural performance by leveraging the complementary strengths of timber and concrete. In TCC floors, reinforcement, such as steel meshes, serves several purposes, including preventing shrinkage cracks in the concrete layer and providing redundancy to ensure structural safety under unexpected conditions. This section focuses specifically on the role of reinforcement in controlling shrinkage, a critical factor in maintaining the integrity of the composite system. The integration of reinforcement offers versatile applications, both within TCC systems themselves and in broader construction contexts, where their hybrid nature proves advantageous. However, the practical implementation of reinforcement in TCC systems introduces challenges, including material compatibility, construction precision, and cost-effectiveness. Additionally, ensuring long-term durability requires addressing concerns such as moisture resistance, fatigue under cyclic loading, and corrosion protection. These aspects underscore the complexity and significance of reinforcement in TCC floor systems within modern construction practices.

TCC - Reinforcement design methodology according to the Eurocodes
The design of TCC floors must also account for reinforcement requirements. According to Eurocode 5, which covers the structural design of timber structures, timber–concrete composite TCC systems, and general rules for buildings, minimum reinforcement is prescribed to control cracking in the concrete at the serviceability limit state [67]. Two approaches are specified in the code for determining this minimum reinforcement.

In practice, the reinforcement in TCC slabs is rarely activated in tension, as the concrete layer primarily resists compressive stresses. Consequently, most designs adopt only the prescribed minimum reinforcement, typically determined from tabulated values that depend on the concrete strength class and the thickness of the concrete topping. This table can be found in table 2.3. This reinforcement primarily serves to limit shrinkage cracking of the concrete rather than contributing to the load-bearing capacity under live loads.

Table 2.3: Design table for minimum reinforcement in TCC floors[67]

CONCRETE CLASS	RC DECK THICKNES [cm]																			
	5		6		7		8		10		12		14		16		18			
C 12/15	[a]0,80	Ø5/150	[a]0,80	Ø5/150	[a]0,80	Ø5/150	[a]0,80	Ø5/150	[a]0,80	Ø5/150	[a]0,80	Ø5/150	0,90	Ø5/150	1,03	Ø5/150	1,16	Ø5/150		
		Ø5/150		Ø5/150		Ø5/150		Ø5/150		Ø5/150		Ø5/150		Ø5/150		Ø5/150		Ø5/150		
C 16/20	[a]0,80	Ø5/150	[a]0,80	Ø5/150	[a]0,80	Ø5/150	[a]0,80	Ø5/150	[a]0,80	Ø5/150	0,92	Ø5/150	1,07	Ø5/150	1,22	Ø5/150	1,37	Ø6/150		
		Ø5/150		Ø5/150		Ø5/150		Ø5/150		Ø5/150		Ø5/150		Ø5/150		Ø5/150		Ø6/150		
C 20/25	[a]0,80	Ø5/150	[a]0,80	Ø5/150	[a]0,80	Ø5/150	[a]0,80	Ø5/150	0,88	Ø5/150	1,06	Ø5/150	1,24	Ø5/150	1,41	Ø6/150	1,59	Ø6/150		
		Ø5/150		Ø5/150		Ø5/150		Ø5/150		Ø5/150		Ø5/150		Ø5/150		Ø6/150		Ø6/150		
C 25/30	[a]0,80	Ø5/150	[a]0,80	Ø5/150	[a]0,80	Ø5/150	0,84	Ø5/150	1,04	Ø5/150	1,25	Ø5/150	1,46	Ø6/150	1,67	Ø6/150	1,88	Ø7/150		
		Ø5/150		Ø5/150		Ø5/150		Ø5/150		Ø5/150		Ø5/150		Ø6/150		Ø6/150		Ø7/150		
C 30/37	[a]0,80	Ø5/150	[a]0,80	Ø5/150	0,82	Ø5/150	0,93	Ø5/150	1,16	Ø5/150	1,40	Ø6/150	1,63	Ø6/150	1,86	Ø6/150	2,09	Ø7/150		
		Ø5/150		Ø5/150		Ø5/150		Ø5/150		Ø5/150		Ø6/150		Ø6/150		Ø6/150		Ø7/150		
C 35/45	[a]0,80	Ø5/150	[a]0,80	Ø5/150	0,90	Ø5/150	1,03	Ø5/150	1,28	Ø5/150	1,54	Ø6/150	1,80	Ø6/150	2,05	Ø7/150	2,31	Ø7/150		
		Ø5/150		Ø5/150		Ø5/150		Ø5/150		Ø5/150		Ø6/150		Ø6/150		Ø7/150		Ø7/150		
C 40/50	[a]0,80	Ø5/150	0,84	Ø5/150	0,98	Ø5/150	1,12	Ø5/150	1,40	Ø6/150	1,68	Ø6/150	1,96	Ø7/150	2,24	Ø7/150	2,52	Ø7/150		
		Ø5/150		Ø5/150		Ø5/150		Ø5/150		Ø6/150		Ø6/150		Ø7/150		Ø7/150		Ø7/150		
C 45/55	[a]0,80	Ø5/150	0,92	Ø5/150	1,07	Ø5/150	1,22	Ø5/150	1,52	Ø6/150	1,83	Ø6/150	2,13	Ø7/150	2,44	Ø7/150	2,74	Ø8/150		
		Ø5/150		Ø5/150		Ø5/150		Ø5/150		Ø6/150		Ø6/150		Ø7/150		Ø7/150		Ø8/150		
C 50/60	0,82	Ø5/150	0,99	Ø5/150	1,15	Ø5/150	1,32	Ø6/150	1,64	Ø6/150	1,97	Ø7/150	2,30	Ø7/150	2,63	Ø8/150	2,96	Ø8/150		
		Ø5/150		Ø5/150		Ø5/150		Ø6/150		Ø6/150		Ø7/150		Ø7/150		Ø8/150		Ø8/150		
C 55/67	0,84	Ø5/150	1,01	Ø5/150	1,18	Ø5/150	1,35	Ø6/150	1,68	Ø6/150	2,02	Ø7/150	2,36	Ø7/150	2,69	Ø8/150	3,03	Ø8/150		
		Ø5/150		Ø5/150		Ø5/150		Ø6/150		Ø6/150		Ø7/150		Ø7/150		Ø8/150		Ø8/150		
C 60/75	0,88	Ø5/150	1,06	Ø5/150	1,24	Ø5/150	1,41	Ø6/150	1,76	Ø6/150	2,12	Ø7/150	2,47	Ø7/150	2,82	Ø8/150	3,17	Ø8/150		
		Ø5/150		Ø5/150		Ø5/150		Ø6/150		Ø6/150		Ø7/150		Ø7/150		Ø8/150		Ø8/150		

REBAR DIAMETER [mm] / AXIAL DISTANCE [mm] $A_{s,req}$ [cm^2/m]

[a]Minimum reinforcement governed by Paragraph 11.3.3(3)

Since TCC slabs are often designed and modelled as simply supported members, they generally lack continuity. However, if reinforcement is intended to transfer horizontal forces, the concrete topping must be continuous across the height of the reinforcement bars. In such cases, the reinforcement must also be verified for tensile capacity under ultimate limit state conditions.

Reinforcement alternatives in TCC floors

Within TCC floors, alternatives to steel reinforcement meshes are mainly related to fibre reinforcement. FRC has been studied extensively as a replacement for steel reinforcement bars and a handful of research regarding TCC floors has used fibres as alternative reinforcement. The residual tensile strength after cracking, a key design parameter for FRC structures, is the mechanical property most significantly affected by fibre reinforcement. In 2009, M. di Prisco et al. showed that some fibres, low-carbon hooked-ends steel fibres, having small size and a low modulus of elasticity, could be used to reduce shrinkage cracking and to enhance fire resistance [68].

In 2002 K. Holschemacher showed that replacing the reinforcement mesh by steel fibre reinforcement (SFRC) functioned similarly to reinforcement mesh. In this study, one mixture using SFRC was chosen based on experiments to be used for the renovation of an existing timber beam ceiling in an older building in Germany. By using SFRC, the need for the concrete cover, as is required with meshes, was eliminated. Resulting in less concrete used and thus adding to sustainability. The study also includes a reference to fibre as a way to reduce emission due to production and transport [18]. A more contemporary study by S. Lecours et al. 2023 used glass fibres and fibre reinforcement to replace the standardly used reinforcement mesh. In this study, push-out tests were also used to assess the shear capacity and the failure modes of the specimens [14]. Using the fibre reinforced concrete, increased the shear capacity for each notch type and prevented shear cracks from forming, reducing scattering at failure.

In 2010 M. LeBorgne used nylon fibres and type I steel fibres in concrete timber composite specimens showing that fibre reinforcement reduces shrinkage of specimens. The specimens were tested in a 4-point bending test. The main failure modes were found to be Horizontal block shear failure, combined tension and bending failure at the inner notch, Combined tension and bending failure at mid span and Concrete buckling in compression [69].

In 2010 another study on fibre reinforcement in TCC took place, focusing on the influence of fibre reinforcement in lightweight concrete on the overall strength of TCC slabs, by H. Kieslich et al. The flexural bending and post-cracking behaviour was tested in a four-point-bending test [70].

Ongoing research in Germany focuses on harnessing the bending load-bearing capacity of the concrete slab in HBV ceilings. The study includes analytical, numerical, and experimental investigations into

the load-bearing behaviour of HBV components reinforced with textiles made from natural fibres. To evaluate which HBV panel variants meet the standards of DIN CEN/TS 19103, push-out tests are conducted to determine the load-bearing capacity and stiffness of the composite joints on panel strips. Typically, only HBV components with notches designed to ensure bonding are tested. Test specimens are being produced with impregnated textile reinforcement made from natural fibres, alongside reference specimens using conventional steel reinforcement. However, these reference specimens feature notches without additional anti-lifting devices to secure the bond. The project is expected to conclude in May 2025 [71].
It should be noted that concern was raised when reducing the concrete layer due to the elimination of concrete cover requirements when using fibre-reinforcement. It reported that an ultra-thin concrete layer led to both reduced strength and stiffness of the specimens significantly, while adhering to vibration requirements [11]. The strength and stiffness of TCC systems using reinforcement alternatives should have similar values to systems using steel meshes. Even though reduced concrete content will lead to less emissions, enough concrete should be present in the cross-section to provide stiffness and strength. Even though studies containing alternatives for reinforcement in TCC are limited and reinforcement not being the focus, it has been a focal point within reinforced concrete as structural elements

2.4. Research gaps and future directions

The literature demonstrates significant progress in understanding the structural behaviour, material choices, and environmental performance of TCC systems. Nevertheless, several gaps remain that limit both the optimisation and wider adoption of these systems.
Firstly, while fibres, FRP, and textile reinforcements have been extensively studied in conventional concrete, their application in TCC remains underexplored. The unique requirements of composite action, such as shrinkage restraint, splitting resistance around connectors, and efficient load transfer between materials, necessitate tailored reinforcement strategies rather than direct extrapolation from existing concrete research.
Secondly, despite promising alternatives such as recycled steel fibres, basalt, or natural fibres, there is a lack of systematic investigation into their long-term durability, structural performance, and compatibility with the thinner concrete layers common in TCC floors.
Thirdly, the environmental dimension, although increasingly acknowledged, is still treated as secondary to structural optimisation. Most studies emphasise strength and stiffness, while fewer integrate life-cycle assessments that account for material production, modified concrete mixes, and EOL scenarios. The absence of standardised test methods and codified design rules for alternative reinforcement further constrains the translation of these findings into practice.

Together, these gaps underscore the need for future research that integrates mechanical, environmental, and economic considerations, thereby supporting the development of more sustainable and widely applicable TCC solutions. Furthermore, this research shows the potential benefits of steel reinforcement alternatives.

3

Case study: DPG media office building

This chapter introduces the case study used to evaluate the structural and environmental performance of timber–concrete-composite (TCC) floor slabs. The case study serves as the reference design for assessing the effects of alternative reinforcement strategies examined in later chapters.

The selected case study building features a representative TCC floor configuration, making it a suitable benchmark for comparison with the alternative reinforcement methods identified in the multi-criteria analysis (MCA) presented in Chapter 4. The chapter begins with an introduction to the case study project, followed by the description of the slab geometry and material properties. It then presents the assessment of the original reinforcement design and its associated environmental footprint. The findings from this chapter establish the baseline against which the performance and sustainability of alternative reinforcement solutions are compared throughout the remainder of the thesis.

3.1. General info

The DPG Media building (Mediavaert) is an office building located on the border of Amsterdam and Duivendrecht. The building was finalised in October 2024 and has a bruto area of 44.691 m2. It is a building existing of 2 levels under ground, and 7 levels above ground, of which the top 6 are a hybrid system of steel and timber, using TCC floor systems. The stability of the system is ensured by a core and diaphragm action in the concrete part of the TCC floor slabs [72]. In figure 3.1 the final building can be seen [73].

Figure 3.1: DPG mediavaert building [73].

3.1.1. Geometrical properties

The floors in the Mediavaert building are single span TCC floor systems. The concrete and timber layer are connected by means of notches and dowels. The cross-section of one of the floor types is given in figure 3.2 [72]. A description of the various TCC components follows.

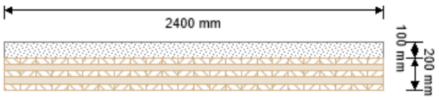

Figure 3.2: Cross-section of TCC floors used in the DPG mediavaert building [72]

Geometrical properties of a cross-section

A general cross-section of the floor is layered as follows: the bottom is a 5-layered CLT slab, with layers of 40 mm, 200 mm thick in total; on top of the CLT slab is a 100 mm reinforced concrete layer, with a mesh of 6 mm diameter, spaced every 150 mm,this mesh spans in both directions [72].

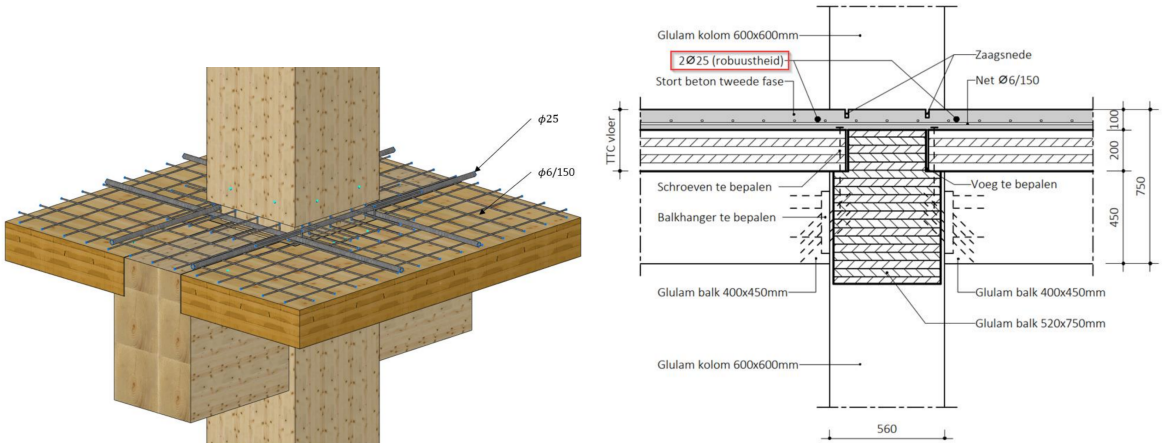

(a) 3D cross-section

(b) Cross-section showing the reinforcement used

Figure 3.3: Cross-section of the floors, with a column [72].

Along the edges of the slabs there are extra reinforcement bars present, these are for robustness of the slabs. The diameter of these is 25 mm, a cross-section with both these reinforcement bars and the reinforcement mesh can be seen in figures 3.3 [72]. At the edges there is an incision in the concrete to prevent hogging moments from developing and thus prevents tension in the concrete due to bending. This incision is taken as a maximum of 15 mm from the top of the concrete layer. This leads to an assumption of the height of the concrete layer as (100 mm - 15 mm =) 85 mm.

Spans

There are several floor spans present in the building, all referred to as a floor type, ranging from 3.00 to 8.10 meters and a width of 2.4 meters (the width of a pre-fabricated CLT panel). The governing floor in the SLS has an effective span of 7.70 meters for the timber and 8.1 for the in-situ concrete top layer. This floor type is referred to as floor type 1, located in the building as can be seen in figure 3.4 [72]. A cross-section of this floor can be seen in figure 3.5, with the total span to the middle of the supporting column being equal to 8.10 meters[72].

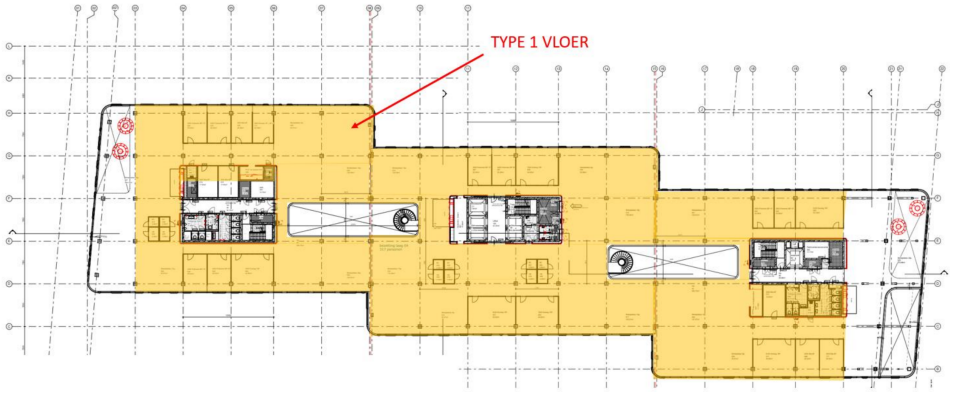

Figure 3.4: Floor plan of the floors used in the DPG mediavaert building [72].

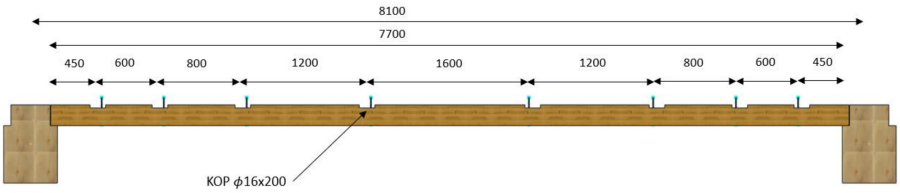

Figure 3.5: Cross-section of TCC floors, type 1 [72].

Connection

The connection between the concrete and the timber is realised by means of notches with dowels. The grooves are spaced in such a way that they are closer to each other at the locations of higher shear forces,closer to the supports. The grooves span the whole width, 30 mm high, reduce the height of the CLT slab and are 150 mm in length. The amount of dowels per groove also increases when the groove is located closer to the supports. This difference in dowels can be seen for floor type 1 in figure 3.6. In the same figure the screws (dowels) used can be seen, in all the floor types the dowels with a diameter of 16 mm and length of 200 mm are used [72].

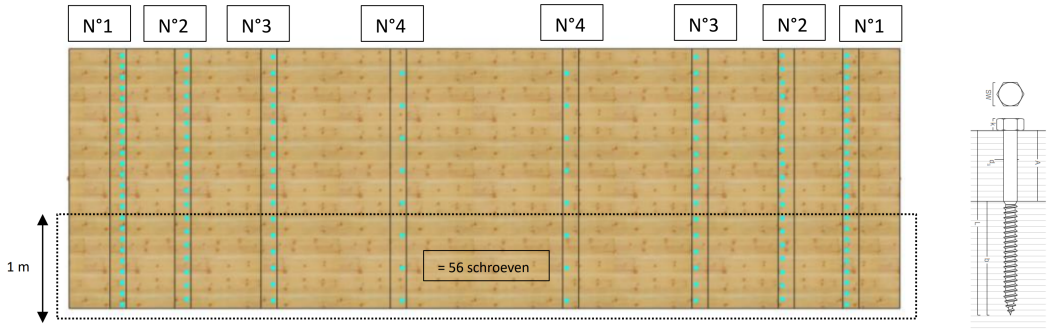

(a) Spacing of dowels

(b) Dowels used

Figure 3.6: Connection details for floor type 1 [72]

3.1.2. Material properties

The reinforcement steel components are made of B500B steel, the E-modulus of this steel type is equal to 210 GPa. The concrete top-layer is of strength class C30/37, with an E-modulus of 330 GPa. The CLT slab is made up of layers of timber of strength class C24, the E-modulus in the grain direction is equal to 120 GPa and orthogonal to the grain the E-modulus is equal to 0 GPa [72].

3.2. TCC floor design process

This section describes the concept developed to assess the influence of changing the regular reinforcement mesh for an alternative reinforcement. Firstly, the design objectives are presented. Next an overview of the checks for a TCC floor regarding the reinforcement and the concrete is given. Finally the influence that several types of alternatives might have on these checks.

3.2.1. Design objectives

The design process of TCC is different from non-composite building materials. These materials can enhance the overall performance while also negatively impacting smaller scale aspects. Thus multiple design objectives can be determined. There are large scale (system wide) objectives, namely:

- Ensuring robustness of the system
- Ensuring diaphragm action of the floors

The robustness ensures a second load path in case of a member collapsing or failing. Making sure that the system is still safe to use in that case. The second one is system wide but more localised as it mainly concerns the floor. The stability of the system is based on the stability core at the location of the staircase and elevator shafts. For the horizontal forces, in the Netherlands mainly due to wind forces and horizontal offset of the building, to be redistributed from the edge of the building, the floor needs to be able to distribute forces in the horizontal plane. This phenomenon is called diaphragm action and is ensured by incorporating tensile members in the concrete top layer. This can be realised as the concrete is cast in situ and thus one big, uninterrupted, structural element.

On a smaller scale, elements, there are two objectives:

- Ensuring comfortable usage of the structure.
- Ensuring safe usage of the structure.

The limit of comfort of usage is also known as the Usability Limit State (ULS) of a structure. For the design of a TCC system this encompasses minimising deformations of the floor slab. This is ensured by calculating the sag of a floor slab induced by the expected loads of the floor element. This resistance to this sag is determined by the stiffness of the separate materials: CLT and concrete, and the connection between the two layers. If the sag is found to be to large, an opposite sag can be introduced to the timber before pouring the concrete. This can be done if the weight of the concrete offsets this opposite sag, as the self weight of the concrete is a load on the system.

Limiting vibrations during the usage of the floor is also analysed as timber is a light material sensitive to vibrating. In floor systems using just timber as floors, this is reduced by adding a screed layer on top,a mixture similar to concrete but made of only small aggregates and cement, to add extra weight to reduce the sensitivity to vibrations. In TCC floor slabs, concrete takes the role of the screed. However, unlike screed, the concrete also increases the stiffness and contributes to the strength and behaviour of the whole floor system. Another limit in the ULS is the crack width in the concrete layer. This is partially to ensure proper behaviour of the concrete in terms of carrying loads, for aesthetics, but also to reduce the chance of harmful substances intruding into the concrete. Through cracks these substances can degrade the reinforcement within and thus reduce the performance capacity of the system on the long term.

Finally, as the structure should be safe to use, there is a Serviceability Limit State (SLS) that all materials and elements have to adhere to. The safety is ensured by comparing the expected response of the system under a specified load, the expected loads increased with set factors, to the design resistance. These are usually then compared by means of a unity check: acting load response divided by designed resistance. Resistance and loading are typically non-uniform across the cross-section. Therefore, design values are calculated over the full cross-section at critical locations along the span. The behaviour and response to the load can be put into several categories, also all checked for in the original design for the whole system:

- Normal capacity: Resistance along the element's axis, compression (negative) and tension (positive). Both must be verified.
- Shear capacity: Resistance to forces perpendicular to the element's axis.

- Bending moment resistance: Resistance to deformation due to bending moments.
- Torsional resistance: Resistance to twisting forces.
- Combined effects: These capacities can interact. Eurocode provides formulas for evaluating their combined contribution.

The checks are usually performed by computing the stresses due to each of these categories and then compare them to the design tensile and compressive capacity of the element. Usually computed for each material as each material has different capacities.

3.2.2. Design checks for reinforcement and concrete in case study

According to the calculation checks in the document provided by Arup, the checks involving the steel reinforcement are as follows [72]:

- SLS: The crack widths are indirectly checked by choosing the minimum reinforcement according to table 9.1 in Eurocode 5 [67].
- ULS: Tensile forces in the concrete slab due to wind forces.

The robustness of the system was assumed to be fulfilled by a set of secondary reinforcement bars as can be seen in figure 3.3. These bars were mentioned to be required, even in the regular design by Dutch legislation. Thus these were kept and the robustness left out of scope in the comparison between the reinforcement types. There were other checks where the concrete had an influence on the checks, depending on the alternative, the concrete characteristic values might change. This might influence the stiffness of the connection and thus a few checks.

The checks involving the concrete are as follows:

- SLS: Floor sag at different stages, the concrete's Young's Modulus influences stiffness of the slab and thus the total sag.
- SLS: Vibrations, the concrete's Young's Modulus influences the floors stiffness and thus the vibration frequency, acceleration and sag with a 1 kN equivalent load.
- ULS: Design shear resistance in the notch, stiffness of concrete is involved.
- ULS: Design shear resistance between concrete and timber in the cross-section, concrete stiffness and compressive strength.

The biggest influences will be in terms of crack width and tensile capacity when changing the reinforcement types. Thus these will be computed for the original design. To ensure a proper comparison, the same dimensions and material properties besides the concrete mix will be used, for the timber and the connection. Though it is worth noting that different floor types mainly differ in span, the cross-sectional heights stay the same, and in the amounts of dowels. In the continuation of the study, the floor type 1 with the maximum amount of dowels, under maximum loading, is considered.

3.2.3. Load cases considered

For the functionality and checks of the structure only one type of loading was considered. The case considered was wind loading perpendicular to the long side of the building (y-direction, see figure 3.7), with a representative value of 5.02 kN/m. Using the load factors and combinations on, the maximum load for which the diaphragm action was checked was found to be equal to 7.56 kN/m.

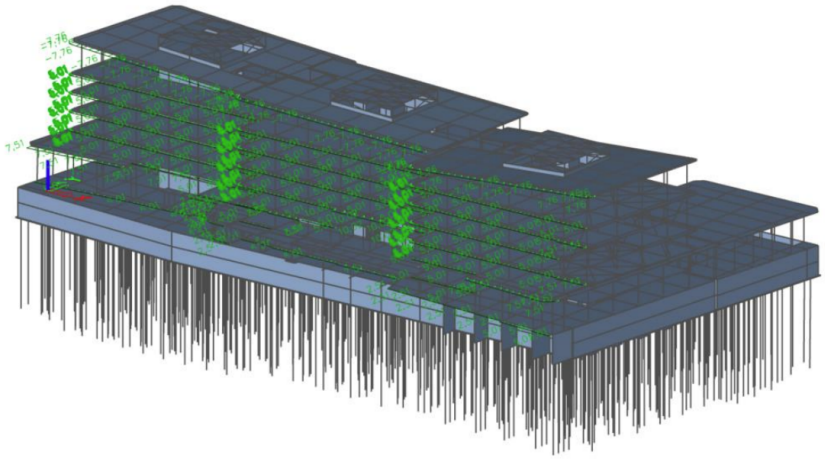

Figure 3.7: Global wind-loading on building in y-direction [72]

3.2.4. Expected behaviour under design loads

With the shrinkage and the wind load being governing in the design of the reinforcement, there are a few ways the stress distribution differs from most reinforcement designs. In most cases a linear or bi-linear stress distribution is found to be governing. However, in case of uniformly applied horizontal loads over the cross-section height, the stress distribution will also be more or less uniformly distributed over the concrete cross-section height, visualised in 3.8.

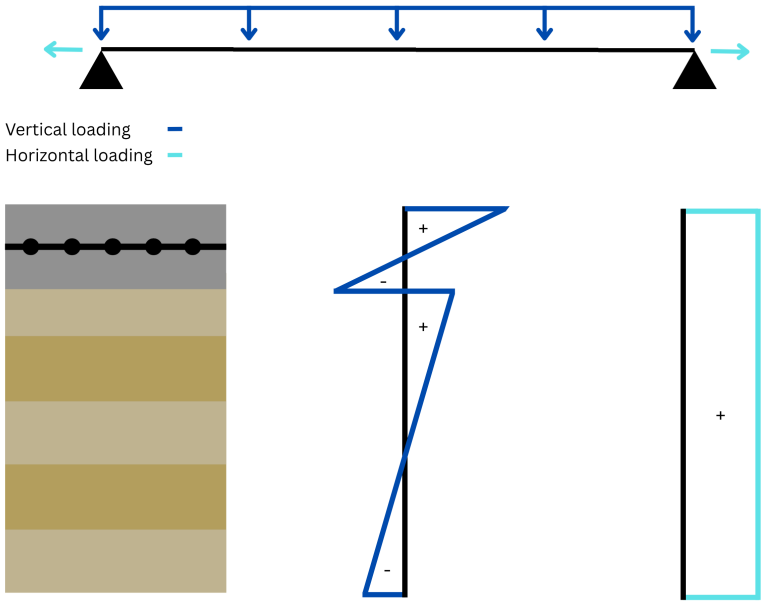

Figure 3.8: Stress distribution over cross-section height for different load cases for a TCC floor.

3.3. Change in behaviour for alternative reinforcement method

The primary focus of the reinforcement alternative is sustainability, while showing promising structural performance when it comes to replacing the standard reinforcement. In addition the alternative should be readily available for application. On top of that, the reinforcement alternative should not be too expensive. To understand the influence of changing the reinforcement on these aspects, a baseline for comparison should be clear.

3.3.1. Change in environmental impact

Some of the alternatives in chapter 2 required a change in concrete mixture. The altered concrete mix would then contain plasticizer, less aggregates and more cement. An increased cement content will not only lead to increased environmental impact, but also to increased shrinkage. This increased shrinkage should be considered when checking crack widths in the concrete.

3.3.2. Change in structural behaviour

Changing the reinforcement can have multiple possible impacts on the behaviour of the floor system.

Firstly, the concrete could change when it comes to characteristic values: tensile strength, compressive strength, E-modulus, Poisson's ratio and density, including reinforcement [52]. Depending on the alternative chosen, this could either increase or decrease.

The change in the concrete's characteristic behaviour could then influence the following: the stiffness of the connection between concrete and timber, the total stiffness of the cross-section, the creep coefficient and the dead-load due to concrete [72].

Beyond the mechanical characteristics changing, the area over which the reinforcement works also changes. In the original design the tensile stresses are distributed by the area of steel in the governing cross-section. If for example fibre reinforcement is used, the tensile stresses will be taken by the whole height of the cross-section, as the reinforcement will be distributed over this whole area. The incision to prevent hogging bending moments should then not be neglected, as this will limit the cross-sectional height over which the tensile forces can be redistributed. The cross-sectional height for the diaphragm action will then be 85 mm instead of the full 100 mm of the concrete layer.

It also worth noting that under the expected loading for which the reinforcement is verified, a more uniformly distributed reinforcement could be beneficial. Thus removing 'spikes' of high concentration as would be present in the case of steel reinforcement bars, see figure 3.8, as all of the tensile stresses need to be redistributed by small areas versus over the whole cross-section height.

3.3.3. Change in design of cross-section

As mentioned previously the height of the concrete layer is determined by a multitude of design objectives the main ones being:

- Minimising vibrations by increasing system weight.
- Minimising crack width to prevent ingression of harmful substances and for aesthetics.
- Ensuring sufficient resistance to acting loads.

The change of reinforcement will impact these objectives. For example, if another material is chosen, with less sensitivity to harmful substances the concrete cover can be reduced and the allowable crack width can be increased as it will be mainly based on aesthetics. However, a reduction of concrete depth will also lead to a decreased weight and make the slab more susceptible to vibrations and a decreased stiffness.

So in a design with less concrete height, which would be more sustainable, the vibration response and sag of the system should be checked. These checks however are left out of scope and a comparison of the same cross-sectional heights as the original design is made.

3.4. TCC floor environmental impact analysis

3.4.1. Impact of original floor design

The floor spans 7.7 meters for the timber, 8.1 meters for the reinforcement and the concrete and has a width of 2.4 meters, using the material data provided by the original calculations, the material volumes and/or weights are calculated to match the functional unit of the EPD's, as can be seen in table 3.2. The beams at the edges, over which the concrete layer continues are kept out of scope. As in further analyses, the concrete layer is kept continuously, this 'extra' bit of span is taken into account with the GWP computations of a floor slab in this section.

The CLT is calculated as a continuous slab with the total span of the floors. The notches/grooves are located as seen in 3.5 and have the same depth as mentioned, reducing the heigh of the CLT slab at the location of the grooves by 30 mm. Using this information the volume is calculated and subsequently the GWP can be seen in table 7.3.

The reinforcement in the concrete slabs can be calculated based on their diameter and spacing, which are 6 mm and 150 mm respectively. Using the density of the material together with the computation of the volume per floor slab leads to the GWP as shown in table 7.3.

The total volume of concrete is computed by assuming a 100 mm height all over the floor slab, with an increase of volume in the notches. This increase is equal to the depth times the length and width of the grooves minus the total volume of notches in the grooves.
Some materials have a set EPD, as does concrete. However, in a part of the study later in this thesis in chapter 7, the admixture of concrete and its material ratio's will be altered. To ensure a concise computation, the ratio's for a concrete mixture of class C30/37 have been used for the quantities [74]. The computation of the GWP in life cycle stages A1-A3 is then based on values from EPD's of these individual materials present in the concrete mixture. The final value of the GWP of the concrete used is then based on sum EPD's and the ratio's of materials. The computation of this can be found in table 3.1 [74–77].

The GWP of this mixture is equal to 123.77 kg CO_2 eq/m^3 of concrete. The total density of the concrete with this mix is found to be 2325 kg/ m^3, the sum of kg material per m^3 of concrete.

Table 3.1: Computation of the GWP value for life cycle stages A1-A3 for concrete class C30/37 [74–77]

Component	kg CO_2 eq/ func unit	func unit	Amount[kg]/ m^3 concrete	kg CO_2 eq/ m^3
Cement (Hoogovencement CEMIII - 42.5 N)	364.00	metric tons	330	0.364·330 = 120.12
Stone (River stone)	1.74	metric tons	1070	1.74E-3·1070 = 1.8618
River sand	2.39	metric tons	750	2.39E-3·750 = 1.79
Water	-	-	175	-
Total	368.13	metric tons	2325.00	123.77

The screws in the notches have been divided into three parts in the volume calculations: head, shaft and thread. All three part have different dimension and to calculate the total volume of one dowel, these separate parts have been calculated first.
For the total amount of screws, the number of screws per notch has been taken from the case study TCC calculation sheet. This resulted in the following amount per notch, considering a slab width of 2.40 meters:

- Notch 1 & 8: 10.0 dowels/m = 24.0 dowels
- Notch 2 & 7: 8.0 dowels/m = 19.0 dowels
- Notch 3 & 6: 6.7 dowels/m = 16.0 dowels
- Notch 4 & 5: 3.3 dowels/m = 7.0 dowels

The total amount of dowels is thus equal to 132 dowels used in a type 1 floor slab. Floor type 1 can be found in chapter 3, figure 3.4. According to the producer (Rothoblaas), one screw of the type KOP16200 weighs roughly 0.264 kg. Using this weight results in a total weight of the screws of 34.848 kg. It is worth noting that not all materials have a volume as their functional unit, thus the mass of materials is also calculated and shown in table 7.2.

Table 3.2: Material volumes from the case study

Material	Length [m]	Width [m]	Height [m]	extra notes	Volume [m^3]
Notches	0.15	2.40	0.03	Total of 8 notches over floor type 1	8.64 E-2
CLT	7.70	2.40	0.20	minus the notch volume	3.69
Concrete	8.1	2.40	0.10	plus the notch volume, minus the dowel head, plus shaft volume	2.03

Material	Diameter [m]	Length [m]	Spacing [m]	nr of elements	Volume [m^3]
Steel Reinforcement mesh (spans width)	0.006	2.40	0.15	$7.7/0.15 = 51.33 \approx 51$	3.46 E-3
Steel reinforcement mesh (spans length)	0.006	7.70	0.15	$2.4/0.15 = 16.00$	3.48 E-3
Steel Reinforcement mesh	(total)				6.94 E-3

Table 3.3: Material quantities from the case study

Material	Density [kg/m^3] [78–80]	Volume [m^3]	kg
CLT	420	3.69	1516.03
Concrete	2325	2.03	4720.68
Reinforcement steel	7850	6.94E-3	54.48
Dowels	-	-	34.848

Material	kg CO_2 eq/f.u.[5]	f.u. quantity	kg CO_2 eq/m^2
CLT carbon capture	-762	3.61 m^3	-148.84
CLT no carbon capture	54	3.61 m^3	10.55
CLT - total	-708	3.61 m^3	-138.29
Concrete - reg cem	123.77	1.92 m^3	13.60
Reinforcement steel	1372.5	54.48 kg	4.05
Dowels	6.88	34.85 kg	12.97

Table 3.4: GWP [4] per m^2 floor - case study

With an overview of the material quantities, functional unit, GWP per functional unit, the GWP for life cycle stages A1-A3 per square meter of floor slab can be found in table 3.4. The total area of a floor slab type 1 is equal to 18.48 m^2.

From table 3.4 the total GWP for one square meter of TCC floor, type 1, is equal to -120.02 kg CO_2 eq. The contribution of the separate materials to the equivalent CO_2 emissions are visualised in figure 3.9 . The inclusion of carbon capture leads to a negative overall percentage and GWP for life cycle stages A1-A3. What is interesting to note, is that when the carbon capture is excluded from the analysis, the emissions from the CLT slab would be larger than that of the reinforcement.

[4]GWP for life cycle stages A1-A3
[5]f.u. = functional unit

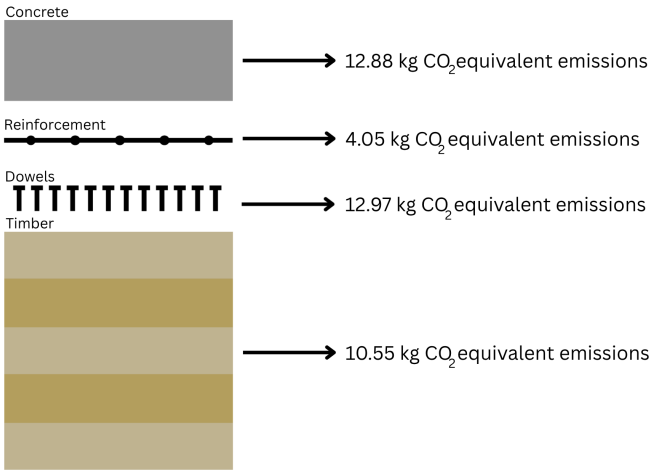

Figure 3.9: Contribution to equivalent CO_2 emissions of materials per square meter of TCC floor slab for regular cement.

What further stands out is the contribution of the reinforcement to the overall GWP value, it is the smallest out of all components whereas the contribution of the dowels is the largest and over 3 times that of the reinforcement. This stands out as the total amount of the reinforcement (in kg of material) is almost twice as large as the dowels.

Impact of changed concrete admixture

The impact of a reinforced concrete element is largely due to the cement in concrete, as is shown in the previous section. It could be of interest to minimise the influence of the cement on the total environmental impact of the total TCC floor slab to analyse the influence of changing the reinforcement in later chapters.
In this case eco$_2$cem is used as an alternative, where it can be employed replacing up to 50 % of cement to ensure a cement class of 42.5N [81]. For this reason 50 % of cement was replaced for the GWP calculations.

Table 3.5: GWP [4] per m^2 floor of the case study

Material	kg CO_2 eq/f.u.[5]	f.u. quantity	kg CO_2 eq/m^2
CLT carbon capture	-762	3.61 m^3	-148.84
CLT no carbon capture	54	3.61 m^3	10.55
CLT - total	-708	3.61 m^3	-138.29
Eco$_2$cem	69.31	2.03 m^3	7.62
Reinforcement steel	1372.5	54.48 $\cdot 10^{-3}$ kg	4.05
Dowels	6.88	34.85 kg	12.97

For the eco$_2$cem variant the total GWP for one square meter of TCC floor, type 1,is equal to -133.21 kg CO_2 eq. The contribution of the separate material is visualised in figure 3.10.

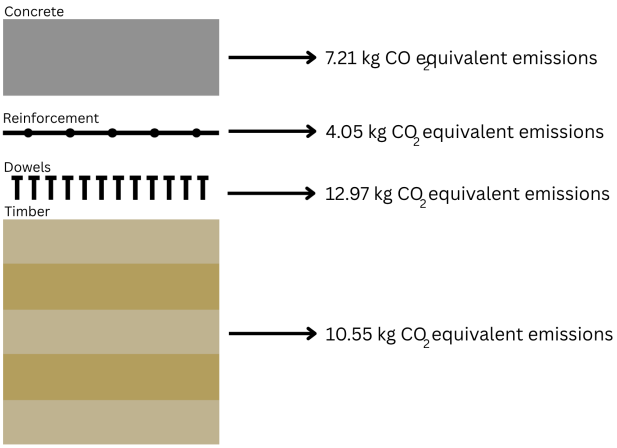

Figure 3.10: Contribution to equivalent CO_2 emissions of materials per square meter of TCC floor slab for eco$_2$cem.

Compared to the regular cement, the partial eco$_2$cem cement replacement leads to a reduction of emissions of the concrete of 44%, 5.67 kg CO_2 equivalent per square meter of TCC floor slab. This leads to a decrease of overall contribution of the concrete of 4 % and an increase of contribution of the reinforcement of 1%, when looking at the whole floor slab.

3.5. Checks for design objective

In the original design by Arup, the TCC slab was also verified. In this section the checks of the previously defined objectives are given.

3.5.1. Crack width

In the original design the crack width was not computed as it was assumed that no tensile stresses were present at the ULS in the concrete layer of the cross-section. Only a table from the Eurocode was used to determine the minimum required steel mesh. This minimum should be in line with the minimum crack width of 0.4 mm [47]. The choice for reinforcement mesh can be seen in figure 3.11. As the smaller diameter is not standard in the Netherlands, the mesh with a 6 mm diameter and 150 mm spacing was chosen in the original design.

Table 9.1 — Minimum reinforcement to control concrete cracking without crack width calculation

CONCRETE CLASS	RC DECK THICKNES [cm]																						REBAR DIAMETER [mm] / AXIAL DISTANCE [mm] A_{req} [cm^2/m]
	5		6		7		8		10		12		14		16		18						
C 12/15	[a]0,80	Ø5/150	[a]0,80	Ø5/150	[a]0,80	Ø5/150	[a]0,80	Ø5/150	[a]0,80	Ø5/150	[a]0,80	Ø5/150	0,90	Ø5/150	1,03	Ø5/150	1,16	Ø5/150					
		Ø5/150		Ø5/150		Ø5/150		Ø5/150		Ø5/150		Ø5/150		Ø5/150		Ø5/150		Ø5/150					
C 16/20	[a]0,80	Ø5/150	[a]0,80	Ø5/150	[a]0,80	Ø5/150	[a]0,80	Ø5/150	[a]0,80	Ø5/150	0,92	Ø5/150	1,07	Ø5/150	1,22	Ø5/150	1,37	Ø6/150					
		Ø5/150		Ø5/150		Ø5/150		Ø5/150		Ø5/150		Ø5/150		Ø5/150		Ø5/150		Ø6/150					
C 20/25	[a]0,80	Ø5/150	[a]0,80	Ø5/150	[a]0,80	Ø5/150	[a]0,80	Ø5/150	0,88	Ø5/150	1,06	Ø5/150	1,24	Ø5/150	1,41	Ø6/150	1,59	Ø6/150					
		Ø5/150		Ø5/150		Ø5/150		Ø5/150		Ø5/150		Ø5/150		Ø5/150		Ø6/150		Ø6/150					
C 25/30	[a]0,80	Ø5/150	[a]0,80	Ø5/150	[a]0,80	Ø5/150	0,84	Ø5/150	1,04	Ø5/150	1,25	Ø5/150	1,46	Ø6/150	1,67	Ø6/150	1,88	Ø7/150					
		Ø5/150		Ø5/150		Ø5/150		Ø5/150		Ø5/150		Ø5/150		Ø6/150		Ø6/150		Ø7/150					
C 30/37	[a]0,80	Ø5/150	[a]0,80	Ø5/150	0,82	Ø5/150	0,93	Ø5/150	1,16	Ø5/150	1,40	Ø6/150	1,63	Ø6/150	1,86	Ø6/150	2,09	Ø7/150					
		Ø5/150		Ø5/150		Ø5/150		Ø5/150		Ø5/150		Ø6/150		Ø6/150		Ø6/150		Ø7/150					
C 35/45	[a]0,80	Ø5/150	[a]0,80	Ø5/150	0,90	Ø5/150	1,03	Ø5/150	1,28	Ø5/150	1,54	Ø6/150	1,80	Ø6/150	2,05	Ø7/150	2,31	Ø7/150					
		Ø5/150		Ø5/150		Ø5/150		Ø5/150		Ø5/150		Ø6/150		Ø6/150		Ø7/150		Ø7/150					
C 40/50	[a]0,80	Ø5/150	0,84	Ø5/150	0,98	Ø5/150	1,12	Ø5/150	1,40	Ø6/150	1,68	Ø6/150	1,96	Ø7/150	2,24	Ø7/150	2,52	Ø7/150					
		Ø5/150		Ø5/150		Ø5/150		Ø5/150		Ø6/150		Ø6/150		Ø7/150		Ø7/150		Ø7/150					
C 45/55	[a]0,80	Ø5/150	0,92	Ø5/150	1,07	Ø5/150	1,22	Ø5/150	1,52	Ø6/150	1,83	Ø6/150	2,13	Ø7/150	2,44	Ø7/150	2,74	Ø8/150					
		Ø5/150		Ø5/150		Ø5/150		Ø5/150		Ø6/150		Ø6/150		Ø7/150		Ø7/150		Ø8/150					
C 50/60	0,82	Ø5/150	0,99	Ø5/150	1,15	Ø5/150	1,32	Ø6/150	1,64	Ø6/150	1,97	Ø7/150	2,30	Ø7/150	2,63	Ø8/150	2,96	Ø8/150					
		Ø5/150		Ø5/150		Ø5/150		Ø6/150		Ø6/150		Ø7/150		Ø7/150		Ø8/150		Ø8/150					
C 55/67	0,84	Ø5/150	1,01	Ø5/150	1,18	Ø5/150	1,35	Ø6/150	1,68	Ø6/150	2,02	Ø7/150	2,36	Ø7/150	2,69	Ø8/150	3,03	Ø8/150					
		Ø5/150		Ø5/150		Ø5/150		Ø6/150		Ø6/150		Ø7/150		Ø7/150		Ø8/150		Ø8/150					
C 60/75	0,88	Ø5/150	1,06	Ø5/150	1,24	Ø5/150	1,41	Ø6/150	1,76	Ø6/150	2,12	Ø7/150	2,47	Ø7/150	2,82	Ø8/150	3,17	Ø8/150					
		Ø5/150		Ø5/150		Ø5/150		Ø6/150		Ø6/150		Ø7/150		Ø7/150		Ø8/150		Ø8/150					

[a]Minimum reinforcement governed by Paragraph 11.3.3(3)

Figure 3.11: Eurocode 5 design table 9.1 for minimum reinforcement [67]

3.5.2. Diaphragm action

In the original design a SCIA model was made of the floor to model the stress distribution due to the horizontal windload. The windload was equal to 5 kN/m, which resulted in a maximum internal force in the X-direction and the Y-direction of 82 kN/m at the corners of the core. The capacity of the reinforcement mesh was also stated to be equal 82 kN/m. It was assumed to be sufficient due to the presence of the secondary reinforcement bars of 25 mm diameter. These bars were discussed in the robustness and were stated to have a capacity of 213 kN, which would be sufficient. Figures of the SCIA model results can be found in figure 3.12

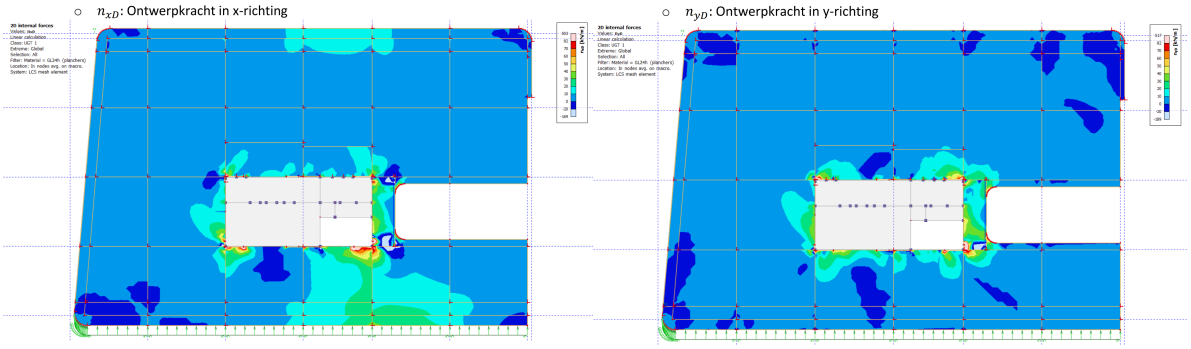

(a) Internal forces in X-direction

(b) Internal forces in Y-direction

Figure 3.12: SCIA model results for internal forces due to windloading

4

Multi Criteria Analysis (MCA) of reinforcement alternatives

In Chapter 2, several reinforcement alternatives were identified. This chapter evaluates them using a Multi-Criteria Analysis (MCA) to select the most promising option for structural modelling in Chapters 5 and 6. The alternatives are assessed against five predefined criteria, with scores assigned and weighted based on their relative importance. The scoring and weighting methodology is explained, and a sensitivity analysis is performed to test the robustness of the results. The highest-scoring alternative is then modelled, and its environmental impact is analysed at the floor slab scale in Chapter 7.

4.1. Solution Alternatives

In this chapter the different alternatives studied are different types of fibre reinforcement. A total of seven different fibre options are considered, based on the literature in section 2. The fibres have been introduced in the literature review and showed promising performance in terms of sustainability, strength and/or ductility. The fibres studied are as shown in table 4.1.

Table 4.1: Reinforcement alternatives and labels

Polypropylene (PP) Fibres	A1
Glass Fibres	A2
Carbon Fibres	A3
Basalt Fibres	A4
Natural Fibres	A5 & A6
Steel Fibres	A7
Basalt Fibre Reinforced Polymer (BFRP) bars	A8
Standard Steel Mesh	A9

In the following paragraphs they will be referred to as alternatives A1, A2, A3, A4, A5, A6, A7, A8 and A9 respectively. A1-A4 and A7 are standard industry fibres; The natural fibres considered in A5 are coconut/coir fibre; In A6 the fibres considered are hemp fibres; In A8 the BFRP rebars will be considered; And in A9 the standard steel reinforcement mesh will be considered. The choice of comparison with the original steel mesh is made to show potential benefits of replacing the steel mesh with another reinforcement type.

4.2. Main criteria and sub criteria

To enable a balanced preliminary evaluation of the proposed reinforcement alternatives, four main criteria have been defined: performance capability C_1, environmental impact C_2, buildability C_3, and

cost C_4. The full overview of the considered criteria can be found in Appendix A.

The structural performance of each alternative is reflected by the performance capability criterion, which estimates how effectively the reinforcement might perform. Practical feasibility is primarily addressed through the buildability and cost criteria.

Together, these four criteria are intended to capture both the technical performance and the contextual feasibility of each alternative within the timber-concrete composite (TCC) floor system.

From all of the sub-criteria in appendix A in Figure A.1, the selection of sub-criteria used in this research is shown in Figure 4.1.The scoring of these selected criteria can be found in 4.4. The criteria assessed in a quantitative manner can be found in the figures in grey. In the following paragraphs, the choice for and all the criteria and sub-criteria are explained in more detail. To evaluate the selected alter-

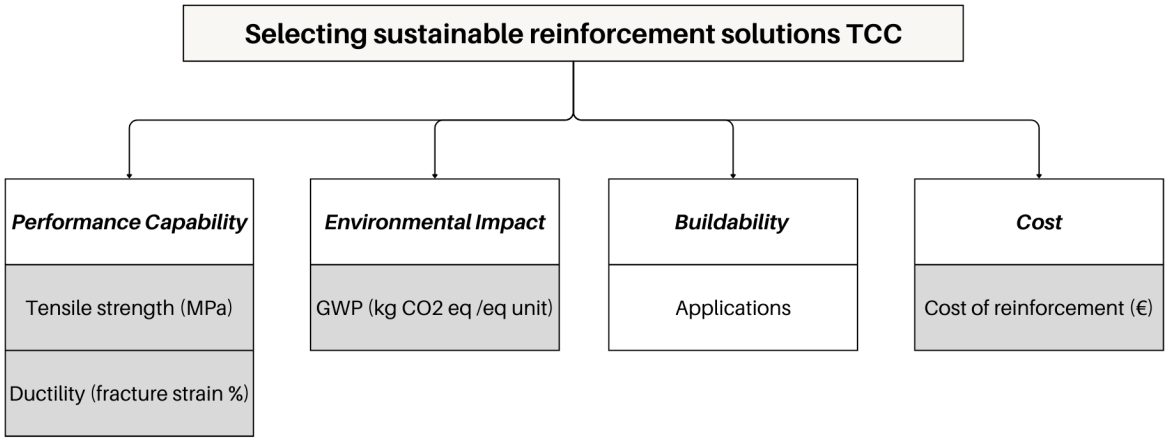

Figure 4.1: Overview of selected criteria

natives in a structured and transparent manner, each main criterion has been further specified through a set of sub-criteria. These sub-criteria capture key performance, environmental, and implementation aspects relevant to the reinforcement material within a TCC slab. Under performance capability, both tensile strength and ductility are included to reflect the mechanical behaviour of the alternative, focusing on its ability to withstand tensile forces and deform under load without failure. For the environmental impact, global warming potential (GWP) is used as a quantitative indicator of the material's carbon footprint during early life cycle stages. Lastly, under buildability, the sub-criterion applications assesses the practical feasibility of implementation by considering prior use, code availability, and the maturity of research. These sub-criteria serve to translate abstract qualities into measurable or classifiable indicators for comparison within the MCA framework.

4.2.1. Performance capability:

Performance capability evaluates the mechanical and durability properties of the alternative, including its tensile strength, stiffness, fatigue resistance, and long-term stability within the composite system. It also considers how well the alternative integrates with the TCC system to maintain composite action. Due to its direct influence on structural integrity and system reliability, this criterion weighs highly.

Performance capability - Tensile strength (quantitative) – C_{11}: One of the main functions of the reinforcement mesh is to take up the tensile forces that are present in case of wind loads acting on the building. The tensile strength of reinforced concrete is dependent on the tensile strength (yield strength) of the reinforcement. As the tensile strength of the reinforcement material influences the performance of the structure, this is chosen as an assessment sub-criterion. The alternative with the lowest tensile strength will be considered the 'worst' and the highest tensile strength will be considered the 'best'.

Performance capability - Ductility (quantitative) – C_{12}: One of the critical performance aspects of reinforcement is its ability to undergo deformation without failure, especially under loading conditions that induce cracking or large displacements. This behaviour is captured by the ductility of the reinforcement, typically expressed in terms of maximum elongation or rupture strain. Higher ductility allows the material to accommodate deformation and redistribute stresses after cracking, which contributes significantly to the structural robustness and energy absorption capacity. As such, ductility of the reinforcement material is chosen as an assessment sub-criterion under performance capability. The alternative with the lowest rupture strain will be considered the 'worst', and the alternative with the highest rupture strain will be considered the 'best'.

4.2.2. Environmental impact:

This criterion assesses the overall ecological footprint of the alternative, considering embodied carbon, energy consumption, pollution, and resource depletion across its life cycle. Sustainable sourcing, carbon sequestration potential, and low-impact processing methods are prioritized. Given the increasing focus on sustainability in construction, this factor holds substantial weight.

Environmental Impact - Global warming potential (GWP) (quantitative) – C_{21}: Measures the partial contribution of the alternative to climate change by quantifying the greenhouse gas emissions (CO_2 equivalent) associated with its production. This excludes carbon emissions from raw material extraction, energy-intensive manufacturing, and degradation over time, as a lot of the more innovative solutions lack information past the A3 stage of the life cycle. Life cycle stages A1-A3 are considered in this criterion, as seen in figure 4.2. For this sub-criterion, alternatives will be ranked based on their total GWP (kg CO_2 equivalent per functional unit). Thus from EPD's the GWP are taken as a comparative value, a lower GWP indicates a more environmentally sustainable option. Using the reinforcement ratio combined with the concrete admixture, the total GWP per m^3 of concrete will be calculated. The alternative with the highest GWP will be considered the 'worst' and the lowest GWP will be considered the 'best'.

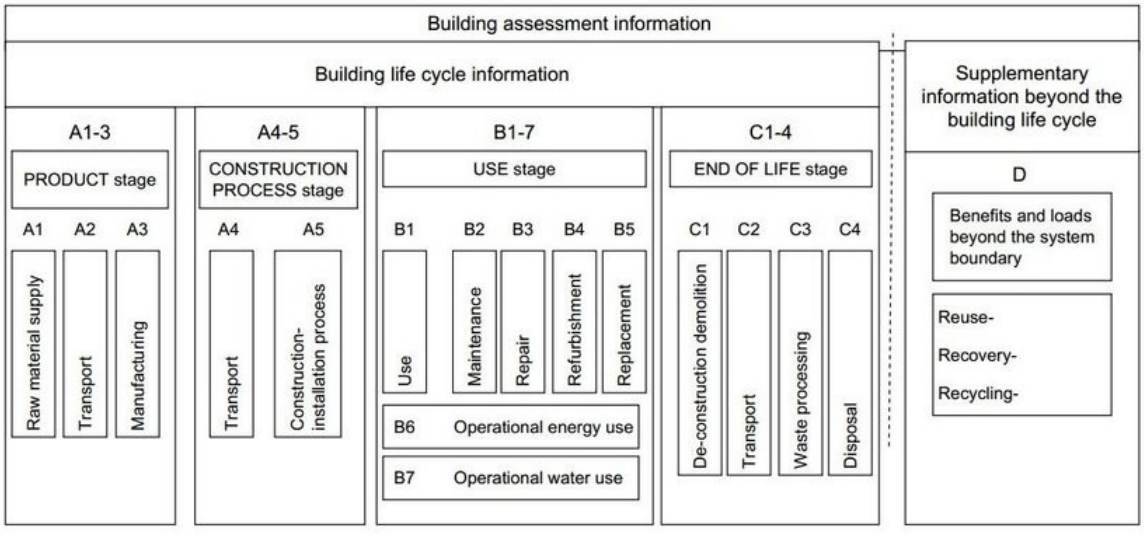

Figure 4.2: Life cycle stages [39]

4.2.3. Buildability:

Buildability reflects the practicality and ease of implementing an alternative reinforcement within a construction project. This includes factors such as the availability of the material, the complexity of its manufacturing process, and whether it has been previously applied in similar structural contexts. The presence of established design guides and standards further enhances buildability by supporting reliable and consistent application. On-site considerations, such as ease of handling, compatibility with existing construction methods, and potential impacts on equipment performance,

also play a crucial role. Alternatives that are easier to produce, specify, and install with minimal disruption to standard workflows are favoured, making buildability a key criterion in the overall assessment.

Buildability - Applications (qualitative) – C_{31}: Considers whether the material has been used a reinforcement in a project or research before and if there are design guides in place for the specific alternative. Six different categories are defined as follows:

- A) Widely applied, clear design codes in place and applied in compression zone as reinforcement before;
- B) Widely applied, specific element codes in place and applied in projects in a similar manner (compression zone to minimise crack width);
- C) Applied in concrete, different application from compression zone in (non) structural elements;
- D) Widely researched, for short term and long term behaviour;
- E) Relatively widely researched, one/two might be missing of the following: short term and long term behaviour
- F) Not widely researched.

4.2.4. Cost:

The cost criterion accounts for the total financial impact of the alternative. A cost-effective alternative must balance affordability with durability to minimize long-term expenses. Since cost efficiency is crucial for large-scale implementation, this criterion receives significant weighting.

Cost - Reinforcement material cost (quantitative) – C_{41}: Assesses the upfront expenses associated with material procurement and processing, from when the alternative would be ready to use in a concrete mixture. Lower initial costs improve the economic feasibility of an alternative. In this analysis, the cost indicated as initial cost is the initial material cost. The alternative with the highest initial material costs will be considered the 'worst' and the lowest initial material costs will be considered the 'best'.

4.3. Scoring methodology of the criteria

For the MCA a set of criteria will be drafted, these criteria will be weighted based on their importance. Then the reinforcement alternatives will be scored on a scale from 0.00-100.00. Per criterion, the 'best' alternative will get a score of 100.00 and the 'worst' will score a 0.00. The alternatives in-between these values will get a score, linearly interpolated between the 'best' and 'worst'. The weights can be chosen in various ways, especially if more than one sub-criterion is chosen to assess per main-criterion. The final score per alternative is then the sum of the total scores per criterion, which is made up of the sum of the weights multiplied by the score of that alternative in that criterion. The alternative that scores the best over the most criteria will be chosen to model in chapters 5 and 6.

4.3.1. Scoring of the criteria

The criteria that will be used to assess reinforcement alternatives in this MCA are the similar to the ones used by P.O. Akadiri et al. [82] . The criteria used in this chapter are slightly altered to fit the assessment of fibres and BFRP. The main criteria will be assigned C_1-C_5, and the sub-criteria will be assigned C_{ij} where i is the main criterion and j is the sub-criterion number. The weights are attached in a similar manner, indicated as W_{ij}. Resulting in the following formula to calculate the score per (sub-) criterion:

$$C_i = \Sigma W_{ij} \cdot C_{ij} \quad (1)$$

$$C_{tot} = \Sigma W_i \cdot C_i \quad (2)$$

4.3.2. Weights of criteria

The total scores of the alternatives will be determined by multiplying the weights per sub-criterion with score, between 0.0 and 100.0, and then take the sum of the weighted scores. In this specific research, as the main driver is sustainability, the environmental impact will be weighed as twice as important as the performance capability, whereas the performance capability is taken as four times as important as buildability and cost. The final weights per criteria are then W_1: 0.5, W_2: 1.0, W_3-W_5: 0.125. Within performance capability the sub-criteria are weighted equally, as they are both valued as being equally important to the performance capability. To not let this one criteria weigh heavier than the others, the sub-criteria get a weight of 0.5, the sum of the two sub-criteria together is equal to 1.0.
The total scores will be a result of taking the sum of the weighted scores of the sub-criteria multiplied by the weight of the main-criterion, as can be seen in formula 2 as seen in 4.3. The weight could be chosen such that:

- All sub-criteria have the same weight, no weight attached to the main-criteria
- All sub-criteria have the same weight, plus weights attached to the main-criteria.
- Different weights for sub-criteria, in such a way that all main-criteria hold the same overall weight - sum of the sub-criteria weights (of one main criterion) = 1.
- Different weights for sub-criteria and different weights for the main criteria.

In this analysis, different weights are assigned to both the main criteria and sub-criteria to account for the imbalance, one criterion includes multiple sub-criteria, while the others have only one.

4.3.3. Scoring of sub-criteria

The scores of the sub-criteria C_{11}, C_{12}, C_{21} and C_{41} are determined by means of linear interpolation. The linear interpolation for the separate sub-criteria is calculated as follows:

$$C_{ij} = (x_i - x_{min})/(x_{max} - x_{min}) \cdot 100 \quad (3)$$

Where:

- C_{ij} is equal to the score of the alternative i for a specific sub-criterion;
- x_i is equal to the value of a specific sub-criterion for the alternative i;
- x_{min} is equal to the minimum value of a specific sub-criterion;
- x_{max} is equal to the maximum value of a specific sub-criterion.

This results in a score of 0.0-100.0 for each alternative in one criterion.

For sub-criterion C_{31}, the scoring is dependent on the category it is classified as. In this sub-criterion the scores are as follows: A) 100.0; B) 75.0; C) 50.0; D) 35.0; E) 15.0; F) 0.0. Where A-F can be found in 4.2.3. For the selected sub-criteria, weights and scoring method, the scoring can be found in the following paragraphs. In appendix D a sensitivity analysis of the weighing and scoring method has been performed.

4.4. Determination of values of the alternatives

To support the multi-criteria analysis (MCA), a comprehensive inventory of relevant data has been compiled for each proposed alternative. The following sub-paragraphs present the quantitative and qualitative values used to evaluate the alternatives across all defined sub-criteria. These inputs form the basis for the final MCA scoring and comparison, ensuring a consistent and transparent assessment framework.

4.4.1. Polypropene fibres

Characteristic values:

- Tensile strength (MPa): 165-600 [83]
- E-modulus (GPa): 4.5 [83]
- Density (kg/m^3): : 900 [83]

- Rupture strain (%): 20 [83].

GWP: For PP-fibres GWP values of 2150 kg CO_2/tonne fibre (A1) and 2210 kg CO_2/tonne fibre (A2) or 4600 kg CO_2/tonne fibre (A1) and 4570 kg CO_2/tonne fibre (A2) were found [84, 85]. The highest value was used for this study as the lower value uses a negative carbon content in their packaging, resulting in a lower GWP value, it is unclear how much this skews the data, thus the higher value is chosen.

Application: One main producers of PP fibres (sika) was found to have a global application of their fibres, in this study only their projects in Europe are considered (UK, Iceland & Turkey included). Roads are defined as outdoor slabs with vehicles driving over them for simplification of classification (including harbour docks and train tracks). Tunnels, as classified, are made up of both traffic tunnels as well as mining tunnels. It is noteworthy that outside of Europe, Australia had more projects using PP fibre [86, 87]. Due to its wide application, multiple (verified) suppliers and the fact that there are no clear design guidelines are in place, this variant is put in class B for buildability. An overview of the applications can be found in table 4.2

Table 4.2: Application of PP-fibres in projects [86, 87]

Type of project	Ground floors	Walls	Roads	Tunnels
Nr. of times applied	2	1	10	6

Reinforcement material cost: For the PP fibres a cost of 5.25 €/150 grams was found through the website of the producer. This then results in a cost of 35,- €/kg [88]

Reinforcement ratio: General dosage recommendation: 0.5 – 2.2 kg/m3 [89]. An optimum dosage of fibre around 0.1–0.5% by volume of mix is recommended for concrete to obtain a proper high temperature resistance [90]. In 2015 M. Mohod showed that a fibre volume of 0.5% gave the best results in a M40 concrete mixture (40 MPa cubic compressive strength) when it comes to the flexural strength of the specimens. The fibre content of 0.5% is a content used in a multiple studies [91, 92].

4.4.2. Glass fibres

Characteristic values:

- Tensile strength (MPa): 2500 [83]
- E-modulus (GPa): 80 [83]
- Density (kg/m^3): 2700 [83]
- Rupture strain (%): 5 [83]

GWP: According to a study by PWC in 2023, a GWP of 1240 kg CO_2 equivalent / tonne glass fibres was found [93]

Application: The application of glass fibre reinforced concrete in existing projects was found to be mainly on interior objects/structures (furniture, cladding, worktops, etc.) and façade panels [94–96]. Glass fibre has not been used on a big scale in floors and other thicker concrete constructions, the main application is lightweight, thin concrete elements. The wide range of suppliers and projects do show a reliable supply chain and consistent performance, thus the fibre will be classified as type C for buildability.

Reinforcement material cost: For glass fibres, the following cost was found 45.25 €per 5 kg. This then results in 9.05 €/kg [97].

Reinforcement ratio: The glass fibre content is usually approximately between 0.1 – 1.5 % by volume depending on the application. For fibre content of 0.3 and 0.5 % this range performed better than the no fibre, by reaching a higher ultimate compressive strength after 28 days [98, 99].

4.4.3. Carbon fibres

Characteristic values:

- Tensile strength (MPa): 3000-7000 [100]
- E-modulus (GPa): 300 [83]
- Density (kg/m^3): 1700 [83]
- Rupture strain (%): 1.5 [83]

GWP: For carbon fibre the following was found for the GWP equivalent emissions, 26700 kg CO_2 eq/ tonne fibre [101].

Application: No big scale applications could be found. At present, carbon fibres are primarily used in the construction industry for structural repair and strengthening applications. While research indicates that carbon fibre-reinforced concrete (CFRC) holds significant potential, its use as a reinforcement material in concrete remains limited and is still undergoing development. In the literature, a lot of studies on carbon fibre reinforcement can be found, both long- and short-term applications. Research into carbon fibre reinforced concrete (CFRC) primarily focuses on enhancing mechanical properties, such as compressive and flexural strength, while also addressing workability challenges and economic considerations for its use in construction. Additionally, there is a strong emphasis on the need for further studies to determine optimal fibre content and to understand the variations in properties due to different fibre and concrete characteristics [102]. The wide range of research shows consistent performance, but the lack of applications indicates a lack of trust in the application, thus the fibre will be classified as type D for buildability.

Reinforcement material cost: The cost of carbon fibre was found to be in a range of 18.42 – 67.02 €per kg of fibres, the average of 42.72 €/kg fibres will be used [103].

Reinforcement ratio: A literature review from 2023 showed that research has looked into carbon fibre percentages (volumetric) of 0.0-2.0 %, with the most frequently analysed value being 0.5 %. The fibre content that resulted in the best 28 day compressive strength was 1 % , of roughly 45 - 70 MPa and flexural strength of roughly 5 - 9 MPa [104].

4.4.4. Basalt fibres

Characteristic values:

- Tensile strength (MPa): 2600- 4840 [105–108]
- E-modulus (GPa): 80-115 [105–109]
- Density (kg/m^3): 1850 - 2750 [105–109]
- Rupture strain (%): 1.2 - 5.6 $\approx$ 3.4 [106–108]

GWP: Literature shows a GWP of 398 kg CO_2 equivalent/tonne basalt fibre [110].

Application: No large scale applications. In the literature, a lot of studies on basalt fibre reinforcement can be found, both long- and short-term applications. According to Jiang et al. in 2014, most research related to basalt fibre reinforcement in concrete is focused on basalt as fibre reinforced polymer bars. Research into fibre reinforced concrete has focused on the general bending strength and flexural modulus of BFRC and cementitious materials, pre-soaking of the fibres, durability of basalt fibres, the long term performance, dynamic compressive strength, deformation, energy absorption capacity, and the effects of basalt aggregates on compressive strength at high temperatures, focusing on performance and durability characteristics. The wide range of research shows relatively consistent performance, but the lack of applications indicates a lack of supply chain and trust in the application, thus the fibre will be classified as type E for buildability [111–116].

Reinforcement material cost: For basalt fibre, a cost of 10.8 €/kg was found [117].

Reinforcement ratio: In general, basalt fibres in concrete have been studied at volumetric percentages of 0.1 -1%. For M30 (C25/30) one paper showed at 0.1% similar compressive strength to no fibres

whereas higher fibre contents resulted in worse performance. The flexural strength was found to be maximum for different fibre lengths at 0.35%. All of these values were for 28 days after casting [109]. Other research found that the compressive strength was highest in a range of 0.1 - 0.3% of fibres, this was equal to 58 MPa at 28 days after casting. Whereas the flexural strength was found to be highest at 0.2 and 0.5% of basalt fibres. The splitting tensile strength was found to be highest at 0.5% [105]. As the concrete compressive strength is decisive for this specific application, the lower range of fibres is taken to be considered [118].

4.4.5. Natural fibres - Coir

Characteristic values:

- Tensile strength (MPa): 158 [119]
- E-modulus (GPa): 4-6 [119]
- Density (kg/m^3): 1150 – 1460 $\approx$ 1300 [119].
- Rupture strain (%): 27.5 [120].

GWP: For coir a GWP of was found 367 kg CO_2 eq/ tonne of fibre [121]. It is worth noting that this is the value of pure coir, without an epoxy which will probably be needed to ensure the durability of the reinforcement. Biobased epoxy and non-biobased epoxy differ greatly when it comes to GWP values, for a more detailed analysis, one would need to figure out how much is needed per tonne fibres [122].

Application: Coir was only found for decorative uses. Research on coconut (coir) fibre reinforcement in construction primarily focuses on its mechanical properties, such as compressive and tensile strength, crack prevention, and overall structural performance. Studies also investigate the material's thermal behaviour and potential for use in fibre-reinforced polymer composites. Despite promising results, current applications are limited due to several challenges. These include reduced flowability of concrete mixes, lower tensile and impact strength compared to other fibres, and poor fibre-matrix compatibility. Additionally, concerns remain over the long-term durability of coconut fibres in harsh environments, highlighting the need for enhanced treatment methods and processing techniques. The lack of comprehensive durability data and a clearly defined optimal fibre dosage further limits its broader structural application. Continued research is needed to overcome these barriers and fully harness the sustainable potential of coconut fibre in construction [107, 123, 124]. Thus this fibre gets placed in buildability category F.

Reinforcement material cost: Without the epoxy, the following was found for coir: 23.99 €/kg [125].

Reinforcement ratio: Literature shows 1.5% increased the compressive strength slightly compared to plain concrete, the split tensile strength, modulus of rupture and shear strength were increased compared to plain concrete for 2%. The plain concrete compressive strength was roughly 21 MPa [126]. Other research showed the best performance for 5 cm long fibres present as 1% of the volumetric content. The compressive strength was roughly equal to 43 MPa. The toughness was the highest for 5 cm length, with 5% fibres, the splitting tensile strength was best for the 1%, with 7.5 cm fibres. For these two categories, the 5 cm, with 1% performed better than the plain concrete. For the modulus of rupture the fibre over 5 cm from a volumetric percentage of 3 performed better than plain concrete [127]. To be able to model the fibre, as much data must be available as possible. As the data from Ali et al. (20212) is more complete than that of Baruah et al. (2007), the latter volumetric percentage (with a focus on compressive strength) will be chosen for the volumetric percentage of the fibres [126, 127].

4.4.6. Natural fibres - Hemp

Characteristic values:

- Tensile strength (MPa): 690 or 530 – 920, average: 700 [128]
- E-modulus (GPa): 15 – 70 [128]
- Density (kg/m^3): : 1450 – 1520 [128]

- Rupture strain (%): 2.8 [128]

GWP: The GWP of hemp can be split into carbon capture and emissions of the processing. These are equal to -1.84 kg CO_2/kg hemp and 113 kg CO_2 eq/ tonne fibre, respectively. The total GWP per tonne fibre then turns out to be 1720 kg CO_2 eq/ tonne fibre [129]. It is worth noting that this is the value of pure coir, without an epoxy which will probably be needed to ensure the durability of the reinforcement. Biobased epoxy and non-biobased epoxy differ greatly when it comes to GWP values, for a more detailed analysis, one would need to figure out how much is needed per tonne fibres [122].

Application: Hemp fibres have been primarily used in the form of hempcrete, a sustainable, lightweight, non-load-bearing building material, commonly applied in interior and partition walls as well as insulation. Research on hemp fibre-reinforced concrete (HFRC) focuses on improving mechanical properties such as compressive strength, splitting tensile strength, and energy absorption capacity, alongside durability aspects like water absorption, carbonation depth, and porosity. Efforts are also directed toward optimizing mix designs and binder combinations to enhance overall performance. However, several limitations persist. These include reduced compressive strength compared to conventional reinforcements, variability in performance, and low tensile strength in unprocessed hemp. Additionally, the lack of industrial infrastructure for effectively separating hemp fibres from shives hampers consistency and scalability [130–133]. Balancing fibre content and density to achieve cost-effective yet high-performing concrete remains a challenge, requiring further development to unlock hemp's full potential in structural applications, thus the fibre is placed in category F for buildability.

Reinforcement material cost: The cost of hemp is roughly 15 €/kg of fibre [134].

Reinforcement ratio: For hemp, a study looked at fibres contents of 0.0 - 1.0 % and it was found the fibre content of 0.75% gave the best results. This gave a compressive strength of roughly 37 MPa and failed at a flexural load of roughly 4.3 MPa [135].

4.4.7. Basalt fibre reinforced polymer (BFRP)

Characteristic values:

- Tensile strength (MPa): The strength of one BFRP bar of 6 mm in diameter is 1250 MPa [136]
- E-modulus (GPa): 55 [136].
- Density (kg/m^3): 2.02 [136]
- Rupture strain (%): 2.3 [137]

GWP: The environmental impact of BFRP is roughly 2690 kg CO_2 eq/tonne BFRP; and roughly 5380 kg CO_2 eq/m^3 material [137]

Application: BFRP is a novel reinforcement type that has been used in a variety of applications. However, a lack of standardized design methods will mean more uncertainties and/or testing of specimens before it can be applied. The reinforcement alternative has proven itself as a possible steel replacement, but there are some uncertainties, there is also a wide scale of research into the behaviour of the material, so this alternative will be classified as class C [137, 138].

Reinforcement material cost: BFRP costs roughly 2.4 €/kg of material [137].

Reinforcement ratio: Research showed a total experiment ratio of 0.98 +/- 0.11 and 0.88 +/- 0.02 to result in acceptable behaviour in shear [139]. According to a technical data-sheet of a basalt fibre rebar producer, a basalt rebar of the same dimensions as a steel rebar has a maximum tensile strength that is over 2 times as large as the maximum tensile strength of a steel rebar [136]. This would equate to a safety factor larger than 2. Thus a reinforcement ratio of the same value as the steel reinforcement mesh would be adequate in this preliminary assessment.

4.4.8. Steel fibres

Characteristic values:

- Tensile strength (MPa): 2000 [140]
- E-modulus (GPa): 210 [140]
- Density (kg/m^3): 7800 [140]
- Rupture strain (%): 3.5 [83]

GWP: The fibres are made of 75-80 % of recycled steel, the equivalent CO_2 emissions are as follows: 1530 kgCO_2 eq/tonne fibre (A2) [141].

Application: The first use of steel fibre concrete (SFC) dates back to the early 20th century. Since then, significant experimentation, development of testing methods, and the creation of calculation models have taken place. The regulations available in the Netherlands also date from this period. The most well-known is the CUR Recommendation 111 'Steel fibre Concrete Industrial Floors on Piles – Dimensioning and Execution' (hereafter referred to as CUR 111). Additionally, the CUR reports C245 'Steel fibre Concrete, Knowledge and Knowledge Gaps' and C246 'Steel fibre Concrete, Inventory of Regulations' are available.
Since then, the use, knowledge, and experience with steel fibre concrete have significantly increased. However, regulations in the Netherlands have lagged behind, especially compared to neighboring countries. Notable standards include the DAfStb-Richtlinie Stahlfasernbeton (Germany), fib Model Code 2010 (international), and CNR-DT 204/2006 (Italy). The upcoming version of NEN-EN 1992-1-1 (Eurocode 2) will also include steel fibre concrete. Due to its wide application, multiple (verified) suppliers and being undermined by the fact that there are no clear design guidelines in place, this variant is put in class B for buildability [142–145].

Reinforcement material cost: According to the same supplier as the characteristic values, the costs of the steel fibres is roughly equal to 975 €/ tonne of fibre - 0.975 €/kg fibre [140].

Reinforcement ratio: In the research from Holschemacher et al. (2010), concrete with a volumetric percentage of 0.25% - 0.76 % was tested. Three different steel fibre types were tested in this research. For one of these fibres, all the percentages increased the compressive strength of the specimen, with the most increase for 0.76%, with a compressive strength of roughly 93 MPa. The tensile splitting was also found to be highest for specimen with 0.76 % steel fibres. The post-cracking behaviour was also found to be best for 0.76% steel fibres [146].

4.4.9. Steel mesh reinforcement

A detailed investigation into all the preliminary criteria has been performed and is summarised in B. In this section, are given.

- Tensile strength (MPa): 400 - 600 ≈ 500[47]
- E-modulus (GPa): 200 [47]
- Density (kg/m^3): 7800 [140]
- Rupture strain (%): 5 [136]

GWP: For A1-A3 the EPD of van Merksteijn International B.V., accessed through the MRPI database, gives the following value for the GWP per tonne of reinforcement steel mesh, 455 kg CO_2 equivalent/-tonne of rebar mesh (made out of sustainably produced steel) [147]. For another rebar mesh, made of virgin materials, the GWP is equal to 2320 kg CO_2 equivalent/tonne rebar mesh, accessed through the International EPD System library [79]. The keywords steel mesh, with Product Category – Construction Products, PCR – Being updated – Construction products (EN 15804 +A2), in the Geographical scope of Europe were used to look for reinforcement mesh EPD's [148]. For this analysis, the average of these two GWP values will be used.

Application: Concrete reinforcement is a widely used application of steel as a component in the construction industry with K. Kwon estimating a use of roughly 950 million tonnes in 2019 [48]. There are design codes in place that ensure safe design of structures using steel reinforcement, the lack of design codes for materials such as fibre reinforcement can make it difficult to apply them on a bigger

scale in projects. Reinforcement steel has been used for over a century, with the first specifications related to reinforcement steel dating back to the 1910's [44]. In the Netherlands the first guidelines for quality of steel rebar date back to 1968 and currently can be found in NEN-EN 10080 [45, 46]. The guidelines related to designing with reinforcement steel can be found in Eurocode 2 for concrete structures [47]. Because of this wide applications and design standards in place, this alternative will be categorized as class A.

Reinforcement material cost: The specific cost of reinforcement is dependent on the supplier. The supplier for the reinforcement meshes in the DPG building is unknown, data for the price reinforcement meshes has been taken from betonstaal [149]. From their website, the price per tonne of mesh is roughly equal to €900.50 (assuming more than 30 meshes were used for the whole building, 1 mesh is approximately 10 m^2 and the drawings show 1368.8 m^2 in rebar meshes) [149].

Reinforcement ratio: The volumetric reinforcement percentage has a set limit in reinforced concrete. For reinforcement bars this is equal to 0.04 Ac, which, if the concrete cross-section is considered to be 100%, results in 4% maximum of reinforcement steel, according to Eurocode 2 section 9.2.1.1 [47]. In the DPG floor type 1 the reinforcement ratio was found to be approximately 0.38%, as can be seen in Appendix C.

4.5. Analysis of alternatives

Based on the previously defined criteria and compiled data, the multi-criteria analysis (MCA) is carried out in this section. Each alternative is evaluated against the selected sub-criteria using the assigned weighting, next paragraph, and scoring system. The resulting scores are then used to compare the overall performance of the alternatives, allowing for a balanced assessment of structural capability, environmental impact, buildability, and cost within the context of a TCC floor system. In table 4.3 an overview of all the values used for the scoring can be found. A sensitivity analysis of the scoring method can be found in Appendix D.

Table 4.3: Used values for scoring

	PP-Fibre	Glass-Fibre	Carbon-Fibre	Basalt-Fibre	Coir-Fibre	Hemp-Fibre	BFRP	Steel-Fibre	Steel Mesh
Tensile strength (MPa) C_{11}	383.50	2500.00	5000.00	3720.00	158.00	700.00	1250.00	2000.00	500.00
Rupture strain (%) C_{12}	20.00	5.00	1.50	2.78	27.50	2.80	2.30	3.50	5.0
GWP- regular cement (kg CO_2 eq/m^3 of concrete) C_{21}	217.40	213.05	471.60	202.60	203.23	179.80	156.91	288.46	177.40
GWP- eco2cem (kg CO_2 eq/m^3 of concrete) C_{21}	135.22	130.85	389.56	119.76	121.52	97.89	97.55	206.55	118.05
Buildability Category C_{31}	B	C	D	E	F	F	C	B	A
Cost(€/m^3 of concrete reinforcement) C_{41}	135.45	456.30	435.74	57.13	311.87	111.38	55.68	57.04	26.86

4.5.1. The scoring of the criteria

Performance capability

Tensile strength For this sub-criterion, the tensile strength of the materials is compared to each other. The maximum value is 5000 MPa for carbon fibres and the lowest value is that of coir, with 158 MPa. In table 4.4 the values are given and the linearly interpolated scores, using formula 3, are given.

Ductility For this sub-criterion, the rupture strain/maximum strain of the materials is compared

Table 4.4: Tensile strength of alternatives [47, 83, 100, 105–108, 119, 128, 136, 140]

	PP-Fibre	Glass-Fibre	Carbon-Fibre	Basalt-Fibre	Coir-Fibre	Hemp-Fibre	BFRP	Steel-Fibre	Steel Mesh
Tensile strength (MPa)	383.5	2500	5000	3720	158	700	1250	2000	500
Score C_{11}	4.66	48.37	100	73.56	0	11.19	22.55	38.04	7.06

to each other. The maximum value is 27.5 % for coir fibres and the lowest value is that of carbon, with 1.5%. In table 4.5 the values are given and the linearly interpolated scores, using formula 3, are given.

Table 4.5: Ductility (strain) of alternatives [83, 106–108, 120, 128, 136, 137]

	PP-Fibre	Glass-Fibre	Carbon-Fibre	Basalt-Fibre	Coir-Fibre	Hemp-Fibre	BFRP	Steel-Fibre	Steel Mesh
Rupture strain/Maximum elongation (%)	20	5	1.5	2.775	27.5	2.8	2.3	3.5	5
Score C_{12}	71.15	13.46	0.0	4.9	100.00	5.00	3.08	7.69	13.46

Environmental Impact - GWP

For the GWP per alternative, the volumetric amount of reinforcement solution per m^3 is multiplied with the density of the solution to get to the amount of reinforcement in kg/m^3. This value is multiplied with the equivalent emissions per kg of reinforcement solution to get to the emission for the alternative applied in 1 m^3 of concrete. The emissions due to the concrete mixture are also taken into account, by subtracting the volume, in percentages, from the total volume multiplying this with the density of concrete and multiplying that with the emissions of the concrete mixture.
The equivalent emissions of the concrete mix differ for the fibres and the reinforcement bars, steel mesh and BFRP, because for the fibres, the large aggregates are removed, plasticizer is added and the amount of cement is increased.
Another distinction has been made to eliminate the impact of the different cement contents, thus resulting in a comparison more based on the GWP values of the reinforcements and less on the concrete (cement) of a structure. The values used for 1 m^3 regular concrete is taken as 123.77 kg CO_2 eq, for the concrete using 50 % eco$_2$cem 1 m^3 causes 69.31 kg CO_2 equivalent emissions [74–77, 150, 151]. For FRC the regular cement concrete mix results in 188.21 kg CO_2 equivalent per m^3 concrete. Whereas the 50 % eco$_2$cem concrete mix for FRC results in 105.69 kg CO_2 equivalent per m^3 concrete [74–77, 150–153]. The argumentation for the used ratios of materials in concrete, calculations of these values and an example of how the values for scoring are calculated can be found in Appendix C.
Performing the calculations as shown in Appendix C then results in the values seen in table 4.6 and 4.7 for the resultant GWP for each alternative reinforcement.

Table 4.6: GWP of alternatives - regular cement [84, 85, 93, 101, 110, 121, 129, 137, 141, 147, 148]

	PP-Fibre	Glass-Fibre	Carbon-Fibre	Basalt-Fibre	Coir-Fibre	Hemp-Fibre	BFRP	Steel-Fibre	Steel Mesh
GWP (kg CO_2 eq/m^3 of concrete)	217.4	213.05	471.60	202.60	203.23	179.80	156.91	288.46	177.40
Score C_2	80.78	82.16	0	85.640	85.28	92.72	100	58.19	93.49

Buildability - Applications

The classification of the alternatives are mentioned in section 4.3, the explanation per alternative is given in appendix B. In table 4.8 an overview of these classifications and the scores as a result are given.

Table 4.7: GWP of alternatives - eco2cem [84, 85, 93, 101, 110, 121, 129, 137, 141, 147, 148]

	PP-Fibre	Glass-Fibre	Carbon-Fibre	Basalt-Fibre	Coir-Fibre	Hemp-Fibre	BFRP	Steel-Fibre	Steel Mesh
GWP (kg CO_2 eq/m^3 of concrete)	135.22	130.85	389.56	119.76	121.52	97.89	97.55	206.55	118.05
Score C_2	87.10	88.60	0.00	92.39	91.79	99.88	100	62.67	92.98

Table 4.8: Buildability scores and classes [44–48, 86, 87, 94–96, 102, 107, 111–116, 123, 124, 130–133, 137, 138, 142–145]

	PP-Fibre	Glass-Fibre	Carbon-Fibre	Basalt-Fibre	Coir-Fibre	Hemp-Fibre	BFRP	Steel-Fibre	Steel Mesh
Buildability category	B	C	D	E	F	F	C	B	A
Score C_3	75.0	50.0	35.0	15.0	0.0	0.0	50.0	75.0	100.0

Cost - Reinforcement material cost

For the cost per alternative, the material cost for the reinforcement, per m^3 of reinforced concrete, is calculated and shown in table 4.9, an example of the calculations can be found in appendix B.

Table 4.9: Reinforcement costs [88, 97, 103, 117, 125, 134, 137, 140, 149]

	PP-Fibre	Glass-Fibre	Carbon-Fibre	Basalt-Fibre	Coir-Fibre	Hemp-Fibre	BFRP	Steel-Fibre	Steel Mesh
Cost (€/m^3 of concrete reinforcement)	135.45	456.30	435.74	57.13	311.87	111.38	55.68	57.04	26.86
Score C_4	74.71	0.0	4.79	92.95	33.63	80.32	93.29	92.97	100

4.5.2. Total scores

The total score, using the weights per main-criterion and formulas 1 and 2, are shown in table 4.10 and 4.11. From tables 4.12 and 4.13, it can be seen that for both the normal concrete and the more sustainable concrete, BFRP comes out on top, followed by either the regular reinforcement mesh or basalt fibre reinforcement.

Table 4.10: Total scores of the normal concrete mix - calculations

	w_i	w_{ij}	PP-Fibre	Glass-Fibre	Carbon-Fibre	Basalt-Fibre	Coir-Fibre	Hemp-Fibre	BFRP	Steel-Fibre	Steel Mesh
Score $C_{1j} \cdot w_{1j}$	0.5	0.5	4.66	48.37	100.00	73.56	0.0	11.19	22.55	38.04	7.06
		0.5	4.66	48.37	100.00	73.56	0.0	11.19	22.55	38.04	7.06
Score $C_2 \cdot w_2$	1.0	1.0	80.78	82.16	0.00	85.64	85.28	92.72	100	58.19	93.49
Score $C_3 \cdot w_3$	0.125	1.0	75.0	50.0	35.0	15.0	0.00	0.00	50.0	75.0	100.00
Score $C_4 \cdot w_4$	0.125	1.0	74.71	0.00	4.79	92.95	33.63	80.32	93.29	92.97	100.00

Table 4.11: Total scores of the eco_2cem concrete mix - calculations

	w_i	w_{ij}	PP-Fibre	Glass-Fibre	Carbon-Fibre	Basalt-Fibre	Coir-Fibre	Hemp-Fibre	BFRP	Steel-Fibre	Steel Mesh
Score $C_{1j} \cdot w_{1j}$	0.5	0.5	4.66	48.37	100.00	73.56	0.0	11.19	22.55	38.04	7.06
		0.5	4.66	48.37	100.00	73.56	0.0	11.19	22.55	38.04	7.06
Score $C_2 \cdot w_2$	1.0	1.0	87.10	88.60	0.00	92.39	91.79	99.88	100	62.67	92.98
Score $C_3 \cdot w_3$	0.125	1.0	75.0	50.0	35.0	15.0	0.00	0.00	50.0	75.0	100.00
Score $C_4 \cdot w_4$	0.125	1.0	74.71	0.00	4.79	92.95	33.63	80.32	93.29	92.97	100.00

Table 4.12: Total scores of the normal concrete mix

	PP-Fibre	Glass-Fibre	Carbon-Fibre	Basalt-Fibre	Coir-Fibre	Hemp-Fibre	BFRP	Steel-Fibre	Steel Mesh
Performance Capability	18.95	15.46	25.00	19.62	25.00	4.05	6.41	11.43	5.13
Environmental Impact	80.78	82.16	0.00	85.640	85.28	92.72	100	58.19	93.49
Buildability	18.75	12.50	8.75	3.75	0.00	0.00	12.50	18.75	25.00
Cost	18.68	0.00	1.20	23.24	8.40	20.08	23.24	25.00	23.32
Total score	108.84	96.14	17.47	108.79	101.93	104.66	121.95	82.80	120.89

Table 4.13: Total scores of the eco$_2$cem concrete mix

	PP-Fibre	Glass-Fibre	Carbon-Fibre	Basalt-Fibre	Coir-Fibre	Hemp-Fibre	BFRP	Steel-Fibre	Steel Mesh
Performance Capability	18.95	15.46	25.00	19.62	25.00	4.05	6.41	11.43	5.13
Environmental Impact	86.66	88.15	0.00	91.93	91.33	99.38	100	62.36	92.51
Buildability	18.75	12.50	8.75	3.75	0.00	0.00	12.50	18.75	25.00
Cost	18.68	0.00	1.20	23.24	8.40	20.08	23.24	25.00	23.32
Total score	124.2	109.86	29.97	124.88	120.48	113.34	125.16	94.63	122.48

4.5.3. Sensitivity analysis

To evaluate the robustness of the MCA, a comprehensive set of sensitivity analyses was conducted. These analyses, detailed in Appendix D, examined how variations in scoring methodology, weighting schemes, and input assumptions influenced the final outcomes. The objective was to determine whether the main conclusions drawn from the base case remained valid under alternative modelling conditions.

Several interpolation techniques were tested, including linear, logarithmic, and exponential functions. Each was applied in two variants: one transforming the raw input values and another transforming the scores directly. Although the relative rankings of some alternatives fluctuated across these methods, key options such as PP-fibres (A1) and FRP (A8) frequently emerged among the top performers. This consistency suggests that their favourable ranking is not heavily dependent on the specific interpolation technique used.

An alternative scoring method based on ordinal ranking was also explored. This approach assigned ranks to alternatives rather than scores on a continuous scale. While this resulted in a narrower spread of final scores, it still highlighted BFRP and basalt fibre as consistently high-performing options, thereby reaffirming general trends observed in the main analysis.

The effect of altering the weight distribution among criteria was also investigated. Both sub-criteria and main criteria were reweighted in various scenarios to reflect potential shifts in stakeholder priorities. Although these changes led to some reordering of alternatives, regular steel mesh and PP-fibres remained consistently strong performers. In some cases, coir and basalt fibres rose in rank, particularly under weightings that favoured environmental or economic considerations.

To further assess ranking stability, certain alternatives were removed from the analysis. In particular, high- and low-performing options such as BFRP and carbon fibre were excluded in different runs. This led to some shifts in the overall rankings but reaffirmed the relative strength of regular steel mesh and basalt fibre in both the reference cement and eco$_2$cem environments.

Lastly, the sensitivity of results to small variations in input data was tested by expanding variable ranges by ±10%. These adjustments had only a modest effect on the final rankings, demonstrating the resilience of the MCA model to minor uncertainties in the input values.

Across all sensitivity scenarios, a full ranking comparison is provided in Table D.1 in Appendix D. The results show that while individual scores may shift under different assumptions, the core findings remain robust, particularly the favourable performance of FRP, PP-fibres, and regular steel mesh. Moreover, it was observed that for most analysis methodologies, there was barely any difference in performance between the regular cement and the eco$_2$cem for both the best- and worst-scoring variant. This indicates that the choice of binder had limited impact on relative material performance in the sensitivity scenarios considered.

Figure 4.3 gives an overview of plots, representing the amount of times that variant was the worst or the best for various analyses, with the regular cement in red and the eco$_2$cem in green. Figure 4.4 gives an overview of the spread of the scores per variant for regular cement and eco$_2$cem separately.

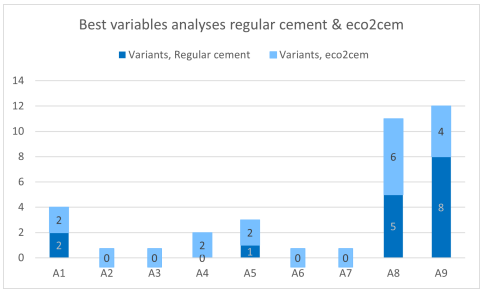

(a) Best scoring alternatives

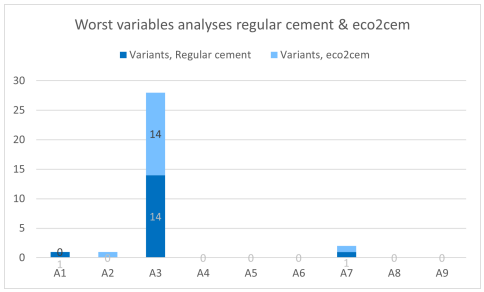

(b) Worst scoring alternatives

Figure 4.3: Scoring from different analyses, regular cement (dark blue) and eco$_2$cem (light blue)

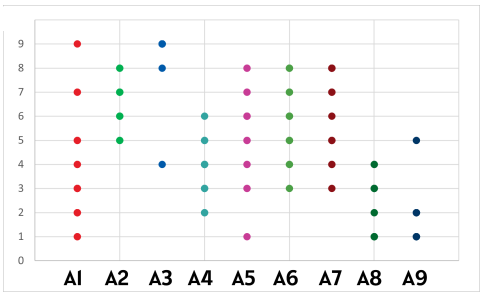

(a) Regular cement

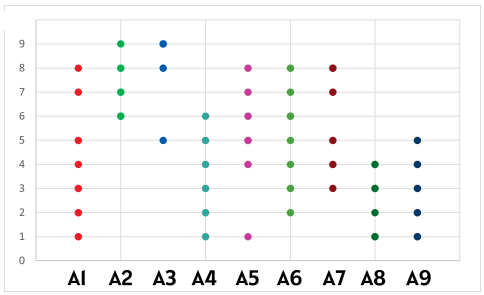

(b) Eco$_2$cem

Figure 4.4: Spread of ranking of alternatives from different analyses methods, methods can be found in appendix D

4.6. Conclusion

This chapter evaluated and compared potential reinforcement alternatives for use in a TCC system, employing a MCA framework that considered structural performance, environmental impact, buildability, and cost. The results of the MCA demonstrated sensitivity to the selected analysis method, scoring system, and weighting factors, highlighting the critical importance of transparent and well-justified parameter choices, as discussed in Appendix D.

Although the Basalt Fibre Reinforced Polymer (BFRP) alternative achieved the highest overall score, it was excluded from final consideration due to findings in Chapter 3, which indicated a uniformly distributed stress profile in the concrete cross-section. This stress distribution favors reinforcement solutions that offer uniform dispersion, making BFRP less suitable for this specific application. Its inclusion in the MCA primarily served to illustrate the potential of advanced fibre-reinforced polymer options, especially given the absence of equivalent FRP variants for other fibres in the comparison.

With BFRP excluded, loose basalt fibre emerged as the most promising candidate, offering a well-balanced performance across all evaluated criteria. Consequently, **Alternative 4 – loose basalt fibre** will be carried forward for further investigation in this study, using a reinforcement ratio of 0.5%, as it was the most frequently used fibre ratio. Thus answering the first sub-question: *"Based on the functional roles and requirements for reinforcement in TCC floor systems, which alternative reinforcement method and material is most suitable for application using a multi-criteria analysis?"*.

The next chapter will focus on assessing its structural behaviour through finite element modelling and crack width analysis and its environmental impact is analysed at the floor slab scale in Chapter 7.

5

Crack width control

This chapter examines the serviceability performance of the concrete layer in Timber-Concrete-Composite (TCC) floor slabs, with a focus on crack width control. The primary objective is to evaluate how well the reinforcement strategies developed through the multi-layered Multi-Criteria Analysis (MCA) in Chapter 4 perform when subjected to detailed serviceability checks. Crack width limits defined in Eurocode 2 serve as the benchmark for this comparison. Two complementary methods are used: a simplified analytical approach applied to the original steel-reinforced design, and a detailed numerical simulation using LS-DYNA (version 21.0). The analytical method provides a baseline estimate, while the numerical model offers deeper insight into complex behaviours not captured by simplified calculations.

By comparing these approaches, the chapter assesses the validity and limitations of the MCA-based reinforcement strategies. The numerical model is also validated against the analytical results, highlighting its potential for more accurate serviceability predictions. The analysis is limited to the concrete top layer of the TCC slab, with the timber-concrete interaction incorporated in the final simulation model. The chapter concludes with a discussion on how reinforcement choices influence serviceability, emphasizing the trade-off between analytical simplicity and numerical precision in structural design.

5.1. Shrinkage calculation

To analyse the crack width due to shrinkage, the shrinkage is first computed according to Eurocode 1, chapter 3.1 [47]. According to formula 3.8 from the Eurocode, the total shrinkage ε_{cs} deformation is equal to the relative drying shrinkage ε_{cd} plus the endogenous shrinkage ε_{ca} [47].

The relative drying shrinkage ε_{cd} can be computed using the following formula, 3.9 from the Eurocode [47].

$$\varepsilon_{cd}(t) = \beta_{ds}(t, t_s) \cdot k_h \cdot \varepsilon_{cd,0} \tag{5.1}$$

Where $\varepsilon_{cd,0}$ can be calculated using the following formula:

$$\varepsilon_{cd,0} = 0.85 \left[(220 + 110 \cdot \alpha_{ds1}) \cdot \exp\left(-\alpha_{ds2} \cdot \frac{f_{cm}}{f_{cmo}} \right) \right] \cdot 10^{-6} \cdot \beta_{RH} \tag{5.2}$$

[47]

where:

$$f_{cmo} = 10.0\,\text{MPa}$$

$$\beta_{RH} = 1.55 \left[1 - \left(\frac{RH}{RH_0} \right)^3 \right] \tag{5.3}$$

$$\alpha_{ds1} = 4.0, \quad \alpha_{ds2} = 0.12$$

$\varepsilon_{cd,0}$ is then found to be equal to 0.40 ‰. k_h can be found in Table 3.3 in Eurocode 1 and is equal to 0.85, based on h_0 [47].

Thus,

$$\varepsilon_{cd}(t) = 0.34\,\text{mm/m} \quad \text{at } t = \infty$$

The autogenous shrinkage ε_{ca} can be computed using:

$$\varepsilon_{ca}(\infty) = 2.5\,(f_{ck} - 10) \cdot 10^{-6} \tag{5.4}$$

[47]

This then results in:

$$\varepsilon_{ca} = 0.05\,\text{mm/m}.$$

The total shrinkage is then equal to: $\varepsilon_{cs} = \varepsilon_{cd} + \varepsilon_{ca} = 0.34 + 0.05 =$ **0.39 mm/m**. This value will be used for computing the stresses due to shrinkage in the rest of this thesis.

5.2. Description analytical analysis

This section outlines the analytical approach used to estimate crack widths in the TCC floor slab at the serviceability limit state. The method follows Eurocode 1 provisions for reinforced concrete, adapted to account for the specific configuration of a timber–concrete composite system. The analytical calculations serve as a benchmark for comparison with the numerical model, providing a simplified yet transparent framework for evaluating reinforcement performance. In the calculations a concrete floor slab, with the concrete dimensions of type 1, see chapter 3, is considered and analysed per meter in width. The values used in these calculations can be found in table 5.1.

Table 5.1: Values used for shrinkage calculation

$f_{ck}/f_{ck,cube}$ (MPa)	30/37
Cement class	N
E_c (GPa)	30.00
f_{cm} (MPa)	38.00
$f_{cm}(t_0)$ (MPa)	22.73
$f_{ck}(t_0)$ (MPa)	14.73
f_{ctm} (MPa)	2.90
$f_{ctm}(t_0)$ (MPa)	1.73
Time of loading t_0 (days)	3.00
Age of start drying shrinkage t_s (days)	3.00
Age of concrete at t = ∞ (days)	∞
Relative Humidity (%)	65.00
width - b - (mm)	1000.00
height - h - (mm)	100.00
Area of the cross-section of concrete A_c (m^2)	0.10
Circumference of the cross-section exposed to shrinkage - u - (cm)	100.00
h_0 fictional thickness of the cross-section (mm)	A_c / u = 200.00
concrete cover - c - (mm)	66.00
E_s (GPa)	200.00
Diameter (mm)	6.00
Spacing (mm)	150.00
A_s (per meter) (mm^2)	188.50
The distance from the top of the slab to the middle of the reinforcement - d - (mm)	66

5.2.1. Eurocode method

Under serviceability limit state (SLS) there are some maximum values to adhere to, one of them being the maximum crack width. In the Netherlands this value is equal to 0.4 mm for indoor concrete elements. For elements under bending loading there is a minimum reinforcement that can be taken from tables, where no computations are needed. These tables can be used only when there is no significant axial tension. In the design of floor type 1,see chapter 3, there is no major axial tension under SLS loading, just the tension due to shrinkage.

To compute the crack width, chapter 7 can be used from Eurocode 1 [47].

5.3. Description numerical model

The numerical analysis was carried out using a finite element (FE) model developed to simulate the cracking of the TCC floor slab. The purpose of this model was to evaluate whether reinforcement is capable of limiting crack widths caused by shrinkage strains. Without such a model, the thesis would lack a proper validation of both the original design and alternative reinforcement layouts, and would relying solely on conservative analytical calculations.

In contrast to the analytical crack width approach presented in the previous section, which represents a lowest-level, conservative approximation, the FE model allows for a more detailed investigation of crack development and stress redistribution. While analytical methods are safe but often overestimate cracking, the FE model provides higher-fidelity predictions, enabling a more nuanced understanding of slab behaviour under shrinkage strains.

This section first introduces the purpose and scope of the model, then sets out the assumptions and simplifications made. Subsequently, the modelling environment, geometry, boundary conditions, materials, and loading definitions are described. Finally, the key results are summarised and discussed in relation to the research question.

5.3.1. Purpose and scope

The main objective of the FE model is to assess the performance of reinforced slabs compared to unreinforced slabs with respect to crack formation. Specifically:

- To determine whether reinforcement is sufficient to limit crack widths caused by shrinkage strains.
- To complement the analytical calculations by providing a higher-resolution description of stress redistribution.
- To serve as a validation step for the design assumptions in the case study.

Three slab configurations were analysed: an unreinforced concrete slab, a steel mesh reinforced concrete slab and a basalt fibre reinforced concrete slab.

5.3.2. Core assumptions

To balance model complexity with computational efficiency, several key assumptions were adopted:

- **Geometry:** As the TCC top layer spans in two directions, the concrete slab is modelled as a two-way spanning slab, simply supported along all edges. As the concrete slab is continuous along both directions during the development of shrinkage, a cut out from the whole floor will be restrained by the surrounding concrete. The restriction of deformation causes tensile strains to develop.
- **Reinforcement:** The reinforcement is modelled as a composite layer with perfect bond to the concrete; mechanical properties being equivalent values of both the concrete and the reinforcement present in this layer. These equivalent values are based on the fraction of reinforcement in that layer and computed for the layer by the software.
- **Components excluded:** Timber slab and grooves were not modelled; vertical loading and time-dependent effects (creep, shrinkage evolution) were ignored. In the final model, the connection between the two layers is represented by discrete beam elements (spring elements) with properties aligning with those computed for the studied lay-out of the TCC floor slab.

- **Material:** Material Type 172 from LS-DYNA's catalogue was used, following Eurocode 2 formulations. The material law captures concrete cracking in tension, crushing in compression, and reinforcement yield, hardening and failure. The material is initially isotropic, represented with a non-rotating smeared crack approach in tension and a plasticity model in compression.

5.3.3. Implementation in LS-DYNA

Software and modelling environment

All finite element simulations in this chapter were carried out in LS-DYNA (version 21.0). The software was chosen for its ability to capture concrete cracking behaviour under imposed strains, offering robust constitutive models specifically for reinforced concrete structures. The analysis was restricted to the tensile stress response under shrinkage loading, without inclusion of creep, relaxation, or staged loading.

Geometry and layout

The model geometry is based on Floor Type 1 from the case study in Chapter 3. All slab dimensions, reinforcement layout, and cover thickness were taken directly from the case study to ensure consistency. This lead to a model of 100 mm thickness, 2.4 m wide and 8.1 m long. The mesh size used is the models is 50 mm x 50 mm, this was found to relatively realisticly represent a cracking pattern in a concrete slab.

Boundary conditions

The slab was modelled as simply supported along its short and long edges, replicating a two-way spanning system. Constraints were imposed to prevent rigid-body motion while still allowing realistic flexural deformation by restraining the nodes along the edge. To avoid stress concentrations at the corners, the nodes in the corners are thus not constrained.

In figure 5.1 the location and the boundary conditions on the slab can be seen. These are pinned in x,y and z direction.

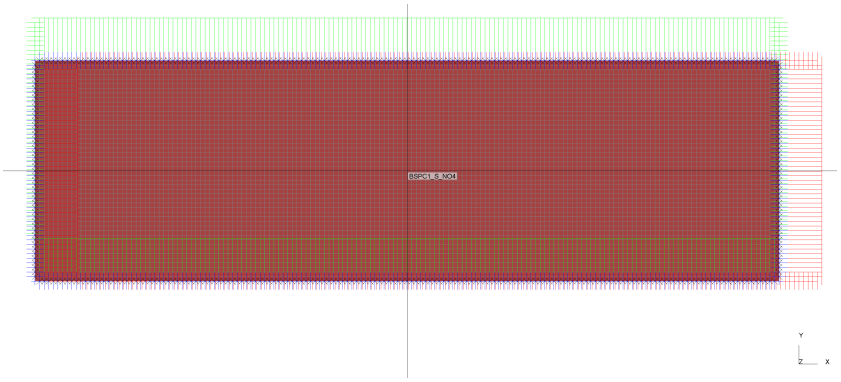

Figure 5.1: Locations of nodes for boundary conditions

Material model

The shell type used in this analysis is a fully integrated shell element to improve running time of the model. Material Type 172 from the LS-DYNA material library was used for shell and Hughes–Liu beam elements, which is the standard for discrete beams in the soft-ware. This material can represent plain concrete, reinforcing steel, or a smeared combination of both. The following key features are included:

- Concrete cracking in tension (non-rotating smeared crack model[1]).
- Concrete crushing in compression (plasticity-based).
- Reinforcement yielding, hardening, and ultimate failure.
- Thermal sensitive concrete and steel.

[1]The smeared cracking model 'smears out' the cracking strain over an element, sticking to the pre-defined mesh size. As a result, the localisation of the cracks is influenced by the material's post-peak toughness [154].

Material properties and governing equations were taken from Eurocode 2 (EC2). A simplified but accurate response was obtained by specifying the following inputs:

- For plain concrete: RO (denisty [kg/m^3]), $ET36$ (Elastic modulus [Pa]), F_C (Mean compressive strength [Pa]), F_T (Tensile strength [Pa]) and F_{CC} (actual compressive strength of concrete[Pa]).
- For reinforced concrete: $Y_{M,REINF}$ (Young's modulus of reinforcement), $SUREINF$ (ultimate stress of the steel), $FRACRX$ and $FRACRY$ (reinforcement fractions in x- and y-directions).
- For the thermally induced strain; the thermal expansion coefficient for both materials is taken as that of concrete; 10 e-6 [1/K]. Both materials have the concrete thermal expansion coefficient, as the shrinkage load is introduced as a thermal load.

The material was modelled as a composite with several layers of the mentioned material models. A visual representation of the resulting layers can be found in figure 5.2.

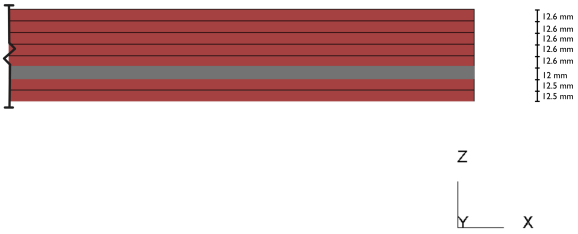

Figure 5.2: Cross-section of the model with dimensions

The slab is split up into 8 layers the top four layers are made up of concrete in each model, with a thickness of 0.0126 m, the fifth layer is the reinforcement layer in the models in which reinforcement is present and is made up of one layer of spread out reinforcement (reinforcement ratio of 0.0157 in both x and y direction), with a thickness of 0.012 m. Finally, the bottom is split up into two layers of 0.0125 m out of concrete for each model.

For the fibre reinforcement the following values were used, with the f_{ck} being derived from the Eurocode as f_{ck} = f_{cm} -8 MPa [47]. According to one piece of research the following inputs for the models are found [155] and can be seen in table 5.2

Table 5.2: Mechanical properties used for modelling of fibre reinforcement

Reinforcement Ratio (% of volume)	0.5
Fibre length (mm)	12
Compressive strength (MPa)	68
Tensile strength (MPa)	3.35
Flexural strength (MPa)	5.75
E-modulus (GPa)	44.5

The rupture strain and Poisson's ratio was taken the same as unreinforced concrete, even though sources mention an increase in strain, they did not mention the value or rate of increased strain.

Mesh size and elements

Shell elements were used for the concrete layer, and the reinforcement bars. A uniform mesh of 50×50 mm was applied across the slab. This provides consistent resolution of shrinkage-induced stresses while keeping the computational time manageable.

The connection between the concrete layer was represented by implementing discrete beams along the axis of the notches. The discrete beams are spring elements with a linear spring stiffness. These values were found in the documentation of the original design as $K_{ser,x}$ = 150000 N/mm and $K_{ser,y}$ = 1 N/mm, and used in the design.

Loading
Shrinkage was modelled through a thermal analogy. An imposed temperature drop ΔT was applied such that the resulting thermal contraction equal to the shrinkage strain:

$$\Delta T = \frac{\varepsilon}{\alpha} \tag{5.5}$$

where α is the thermal expansion coefficient of concrete ($1 \cdot 10^{-5}$ °C^{-1}). This method enabled shrinkage strains to be applied consistently across the slab without explicitly modelling time-dependent evolution. The load is slowly increased, as LS-Dyna is a dynamic modelling software, to prevent sudden spikes in stresses and unexpected behaviour. Additionally, damping was introduced to minimize excessive dynamic responses, complementing the incremental loading strategy.

5.4. Analytical analysis Calculations

This section presents the step-by-step analytical calculations for estimating crack widths. The procedure includes the determination of tensile stresses, reinforcement strain, and crack spacing, following Eurocode 2 guidelines. The calculations provide a baseline for evaluating the adequacy of reinforcement in controlling crack development under service loads. According to Eurocode 1, chapter 7.3.4, the formula for the total crack width is as follows:

$$w_k = s_{r,\max}(\varepsilon_{sm} - \varepsilon_{cm}) \tag{5.6}$$

where:

$s_{r,\mathbf{max}}$ maximum crack spacing;

ε_{sm} average strain in the reinforcement under the applied loading, including the effect of prescribed deformation and accounting for tension stiffening. Only strain relative to the zero strain of the concrete at the same level is considered;

ε_{cm} average concrete strain between cracks.

The difference $\varepsilon_{sm} - \varepsilon_{cm}$ can be computed as:

$$\varepsilon_{sm} - \varepsilon_{cm} = \frac{\sigma_s - k_t \frac{f_{ct,eff}}{\rho_{p,eff}}(1 + \alpha_e \rho_{p,eff})}{E_s} \quad \geq \quad 0.6\,\frac{\sigma_s}{E_s} \tag{5.7}$$

where:

σ_s tensile stress in the reinforcement, assuming the cracked cross-section:

$$\sigma_s = \frac{M}{A_s \cdot z}$$

Where:

- M is the moment causing tension in the reinforcement;
- and z is the lever-arm of the moment.
- and x is the height of the concrete compressive zone

$$z = d - x$$

α_e ratio of steel to concrete modulus:

$$\alpha_e = \frac{E_s}{E_{cm}} \tag{5.8}$$

$\rho_{p,\text{eff}}$ effective reinforcement ratio, defined as

$$\rho_{p,\text{eff}} = \frac{A_s}{A_{c,\text{eff}}}$$

with effective height under tension $A_{c,\text{eff}}$, using b and $h_{c,\text{eff}}$ where

$$h_{c,\text{eff}} = \min\left(2.5(h-d),\ \frac{h-x}{3},\ \frac{h}{2}\right) \tag{5.9}$$

k_t factor depending on load duration:

- short term: $k_t = 0.6$,
- long term: $k_t = 0.4$.

k_t factor depending on load duration:

- short term: $k_t = 0.6$,
- long term: $k_t = 0.4$.

$s_{r,max}$, the maximum spacing between cracks, using the concrete cover c, can be calculated as follows:

$$s_{r,\text{max}} = k_3 c + \frac{k_1 k_2 k_4\, \phi}{\rho_{p,\text{eff}}} \tag{5.10}$$

For the calculation of the height of the concrete compressive zone, formula 4.37 from *Concrete Structures under Imposed Thermal and Shrinkage Deformations: Theory and Practice* (2011) is used [156]. The formula is:

$$x = d \cdot \left[-\alpha_e \rho_1 \alpha_{ts} + \sqrt{\left(\alpha_e \rho_1 \alpha_{ts}\right)^2 + 2\alpha_e \rho_1 \alpha_{ts}}\right] \tag{5.11}$$

In the crack it holds:

$$\alpha_{ts} = 1, \quad \alpha_e = \frac{E_s}{E_c} = \frac{200 \cdot 10^3}{30 \cdot 10^3} \approx 7, \quad d \approx 66\,\text{mm}, \quad \rho_l = \frac{A_s}{bl} = 0.00188 \tag{5.12}$$

This then results in:

$$x = 9.67\,\text{mm}, \quad h_{c,eff} = 30.11\,\text{mm}, \quad A_{c,eff} = 30111.13\,\text{mm}^2, \quad \rho_{p,\text{eff}} = 0.0063, \quad z = 68.48\,\text{mm}.$$

Using the following formulas, the tensile stress in the reinforcement at cracking can be computed [156].
The formula for the flexural tensile strength $f_{ctm,fl}$ is:

$$f_{ctm,fl} = (1.6 - h)\, f_{ctm} \ > \ f_{ctm} \tag{5.13}$$

The formula for the cracking moment M_{cr} is:

$$M_{cr} = W \cdot f_{ctm,fl} = \frac{bh^2}{6} f_{ctm,fl} \tag{5.14}$$

The formula for the steel stress directly after cracking is:

$$\sigma_{s,cr} = \frac{M_{cr}}{A_s\left(d - \frac{x}{3}\right)} \tag{5.15}$$

The flexural tensile strength is found to be equal to 4.35 MPa and the cracking moment is equal to 7.25 kNm/m.

In the case of shrinkage, the resulting stresses can be calculated as follows:

$$\sigma_{s,cs} = \varepsilon_{cs} \cdot E_s \tag{5.16}$$

Table 5.3: Tensile stresses and the crack width according to Eurocode 1

	σ_s [MPa]	$\varepsilon_{sm} - \varepsilon_{cm}$ [mm/mm]	$s_{r,max}$ [mm]	w_k[mm]
Cracking moment induced cracking scenario	561.62	0.00303	377.14	1.14
Shrinkage induced cracking scenario	78	0.000361	536.91	0.19

Table 5.3 shows that the crack width under the shrinkage strain is smaller than the crack width under the cracking moment. With the crack width under the shrinkage induced stresses being equal to 0.19 mm. This would fulfill the requirements under the Eurocode requirements in the SLS ($\leq$ 0.4 mm).
With ε_{cs} = 0.39 mm/m ε_{ct} = 0.12 mm/m, the strain due to shrinkage is larger than the maximum tensile strain what the concrete can withstand. But the crack width of the shrinkage is smaller than that of the cracking moment. This leads to the conclusion that the concrete undergoing shrinkage strain is in the crack formation stage.

5.5. Results

The results section compares the outcomes of both approaches, providing insight into the advantages and limitations of each. The findings are structured into two subsections:

5.5.1. Analytical approach

As mentioned previously. The strain due to shrinkage of concrete is found to be equal to 0.39 mm/m which then results in a crack width of 0.19 mm and a crack spacing of 536.91 mm.
The concrete slab is found to be in the crack formation stage when analysed under shrinkage loading. The maximum allowed crack width according to the Eurocode is 0.4 mm for indoors SLS-loading conditions [47]. A unity check for the crack width according to the numerical approach would then be 0.48 < 1.0, thus the steel reinforcement mesh is determined to be sufficient.

5.5.2. Numerical approach

The numerical simulation outcomes are presented, including visualisations of crack development and stress distributions. In Appendix E the model results used to validate the final models and the development of the crack widths can be found. The program can compute the strain due to cracking of the concrete, by multiplying the strain the element width (50 mm). The crack widths need to be compared to a maximum crack width. The maximum crack width according to the Eurocode would be 0.4 mm, however literature suggests an allowable crack width for non-corrosion susceptive material to be 0.7 mm for indoors applications [157].

Unreinforced concrete slab

The unreinforced slab shows better behaviour in terms of limiting the crack width for the model with discrete beams, though the difference is very small.

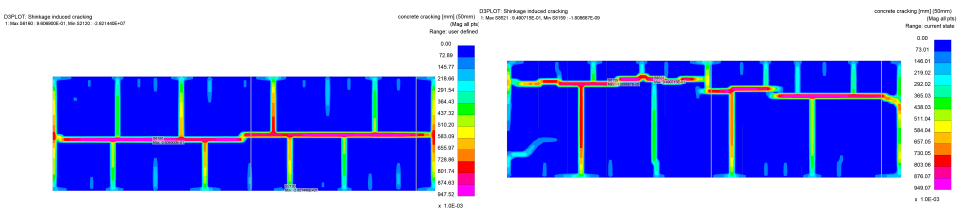

(a) Shrinkage cracks at t=8.0, model without beams **(b)** Shrinkage cracks at t=8.0, model with beams

Figure 5.3: Resultants from LS-Dyna for model without reinforcement

Steel mesh reinforced concrete slab

The resulting shrinkage cracks for time t = 8 seconds are shown in figure 5.4. It can be seen that the cracks are more spread out over the slab and that the cracking width is smaller for the model version with discrete beams. However, the value is bigger than computed using hand calculations.

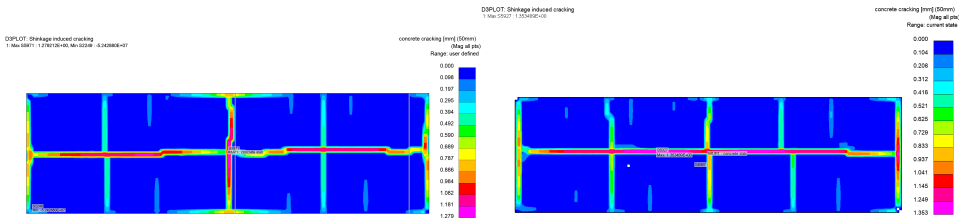

(a) Shrinkage cracks at t=8.0, model without beams **(b)** Shrinkage cracks at t=8.0, model with beams

Figure 5.4: Resultants from LS-Dyna for model with reinforcement

Basalt fibre reinforced concrete slab

As can be seen in figure 5.5, the model with the beams perform better in terms of limiting the crack width of the slab.

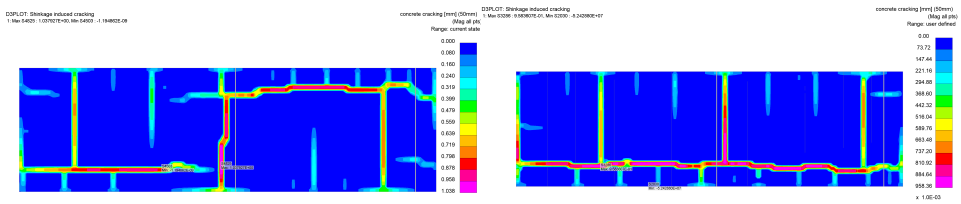

(a) Shrinkage cracks at t=8.0, model without beams **(b)** Shrinkage cracks at t=8.0, model with beams

Figure 5.5: Resultants from LS-Dyna for model with basalt reinforcement

5.6. Conclusion

The computed shrinkage according to the Eurocode, used throughout this chapter, was found to be equal to 0.39 mm/m. The analytical approach, using formulas from the Eurocode showed a maximum crack width of 0.19 mm. The models, under the same applied load also showed cracking. The smallest crack width for this model, including the connection of the concrete to the timber slab was for the non-reinforced model. The crack width for basalt concrete was larger than for the model without reinforcement. Finally, the largest crack width was found to be for the model with steel mesh reinforcement. The values can be found in table 5.4.

Table 5.4: Resultant crack widths for the different models

	No reinforcement	Steel mesh reinforcement	Basalt fibre reinforcement
Crack width [mm], without beams	0.96	1.28	1.04
Crack width [mm], including beams	0.95	1.35	0.96

Both the steel mesh and basalt fibre reinforced models exhibited larger crack widths than the non-reinforced model. This outcome can largely be attributed to the way reinforcement was incorporated into the numerical model. For the steel reinforcement mesh, the reinforcement was modelled using equivalent mechanical properties based on the reinforcement ratio, rather than as discrete bars. In reality, steel bars are distributed throughout the concrete and directly take over tensile stresses once cracking begins. This redistribution reduces crack widths and influences how cracks initiate and propagate. The simplified modelling approach, which does not capture this discrete interaction, likely overestimates crack widths. This is further supported by the significant discrepancy between the analytical and numerical results.

Similarly, the basalt fibre reinforcement model showed relatively large crack widths, which may be due to the post-cracking behaviour of fibre-reinforced concrete. While fibres can enhance the tensile strength of concrete, they also lead to higher tensile stresses at the moment of cracking. These stresses must be immediately carried by the fibres, potentially resulting in wider cracks. Moreover, the model treated the concrete slab as a continuous, homogeneous material, whereas in reality, the discrete nature of fibres plays a crucial role in early crack development.

Therefore, the large crack widths observed in both reinforced models do not necessarily indicate that steel mesh or basalt fibres are ineffective in controlling shrinkage-induced cracking. Rather, they highlight limitations in the current modelling approach, which may not accurately capture the complex behaviour of reinforced concrete under shrinkage. As the model uses a smeared cracking model, in which crack width is heavily dependent on mesh-size. Which be critical for localisation of cracks and development.

When comparing the results of the models and assuming that in the original design the reinforcement is sufficient, a smaller crack width with the fibre reinforced model than the regular reinforced model can be assumed. Thus the fibre alternative is deemed sufficient. But before applying in a real life scenario, doing a physical test to confirm the shrinkage behaviour is advised. Thus concluding the answer for the first part of the 'mechanical performance' element of the second sub-question: *"How does the most suitable alternative reinforcement method and material compare to an existing case study design based on their individual mechanical and environmental performances?"*.

The second step of the comparison of the mechanical performance is preformed in the next chapter by analysing the diaphragm action of the concrete layer in a TCC floor system.

6

Diaphragm action of the TCC floor system

This chapter investigates the ultimate strength and structural safety of the Timber-Concrete-Composite (TCC) floor slab under extreme wind loading conditions, with the primary aim of validating the multi-layered Multi-Criteria Analysis (MCA) developed in Chapter 4. By comparing the MCA-derived reinforcement alternative to the conventional steel mesh, the chapter tests whether the MCA method can reliably guide reinforcement design under ultimate limit state conditions. Using consistent slab geometry and loading configurations, both reinforcement strategies are modelled and analysed for their stress distribution and tensile capacity.

The analysis is conducted through parametric modelling in Rhinoceros 3D and Grasshopper, with structural simulations performed in GSA Oasys (version 10.2). This side-by-side comparison provides a detailed-level verification of the MCA method, highlighting its strengths and limitations when applied to real-world structural safety scenarios. The chapter ultimately assesses how well the MCA-informed reinforcement performs under extreme loading, offering insights into its practical applicability and the trade-offs between design innovation and structural reliability.

6.1. GSA model for a TCC floor systems

A numerical analysis was carried out using a finite element (FE) model to simulate the stress distribution of different reinforcement materials under the same horizontal wind load. This section introduces the modelling software and assumptions on which the models are based.

6.1.1. Purpose and scope

The main purpose of the models is to check if the capacity of the reinforcement is sufficient for the applied wind loading. Specifically:

- To determine the stress distribution in different reinforcement material scenarios.
- To serve as a validation step for the design and multi criteria analysis assumptions.

Two different reinforcements were included in this analysis, the originally designed reinforcement mesh and basalt fibre reinforcement. The only difference between these models is the stiffness of the concrete layer. The tensile stresses are then compared between the different reinforcement materials maximum tensile capacity.

6.1.2. Core assumptions

The model is constructed to balance the complexity with the computational efficiency, to achieve this, several key assumptions were adopted:

- Mesh size of 150 mm x 150 mm

- For the analysis, conform the original design, the concrete layer of the TCC ensures diaphragm action (the timber part of the floor is left out of consideration).
- The only force action upon the floor slab is a horizontal wind force with a value of 5.01 kN/m along the floor edge.
- Different parts of the building are completely disconnected.
- The concrete stability core walls are connected in a fixed manner.
- All beams and columns are connected in a pinned manner (not moment resistant).

6.1.3. Implementation in GSA and Rhino

Software and modelling environment

All finite element simulations in this chapter were carried out in GSA Oasys (version 10.2). Rhinoceros 3D (version 8) was used to generate the slab geometry, while Grasshopper served as the parametric interface to efficiently transfer the model into GSA. Within GSA, the analysis was performed to evaluate the stress distribution in both the longitudinal (x) and transverse (y) directions under horizontal wind loading.

Elements and layout

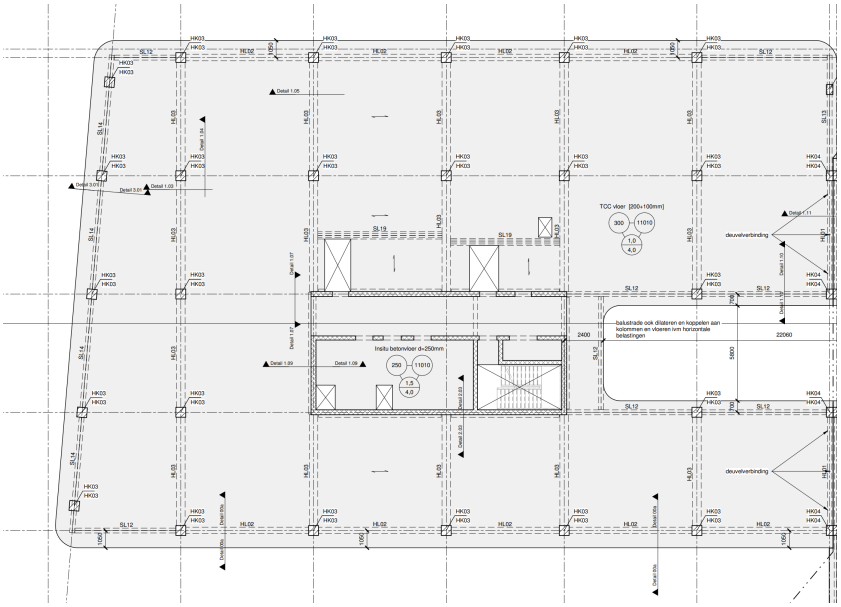

Figure 6.1: Floor plan with beam annotations

The model uses several elements, the beam labels can be found in fig 6.1 the dimensions are noted in table 6.1. The values for the stiffness stem from documents of the original project, used in the model for the stability core. The steel used for the beams was S355 and timber class used was C24.

Table 6.1: Values mechanical properties and dimensions used for the GSA model

Element	E-Modulus (GPa)	Dimensions
Floorslab normal reinforcement	31.25	h = 100 mm
Floorslab normal reinforcement	43	h = 100 mm [155]
Concrete core inside walls	3.8	t = 250 mm
Concrete core outside walls	10	t = 300
Concrete core inside beams	3.28	t = 250 mm
Concrete core outside beams	10	t = 250 mm
Concrete core floor slab	0.001	h = 250 mm
SL12	210	HEA 360A
SL13	210	HEA340A
SL14	210	HEA320A
SL19	210	HE240B + 440 x 15
HL01	13	260 x 750
HL02	13	400 x 450
HL03	13	520 x 750

A visual of the rhino model is shown in figure F.4. Figures of the seperate elements can be found in appendix F.

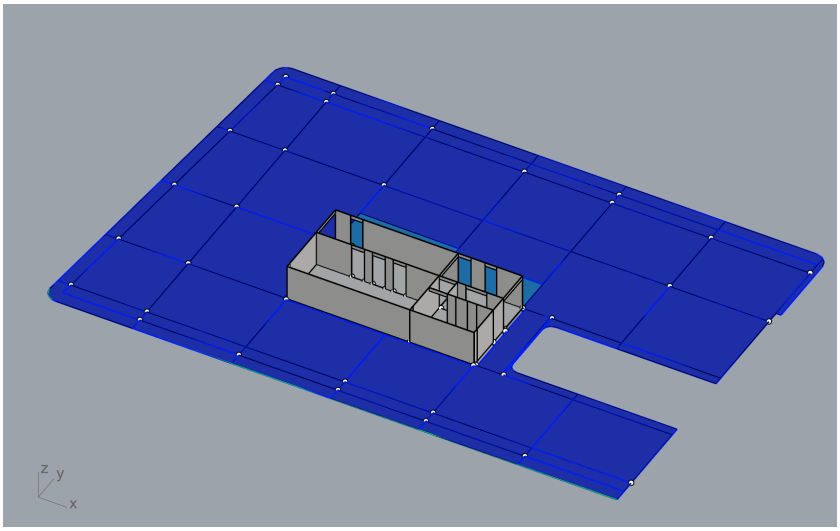

Figure 6.2: Showcasing the rhino model of the floor slab studied in this chapter

All materials are modelled linear elastically. The model is split up in the beams, the floors and the core. In this modelling software, when having adjacent elements are assumed to have perfect bonding. It could be argued that this is not the case and a more detailed model would be needed to analyse the influence of the connections on the stress distribution. This limiting factor needs to be taken into account when analysing the different modelling methods.

Boundary conditions

The slab will not be loaded vertically and no weight will be added to the slab, accordingly no supports in the z-direction were placed at the location of the columns.

As the floor redirects the forces to the stability core, the floor will be fixed at the base and top of the core. A figure of the core in the model and its restraints can be found in Appendix 6.1. The floor slabs and the beams are pinned to the core, allowing for rotation.

Loading
The horizontal wind loading used in the case study is equal 5.01 kN/m (without load factor). The value for the horizontal wind force used in the analysis is equal to 7.56 kN/m (with load factor).

6.2. Model analysis Results

The original design was checked for tensile stresses in both the x- and y-direction. For this analysis, first the stress due to the ULS windloading are computed and then checked against the tensile capacity of the reinforcement materials.

The SCIA model, shown in chapter 3, shows a maximum internal tensile force of 82 kN/m. This value is used as a secondary validation of the capacity under ULS loading of the reinforcement methods.

6.2.1. Regular reinforcement

Figure 6.3 shows the 2D plots of the resultant internal forces due to ULS wind loading. The partial factor for computing the unity check when assessing a steel member is equal to 1.15. Using the following formula from the Eurocode, the maximum design tensile strength is then:

$$\sigma_{std} = \frac{\sigma_{st}}{\gamma_s} = \frac{500}{1.15} = 435\text{MPa} \tag{6.1}$$

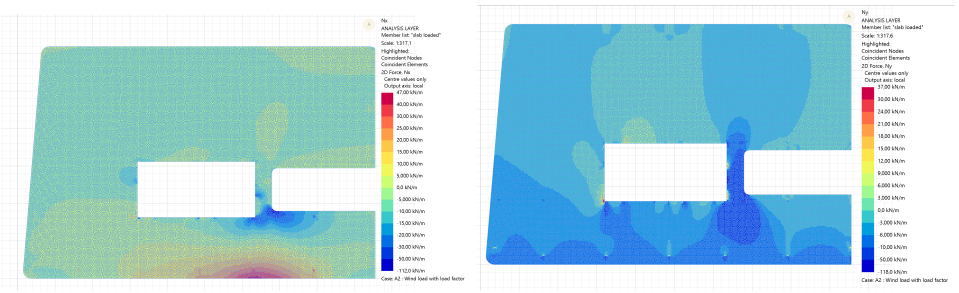

(a) Nx(kN/m) **(b)** Ny(kN/m)

Figure 6.3: Showcasing the resultant internal forces from the GSA model

The maximum internal tensile force is equal to 44.73 kN/m. The reinforcement mesh, with a design tensile capacity of 435 MPa and a total area of reinforcement of 188.5 mm^2, the total design tensile capacity of the reinforcement mesh is found to be equal to 82.00 kN/m. This results in a unity check of 44.73/82.00 = 0.55 < 1.0. Thus the tensile capacity of the reinforcement mesh is not reached.

For the original maximum internal tensile force of 82 kN/m a unity check of exactly 1.0 can be found. A unity check of exactly 1.0 is usually not deemed sufficient, which is solved by adding the capacity of the secondary steel bars for stability to the steel area sued in the verification. This method would result in a unity check way less than 1.0.

6.2.2. Alternative reinforcement

Figure 6.4 shows the 2D plots of the resultants internal forces due to ULS wind loading. According to the fib, the partial factor for fibre reinforced concretes is equal to 1.5 [158]. The design tensile strength is then:

$$f_{ctd} = \frac{f_{ck}}{\gamma_F} = \frac{3.35}{1.5} = 2.23\text{MPa} \tag{6.2}$$

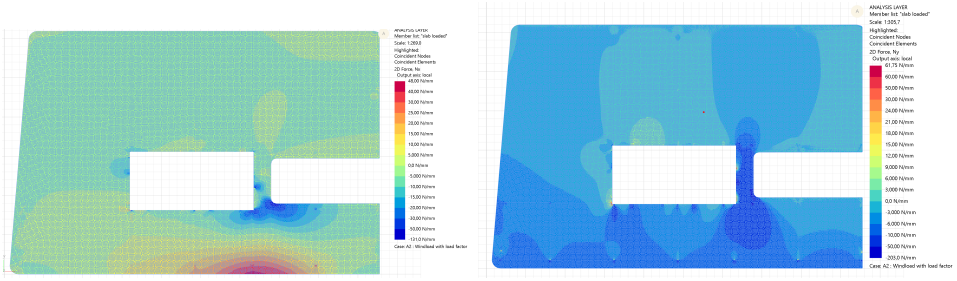

(a) Nx(kN/m) **(b)** Ny(kN/m)

Figure 6.4: Showcasing the resultant internal forces from the GSA model for the basalt fibre reinforcement

The maximum internal tensile force is equal to 58.00 kN/m. The basalt reinforced concrete has a tensile design capacity of 2.23 MPa and acts over a height of 85 mm, resulting in a tensile design capacity per meter span of 189.55 kN/m. A unity check would then be 58.00/189.55= 0.31 < 1.0.

For the original SCIA model, an internal tensile force of 82.00 kN/m was found. Using that internal force results in a unity check of 82.00/189.55 = 0.43 < 1.0.

Per meter span, the slab would have a tensile capacity larger than the occurring internal tensile forces for both the GSA model and the original SCIA model.

Table 6.2: Resultant maximum internal forces from GSA

	Regular C37/30 concrete	Basalt reinforced concrete
Max positive Nx [kN/m]	46.63	47.66
Max positive Ny [kN/m]	59.02	61.75

6.3. Conclusions

From the previous paragraphs it can be concluded that both types of reinforcement would suffice under the applied loading, especially when the extra reinforcement for robustness would be included. There are higher internal forces found in the model using fibre reinforcement concrete material model, as compared to the slightly lower internal forces in the model using steel mesh reinforced concrete. This difference in internal forces is most likely due to the difference in E-modulus. A higher E-modulus for the fibre reinforcement material model is likely to lead to a higher internal stresses and thus internal force distribution. It is worth noting that there are some differences between the original model (made in SCIA) and the model shown in this report (made in GSA). The main difference is most likely to stem from the way that boundary conditions can be defined in SCIA versus GSA. Where in SCIA one can define boundary condition along sides of slabs connecting to each other, in GSA bordering slabs are considered to be connected in a fixed manner. This could explain the roughly 40 kN difference between the SICA model results with steel reinforcement mesh and the GSA model of the same reinforcement type.

The values from the basalt fibre reinforced concrete might also need a more realistic representation, as the mechanical input values for the model are taken from one source of literature [155]. The most complete source only contained high compressive strength concrete samples, which resulted in a higher E-modulus compared to the concrete class used in the original design.

To conclude, when looking at the unity checks of the models, both smaller than 1.0, a lot smaller than 1.0, the reinforcement could be considered over designed for the application and loads applied in the models. It is worth mentioning that there is a difference between the original design of Arup, where a maximum of 82 kN/m was found. In this load case, the steel mesh would just suffice with a unity check equal to 1.0. The basalt fibre would then have a unity check of 0.43, which would still be considered an over design. However, as mentioned previously, basalt fibres have low ductility/a brittle failure mechanism, so a low unity check is better. As without failure warnings, a low unity check indicates a safe structure.

In the next chapter, the floor system analysed here, primarily the concrete and reinforcement, is assessed at slab level, including the timber, concrete, reinforcement, and connection, with a focus on environmental impact. Potential design changes based on the observed overdesign are not considered in this assessment. This concludes the analysis of the second research question: *"How does the most suitable alternative reinforcement method and material compare to an existing case study design based on their individual mechanical and environmental performances?"*.

The following chapter will analyse the environmental implications of the alternative reinforcement method and material through a comparison of the global warming potential of the alternative with the DPG design for the whole TCC floor slab.

7

Environmental Impact Analysis

This chapter presents a focused environmental assessment comparing the carbon footprint of the conventional steel mesh reinforcement with the alternative proposed through the multi-layered Multi-Criteria Analysis (MCA) in Chapter 4. While the MCA provided preliminary estimates, this phase deepens the analysis using Environmental Product Declarations (EPDs) and supplementary literature data. The comparison targets the Global Warming Potential (GWP) across life cycle stages A1–A3, which include raw material extraction, transport, and manufacturing.

By quantifying the environmental impact of both individual materials and the complete Timber-Concrete-Composite (TCC) slab system, the study contributes to a holistic framework for sustainable structural optimisation. The findings aim to bridge the gap between theoretical modelling and practical application, offering evidence-based strategies to reduce carbon emissions without compromising structural integrity.

7.1. Methodology

7.1.1. Environmental indicator and life-cycle-stages used

A commonly used metric in the construction industry to assess the sustainability of materials and systems is the carbon footprint or GWP [37]. Ideally, a comprehensive environmental assessment would cover all life cycle stages defined in EN 15978 [39], including production (A1-A3), construction (A4-A5), use (B1-B7), end-of-life (C1-C4), and potential benefits beyond the system boundary (D). However, for the fibre alternative selected in this study, available data is limited to the production phase, represented by life cycle stages A1-A3.

Therefore, the environmental assessment in this thesis focuses on the carbon footprint per square meter of the TCC floor system in a cradle-to-gate approach, evaluating the GWP for the production stage only [40] using data from EPDs, where available.

7.1.2. Qualitative assessment of non-assessed life-cycle-stages

As noted in the previous section, the quantitative environmental analysis in this chapter is restricted to life cycle stages A1-A3 due to data limitations. Nonetheless, insights from literature and EPDs are available for certain materials and elements beyond these stages.

To provide a more holistic perspective, this section presents a qualitative assessment of the remaining life cycle stages (A4-D). This includes an evaluation of the potential impacts during construction, use, and end-of-life phases, with particular attention to the interaction of materials during demolition and recycling processes. While this discussion will offer indicative insights into the environmental behaviour of the materials beyond the production phase, it will not provide quantified data.

7.2. Environmental product declarations

For the environmental impact analysis of the TCC floor systems, the GWP of each material component was assessed using EPDs. These EPDs quantify environmental impacts per life cycle stage according to NEN-EN 15804:2012+A2:2019 for a defined quantity of material. The selection of EPDs was based on their relevance to the Dutch market and representativeness of the materials used in the original and alternative designs.

As a TCC floor is a composite system consisting of several materials, each produced and supplied by different manufacturers using different methods, it is not possible to obtain all EPD data from a single source. To ensure consistency and comparability, EPDs were sourced primarily from the same database used by the Dutch National Environmental Database (NMD), the *Milieu Relevante Product Informatie* (MRPI) database. Where necessary, these were supplemented with data from the International EPD System, with the geographical scope limited to Europe to maintain regional relevance. This approach ensures that variations in environmental impact reflect real differences between materials and scenarios, rather than inconsistencies in data sources.

Cross-Laminated Timber (CLT) The EPD from Stora Enso [159] was selected, as the same supplier's data was used for the mechanical property inputs in the TCC floor calculations. This ensures consistency between the structural and environmental modelling.

Stainless Steel Screws The EPD from Adolf Würth GmbH & Co. KG [160] was selected because it closely aligns with the product specifications used in the structural design, making it a realistic representation of the screws in the original TCC system. Using data from a well-established European manufacturer ensures strong geographical relevance and reduces the risk of inconsistencies that might occur with generic or non-regional datasets.

Concrete Mix Design The mix design follows the VOBN EPD for C30/37 concrete [74], which reflects Dutch industry standards. The proportions of each constituent material were taken directly from this EPD, while the GWP values for those materials were taken from the EPDs of the individual components. This approach was chosen because the alternative reinforcement scenarios in this study use different mix designs, with varying quantities of some materials. Using the same GWP dataset for each material across all scenarios ensures fair and unbiased comparisons.

The additional components and aggregates are represented by the following EPDs:

- Dutch sand: Cascade [76]
- Gravel from the Danish part of the North Sea: Spaansen [77]
- Eco2cem (slag cement): Ecocem Benelux B.V. [150]
- Hoogoven Cement CEM III/B 42.5 N: Hollandse Cement Maatschappij [75]
- Plasticizer: Sika [153]

The value used for 1 m^3 regular concrete is taken as 123.77 kg CO_2 eq. Whereas the concrete using 50 % eco$_2$cem 1 m^3 causes 69.31 kg CO_2 equivalent emissions [74–77, 150, 151].
For FRC the regular cement concrete mix results in 188.21 kg CO_2 equivalent per m^3 concrete. Whereas the 50 % eco$_2$cem concrete mix for FRC results in 105.69 kg CO_2 equivalent per m^3 concrete [74–77, 150–153]. A more detailed calculation can be found in chapter 3 for the regular reinforcement, in Appendix 3 the same method is used,albeit with different material ratios, for the FRC.
The argumentation for the used ratios of materials in concrete, calculations of these values and an example of how the values for scoring are calculated can be found in chapter 3 and Appendix C.

Reinforcement Mesh (B500B) Two EPDs from Merksteijn International B.V. [148] and Gallega [79] were averaged to represent the environmental impact. Both are specific to reinforcement mesh and relevant for the Dutch and European markets. Averaging was necessary to avoid bias, as the GWP values for life cycle stages A1-A3 differed significantly between the two datasets.

Alternative Reinforcement (Basalt Fibre) No certified EPD was available for basalt fibre reinforcement. Instead, environmental impact data from Fořt et al. (2021) [110] was used as an academic approximation, enabling inclusion of this material in the comparative analysis despite the absence of a standardised declaration.

Summary This selection of EPDs provides a consistent, transparent, and realistic representation of environmental impacts for both the reference TCC design and the alternative scenarios. The approach ensures that differences in sustainability performance reflect actual material and design variations, rather than inconsistencies in data sourcing.
An overview of the most important aspects of the EPDs can be found in table 7.1

Table 7.1: GWP [1] data for materials, life cycle stages A1-A3 [74–76, 147, 150, 153, 159, 160]

Element/material	Functional unit	GWP with carbon capture	GWP without carbon capture	GWP total
CLT24	m^3	-762.00	54.00	-708.00
Screws	kg	-	-	6.88
Sand [76]	metric tons	-	-	2.56
Gravel [77]	metric tons	-	-	1.74 E-1
Eco_2cem	metric tons	-	-	30.30
Hoogoven Cement	metric tons	-	-	364.00
Plasticizer	kg	-	-	0.87
Reinforcement steel [147]	metric tons	-	-	455.00
Reinforcement steel [79]	metric tons	-	-	2320.00
Basalt Fibre	metric tons	-	-	398.00

The EPDs are publicly available and accessible through the links down below:

- CLT24, Stora Enso [159]
- Stainless Steel screws, Adolf Würth GmbH & Co. KG [160]
- C30/37 Concrete, VOBN [74]
- Dutch sand, Cascade [76]
- Dutch Gravel, Cascade [77]
- Eco_2cem, Ecocem Benelux B.V. [150]
- Hoogoven Cement CEM III/B 42,5 N, Hollandse Cement Maatschappij [75]
- Plasticizer, Sika [153]
- B500B reinforcement steel, Merksteijn International B.V. [147]
- B500B reinforcement steel, Gallega [79]

7.3. Environmental impact - A comparison of designs

7.3.1. Original design

The calculations for the total environmental impact of life cycle stages A1-A3 can be found in chapter 3. An overview of the results of this chapter can be found in table 7.2 and 7.3.

With an overview of the material quantities in table 7.2, functional unit, GWP per functional unit, the GWP for life cycle stages A1-A3 per square meter of floor slab can be found in table 7.3. The total area of a floor slab type 1 is equal to 18.48 m^2.

[1] kg CO_2 equivalent/functional unit
[4] GWP for life cycle stages A1-A3
[5] f.u. = functional unit

Table 7.2: Material quantities - case study

Material	Density [kg/m^3] [78–80]	Volume [m^3]	kg
CLT	420	3.69	1516.03
Concrete	2325	1.92	4464
Reinforcement steel	7850	6.94E-3	54.48
Dowels	-	34.848	

Table 7.3: GWP [4] per m^2 floor - case study

Material	kg CO_2 eq/f.u.[5]	f.u. quantity	kg CO_2 eq/m^2
CLT carbon capture	-762	3.61 m^3	-148.84
CLT no carbon capture	54	3.61 m^3	10.55
CLT - total	-708	3.61 m^3	-138.29
Concrete - reg cem	123.77	1.92 m^3	12.88
Eco$_2$cem	69.31	1.92 m^3	7.21
Reinforcement steel	1372.5	54.48 kg	4.05
Dowels	6.88	34.85 kg	12.97

From table 7.3 the total GWP for one square meter of TCC floor, type 1, with regular cement is equal to -120.74 kg CO_2 eq. For the eco$_2$cem variant the total GWP for one square meter of TCC floor - type 1 - is equal to -133.621 kg CO_2 eq.

It was mentioned in chapter 3 that the change to 50 % eco$_2$cem leads to and decrease of contribution of concrete to the GWP of the whole TCC floor slab. Whereas it leads to an increase, percentage wise, of the contribution of the reinforcement to the GWP of the whole TCC floor slab.

7.3.2. Alternative reinforcement design

To assess the GWP emissions of an alternative design using alternative reinforcement instead of reinforcement mesh the amount of materials needs to be computed first.
The total amount of CLT and dowels does not change compared to the slab design from the study case, see table 3.2 and 7.4. However, the amount of concrete will be dependent on the amount of fibre used. The volumetric percentage used in chapter 4 was based on average values from literature. In chapters 5 and 6, one fibre with a specific reinforcement ratio was used, the same volumetric percentage is used in this chapter as mentioned in 4, is equal to 0.5%.

It is worth noting that not all materials have a volume as their functional unit, thus the mass of materials is also calculated and shown in table 7.5. It can be noted that the regular reinforced concrete mix has a lower density in table 7.2 than the mix for the alternative reinforcement in table 7.5. The density calculations can be found in Appendix C

With an overview of the material quantities, functional unit, GWP per functional unit, the GWP for life cycle stages A1-A3 per square meter of floor slab can be found in table 7.6. The total area of a floor slab type 1 is equal to 18.48 m^2.

From table 7.6 the total GWP for one square meter of TCC floor,type 1,with regular cement is equal to -117.57 kg CO_2 eq. For the eco$_2$cem variant he total GWP for one square meter of TCC floor, type 1, is equal to -126.21 kg CO_2 eq. The contribution per material can be seen in figures 7.1.

7.4. Conclusion

Tables 7.6 and 7.3 demonstrate that the original design generally results in lower GWP values compared to the alternative reinforcement. For both reinforcement types, using regular cement leads to higher

[6] GWP for life cycle stages A1-A3
[7] f.u. = functional unit

Table 7.4: Material volumes of the alternative reinforcement

Material	Length [m]	Width [m]	Height [m]	extra notes	Volume [m^3]
Notches	0.15	2.40	0.03	Total of 8 notches over floor type 1	8.64E-2
CLT	7.70	2.40	0.20	Minus the notch volume	3.69
Concrete	7.70	2.40	0.10	Plus the notch volume, minus the dowel head- and shaft volume + fibre volume	1.93

Material	Volume[%]	Volume of total cross-section[m^3]	Volume[m^3]
Basalt Fibre	0.5	1.93	9.65E-3

Table 7.5: Material quantities of the alternative reinforcement

Material	Density [kg/m^3] [78–80]	Volume [m^3]	kg
CLT	420	3.69	1516.03
Concrete	2498	1.93	4821.14
Basalt Fibre	2150	9.65E-3	20.75
Dowels	-	-	34.85

GWP than using the alternative eco$_2$cem cement.

GWP values per square meter for reinforcement only:

- Steel mesh: 4.05 $kgCO_2eq/m^2$
- Basalt fibre: 0.45 $kgCO_2eq/m^2$

GWP values for combined concrete and reinforcement:

- Steel mesh: 16.93 $kgCO_2eq/m^2$
- Basalt fibre: 17.4 $kgCO_2eq/m^2$

These results highlight the importance of evaluating the full concrete-reinforcement system rather than focusing solely on individual components. Although basalt fibre has a significantly lower GWP at the reinforcement level, the overall GWP increases when combined with concrete due to the higher cement

Table 7.6: GWP [6] per m^2 floor - alternative reinforcement

Material	kg CO_2 eq/f.u.[7]	f.u. quantity	kg CO_2 eq/m^2
CLT carbon capture	-762	3.61 m^3	-148.84
CLT no carbon capture	54	3.61 m^3	10.55
CLT - total	-708	3.61 m^3	-138.29
Concrete - reg cem	188.21	1.92m^3	16.95
Concrete - eco$_2$cem	105.69	1.92 m^3	10.98
Basalt Fibre	398	20.75E-3 ton	0.45
Dowels	6.88	34.85 kg	12.97

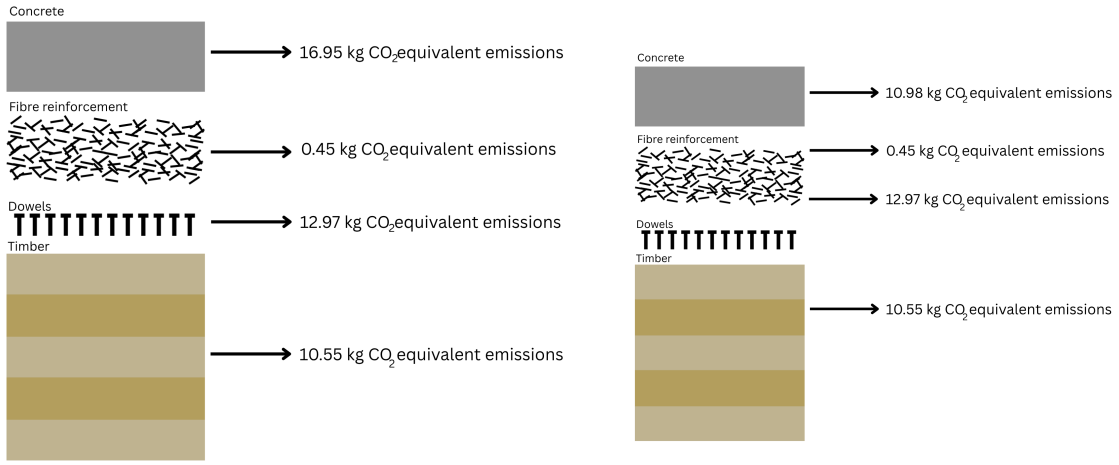

(a) Regular cement concrete

(b) Eco$_2$cem concrete

Figure 7.1: Contribution to equivalent CO_2 emissions of materials per square meter of TCC floor slab.

content required in fibre-reinforced mixes. As fibre reinforcement requires the fibres to bridge gaps created by cracks, rather than relying on aggregates. As a result, the concrete mix needed fewer large aggregates and more cement to achieve the same compressive strength as a standard C30/37 mix. This increase in cement content led to higher emissions.

To isolate the impact of cement type, a mix using eco$_2$cem was analyzed. The adjusted GWP values were:

- Steel mesh with eco$_2$cem: 11.26 $kgCO_2eq/m^2$
- Basalt fibre with eco$_2$cem: 11.43 $kgCO_2eq/m^2$

Additionally, dowels, despite their small volume, contribute significantly to the total GWP, with a value of 12.97 $kgCO_2eq/m^2$, comparable to the concrete component using regular cement.

In summary, while basalt fibre offers clear environmental benefits at the material level, its integration into the full TCC floor system can lead to higher overall GWP due to increased cement usage. This underscores the need for holistic assessment when selecting sustainable construction materials. Thus concluding the answer to the second sub-question: *"How does the most suitable alternative reinforcement method and material compare to an existing case study design based on their individual mechanical and environmental performances?"*.

The following chapter builds upon the findings presented here and in previous chapters by critically reflecting on the methodologies applied and examining how underlying assumptions have influenced the outcomes. This reflection serves as a foundation for integrating technical performance and environmental impact into a unified optimisation strategy.

8

Discussion

This chapter reflects on the findings presented in the previous sections and considers their broader implications for Timber-Concrete-Composite (TCC) design and sustainable construction. The results from both mechanical and environmental analyses are revisited to assess how well basalt fibre reinforcement aligns with the thesis's overarching goal: integrating structural performance and environmental impact into a holistic evaluation framework. Particular attention is given to the limitations of the modelling approaches, the assumptions made during the Multi-Criteria Analysis (MCA), and the trade-offs encountered between mechanical efficiency and sustainability. Through this critical reflection, the feasibility of basalt fibre as a viable alternative to conventional steel reinforcement in TCC floor systems is examined.

8.1. Multi-criteria analysis

The primary objective of this thesis was to holistically evaluate reinforcement alternatives in TCC floor systems, integrating both mechanical performance and environmental impact into the decision-making framework. This was achieved through a MCA, which, although effective, revealed several limitations. Notably, the MCA proved highly sensitive to the weighting of criteria and the method used to interpolate scores across alternatives. This sensitivity introduces uncertainty into the ranking process and underscores the need for transparent and well-justified weighting strategies.

The process of assigning weights in MCA is inherently subjective, as there is no universally accepted scientific method to do so. In Chapter 4.4, the weighting approach was guided by previous research that successfully applied MCA to material selection. In these studies, expert judgment played a key role in determining weights, an approach that, while informed and valuable, naturally reflects human perspectives. This underscores a key characteristic of MCA: its flexibility allows for expert input, but also means that outcomes may vary depending on the context and the stakeholders involved. However, this subjectivity also allows MCA to be tailored to specific needs and preferences, making it adaptable across various applications.

Another important consideration is the limited scope of criteria used in the MCA. For structural performance, the analysis focused exclusively on tensile strength and ductility, rather than evaluating comprehensive structural behavior. This choice was largely due to the absence of standardized design methodologies that translate fibre properties into fibre-reinforced concrete performance. As previously discussed, the behavior of fibre-reinforced concrete is influenced by a broader range of factors, including fibre length, bond strength, orientation, and modulus of elasticity, which were excluded due to the lack of standardized data.

Consequently, the MCA may not fully capture the real-world performance of the alternatives. Nonetheless, the reduced number of criteria contributes to the simplicity of the analysis. A more concise set of criteria also minimizes the risk of overlooking complex interdependencies between them, which can be a challenge in more elaborate decision models.

8.2. Finite element models

In essence, a model serves as a simplified representation of reality, designed to answer questions about complex systems. This principle was central to the modelling approach adopted in this research. However, not all models are created equal, each serves a distinct purpose. Therefore, the following sections provide reflections on both the general modelling methodology and the specific software tools used, in relation to the objectives of this study.

8.2.1. General

Material properties

The finite element models developed in this study were based on material properties sourced from a single literature reference. In some instances, key parameters, such as the E-modulus and compressive strength, did not align with the concrete strength class used in the case study.
This mismatch led to an overdesign of the alternative reinforcement in terms of compressive strength. While this may have enhanced mechanical performance, it complicates direct comparisons with the original design. Reducing the compressive strength of the concrete mix could potentially lower its tensile strength.
However, given the low unity check values observed for the basalt fibre alternative, this reduction may be acceptable. Moreover, a lower compressive strength could reduce cement content, thereby improving the environmental profile of the design.

Loading conditions

In the original design, it was assumed that no tensile stresses were present in the concrete portion of the composite cross-section. Literature suggests that such stress distributions occur only under conditions of full composite action, an idealized scenario rarely achieved in practice. In reality, partial composite action introduces tensile stresses that could affect both serviceability limit state (SLS) and ultimate limit state (ULS) calculations. For instance, these stresses could increase the load used to compute crack widths or internal forces.

Despite this, tensile stresses were excluded from the scope of this analysis to maintain consistency with the original design. This decision was made to preserve simplicity and ensure compatibility between the original and alternative reinforcement evaluations.

8.2.2. LS-DYNA

To investigate shrinkage-induced cracking and diaphragm action, LS-DYNA models were developed using a combination of 2D shell elements, 1D discrete beam elements, and a smeared cracking approach. Reinforcement was represented through a smeared equivalent material, derived from the reinforcement ratio. While this modelling strategy proved effective for the study's objectives, it comes with notable limitations.

Shell elements, though computationally efficient, are less reliable in capturing through-thickness stress variations. Fortunately, the applied loads in this study were relatively uniform across the cross-section, minimizing the impact of this limitation. Deviations in stress distribution were primarily observed in regions with steel reinforcement, where material property differences played a role.

The smeared cracking model distributes cracking strain uniformly across each mesh element, based on a predefined crack-band spacing from Eurocode. This approach does not pinpoint exact crack locations but instead indicates the general regions, typically within 50 mm elements, where cracking is expected. A finer mesh provides a more detailed picture of crack propagation, though the strain remains constant within each element. The model is sensitive to strain localization and post-peak material behaviour, particularly given concrete's brittle nature. Additionally, the crack-band spacing was uniformly applied across all models due to the absence of a method for computing crack spacing in unreinforced concrete. This conservative assumption influences both the predicted crack locations and strain magnitudes, and explains the consistent cracking patterns observed when re-running the same model.

The smeared reinforcement method assumes a uniform tensile capacity across the layer, whereas actual reinforcement is discrete and localized. This simplification affects the distribution of tensile stresses in the concrete and, consequently, the crack patterns. A more precise representation would involve

modelling individual reinforcement bars, but this would significantly increase computational demands, especially given the fine mesh required for the cracking model.

Finally, the structural models were based on symmetrical geometry, material properties, and boundary conditions under uniform loading. In theory, such a system should respond symmetrically, allowing for computational efficiency by modelling only a portion of the structure and mirroring the results. However, the models exhibited asymmetrical behaviour, contrary to expectations. This discrepancy may be attributed to the crack-band spacing not aligning with the structure's length, combined with the sharp post-peak response of the concrete due to its brittle nature.

8.2.3. GSA

The original design was validated using a SCIA model of the entire floor under wind loading. For this research, a comparable model was developed in GSA, a software tool used internally at Arup. GSA was selected to facilitate analysis of the alternative reinforcement options.

Like the LS-DYNA model, the GSA model utilized 2D shell elements to represent the concrete layer. The same limitations regarding shell elements apply, but the method remains suitable due to the relatively uniform stress distribution resulting from the applied loads.

As discussed in Chapter 3, the design includes strategic cuts in the concrete layer to prevent hogging moments in one direction, effectively creating a pinned boundary condition along the spanning direction of the floor slabs. This behavior could not be fully replicated in GSA, as the software automatically applies fixed connections between 2D elements. This modelling constraint led to discrepancies between the SCIA and GSA models.

Nevertheless, given the small differences in maximum internal tensile forces observed between reinforcement alternatives, both were also compared against the original SCIA model results to ensure consistency and reliability.

8.3. Environmental impact analysis

The environmental impact assessment conducted in this thesis focused exclusively on Global Warming Potential (GWP) for life cycle stages A1 to A3. This limitation was primarily due to the lack of available data for subsequent stages.

While this approach offers a useful snapshot of the embodied carbon associated with material production and processing, it does not provide a complete picture of the environmental footprint. Notably, the end-of-life stage, often poorly documented in Environmental Product Declarations (EPDs), was excluded, despite its potential to significantly influence overall impact.

In addition to the limited life cycle scope, the analysis considered only one type of cement/concrete mix. Numerous alternative and more sustainable cement types exist, and their inclusion could have altered the results. Furthermore, other components of the concrete mix,such as the use of recycled aggregates or sand, were also left out of scope, despite their relevance to environmental performance.

Another key limitation in the GWP calculation relates to the dowels used in the TCC floor system. These components were found to contribute substantially to the overall GWP. However, the analysis was based on a single dowel layout per floor slab. While variations in timber and concrete spans were considered across different floor types, the number of dowels varied significantly. The floor type studied in this thesis represented the most extreme loading scenario, requiring the highest number of dowels. In other areas of the DPG building, where loading conditions are less severe, the GWP would likely be lower.

By focusing solely on the most demanding configuration, the analysis highlights the importance of including all relevant components, and their variations, when assessing the environmental impact of composite systems. A more comprehensive approach would improve the accuracy and applicability of the findings across different design scenarios.

8.4. Case study

This study focused on a single cross-section of the TCC floor system, maintaining constant material dimensions, height and width, except for the reinforcement type. It was observed that the basalt

fibre alternative was overdesigned for wind loading conditions, suggesting potential for optimization. By reducing the concrete cross-sectional height, the unity check could be increased while remaining within safe structural limits. This adjustment would also reduce material usage, thereby lowering the environmental impact.

However, such optimization introduces additional design complexity. A lighter concrete layer may increase the system's susceptibility to vibrations, which could affect occupant comfort and long-term performance. Given that concrete was identified as the largest contributor to the system's overall emissions, further exploration of the trade-offs between structural performance and vibration control is warranted.

Incorporating vibration minimization as an additional design objective could lead to more refined and sustainable TCC floor systems. Balancing mechanical efficiency, environmental impact, and serviceability requirements would enable a more holistic and performance-driven design approach.

8.5. Combining model results with the environmental impact

The last sub-question to be considered in this research is: *"To what extent do the mechanical and environmental performances influence each other with the implementation of the most suitable reinforcement method and material?"*. To answer this, the mechanical performance (discussed in Chapters 5 and 6) and the environmental impact (Chapter 7) must be considered together.

This study shows that both aspects are strongly influenced by the concrete mixture rather than the reinforcement alone. Mechanically, the effectiveness of basalt fibre reinforcement depends on its bond with the concrete, while environmentally, the GWP is driven primarily by cement content. Using a conventional amount of fibre reinforcement led to an overdesigned structure with a GWP higher than that of the DPG TCC floor.

Therefore, the concrete mixture acts as the main driver for both mechanical and environmental performance. Cement's high environmental burden and concrete's critical role in structural behaviour create a direct link between these two performance domains. Even when reinforcement is the focus, optimizing the concrete mixture is essential to achieve a balance between strength and sustainability.

9

Conclusion & Recommendations

9.1. Conclusion

This thesis set out to answer the question: *"What are the mechanical and environmental implications of using a suitable alternative reinforcement method and material in timber-concrete-composite (TCC) floor systems, assessed against a case study"*

The objective behind this question was to develop a structured method for evaluating reinforcement alternatives that not only meet structural requirements but also contribute to reducing the environmental footprint of building components. By integrating both mechanical and sustainability criteria into the assessment, the research aimed to support more informed and balanced design decisions in TCC systems. The study focused on identifying viable non-steel reinforcement options and testing their performance through a combination of multi-criteria analysis and detailed numerical modelling, using a real-world floor slab as a reference case. To answer the main question, several sub-questions were proposed, with the first one being: *"Based on the functional roles and requirements for reinforcement in TCC floor systems, which alternative reinforcement method and material is most suitable for application using a multi-criteria analysis?"*. This question was answered using chapter 2, 3 and 4

In chapter 2 and 3, the functions of reinforcement in TCC floor slabs were examined. It was found that, unlike conventional reinforced concrete elements where reinforcement primarily resists tensile forces due to vertical loading, reinforcement in TCC systems serves different purposes. Its main roles are to minimize shrinkage-induced cracking and to ensure horizontal force redistribution to the stability core under lateral loading conditions.
This shift in function is logical when considering the composite nature of the system, where timber replaces reinforced concrete in the tensile zone of the cross-section under governing load cases. As such, the reinforcement in TCC slabs operates predominantly in the compressive zone where it is activated in the horizontal plane.
These key functionalities formed the basis for the mechanical behaviour analysis in the remainder of the thesis. Chapter 2 and 4 the possible alternative methods and materials were discussed and analysed respectively.

Building on the insights of the functional roles of the reinforcement, a Multi-Criteria Analysis (MCA) method was developed to evaluate eight promising alternatives to conventional steel reinforcement bars and compared them to the conventional steel mesh used in the case study of the DPG building. The MCA considered four main criteria: Performance Capability, Environmental Impact, Buildability, and Cost. Structural performance was further divided into two equally weighted sub-criteria: Tensile Strength and Ductility.
The MCA was designed as a low-detail, broad assessment tool to evaluate multiple alternative reinforcement methods and materials cross different functional units with sustainability being the dominant criteria as it is the driver of the research. From this analysis, Basalt Fibre Reinforced Polymer (BFRP) bars emerged as the most desirable option.
However, due to the relatively uniform stress distribution across the cross-section in the relevant load

cases, the best-performing fibre reinforcement alternative was selected for further study. This material was determined to be basalt fibres.
Answering the research question, the most suitable reinforcement material was found to be basalt and the best suited reinforcement method for TCC floors is determined to be fibre reinforcement,

After determining the best suited alternative reinforcement method and material, this alternative is then compared against the DPG design. Chapters 5, 6 and 7 are used to answer the second sub-question: *"How does the most suitable alternative reinforcement method and material compare to an existing case study design based on their individual mechanical and environmental performances?"*

The detailed study focused on a single case: a standard floor element from the DPG Media building. Two key structural aspects were analysed: cracking behaviour due to shrinkage and design capacity under horizontal wind loading.

Finite element models were constructed to simulate crack formation due to shrinkage for the most favourable alternative identified through the MCA, using LS Dyna. These results were compared to an analytical approach for computing crack width under the maximum expected shrinkage strain in the floor system.
The numerical models consistently predicted larger crack widths than the analytical method, 0.95 mm for the non-reinforced model, 0.96 for the basalt fibre reinforce model and 1.35 for the steel mesh reinforced model, suggesting a mismatch between the modelling approach and the intended objective rather than a deficiency in the reinforcement material itself.
When comparing the modelled crack widths to the Eurocode limit of 0.4 mm in the Ultimate Limit State (ULS) phase, all results exceeded this threshold. However, as discussed in Chapter 3, this limit is primarily intended to prevent corrosion of steel reinforcement. Since basalt fibre is not susceptible to corrosion, this limit does not apply.
Instead, the basalt fibre crack widths were compared to a 0.7 mm limit found in literature. Although the unity check still exceeded 1.0, it was closer to the acceptable range than the standard steel mesh.
Assuming the original design's reinforcement was sufficient, the fibre-reinforced model can be expected to produce smaller crack widths than the regular steel-reinforced model.

In addition to shrinkage analysis, a separate GSA model was developed to assess stress distribution in the top concrete layer of the TCC slab under horizontal loading. The results were compared against the tensile capacity of the selected reinforcement method. Both the original design and the alternative reinforcement configuration were modelled to enable a direct comparison of structural performance.
The unity check for the standard steel mesh reinforcement was found to be 0.55 in the GSA model and 1.0 in the SCIA model. For the basalt fibre reinforcement, the brittle nature of the material necessitated an additional safety factor. With this adjustment, the unity check was 0.31 in the GSA model and 0.43 in the SCIA model.
These results indicate that the mechanical performance of the basalt fibre alternative is superior to that of the standard steel mesh, supporting the MCA conclusion.

To assess environmental performance, the Global Warming Potential (GWP) was calculated for all components of the TCC floor slab, covering life cycle stages A1 to A3. These values were computed for both the original design and the alternative reinforcement variant.
The analysis revealed that while the GWP of the reinforcement itself decreased with the use of basalt fibres, the overall GWP of the slab increased. This was primarily due to changes in the concrete mix.
Fibre reinforcement requires the fibres to bridge gaps created by cracks, rather than relying on aggregates. As a result, the concrete mix needed fewer large aggregates and more cement to achieve the same compressive strength as a standard C30/37 mix. This increase in cement content led to higher emissions.
Investigating alternative cement types with lower GWP values yielded similar results, indicating that the environmental impact could not be significantly reduced through mix design alone.

Another notable finding was that the dowels (metal screws) used in the notches had the highest GWP values of all components. This is likely due to the high level of processing required to achieve their specific shape. Although the screws weigh approximately 60% of the reinforcement steel, their GWP was more than three times higher. This highlights the importance of considering all components in environmental assessments, not just the reinforcement material.

Finally, the last research question was answered in chapter 8, reflecting on the information found in

previous chapters. *"To what extent do the mechanical and environmental performances influence each other with the implementation of the most suitable reinforcement method and material?"*. The findings indicate that these two performance aspects are strongly interconnected, primarily through the concrete mixture rather than the reinforcement alone. Basalt fibre reinforcement relies on its bond with concrete for structural efficiency, while the environmental impact in terms of GWP is largely determined by cement content. Using conventional fibre quantities from literature led to an overdesigned structure with a GWP exceeding that of the reference DPG TCC floor. This demonstrates that optimizing the concrete mixture is essential for achieving both structural adequacy and sustainability, even when reinforcement selection is the primary focus.

In summary, this research examined how alternative reinforcement materials can be assessed and compared for their mechanical and environmental performance in TCC floor systems through a case study approach. The mechanical evaluation confirmed that basalt fibre reinforcement meets the functional requirements of TCC slabs and performs better than conventional steel mesh, particularly in horizontal load capacity and crack control. However, the environmental analysis revealed a more complex outcome: while the reinforcement itself has a lower GWP, the overall slab GWP increased due to the cement-rich concrete mix required for fibre performance. This trade-off highlights that material substitution alone does not guarantee improved sustainability and underscores the importance of considering all components and interactions within the system. Ultimately, the findings demonstrate both the potential and limitations of alternative reinforcement in TCC systems and emphasize the need for integrated assessment methods to guide future sustainable design strategies.

Key findings are listed as follows:

1. The MCA identified the basalt fibre reinforced polymer bars as the optimal variant, however the research continued with loose fibres as a focus due to the functionality of reinforcement in the case study. The most optimal loose fibre reinforcement variant was loose basalt fibre.
2. The maximum crack from the model resulted in 1.35 mm for the steel mesh reinforcement. The second largest, reinforced with basalt fibre, was 0.96 mm, slightly higher than the 0.95 mm for the non reinforced model. However, all of these crack widths were larger than the analytically computed 0.19 mm.
3. The resultant internal forces due to horizontal wind loading were found to be very close in maximum tensile value between the regular concrete model and the basalt fibre reinforced concrete model.
4. The basalt fibre reinforced concrete showed sufficient tensile capacity to enable diaphragm action in the top layer of the TCC floors.
5. The originally designed floor slab was found to have a lower total GWP per m^2 of floor slab than the basalt fibre reinforced variant. Even though the reinforcement on its own resulted in lower GWP values, the combination with the altered concrete admixture, which was higher in cement content, resulted in a higher overall GWP.
6. The biggest contributor to the GWP for the TCC floorslab were the shear connectors, connecting the timber- and concrete slabs.

9.2. Recommendations

Based on the findings and reflections presented in this thesis, several recommendations can be made to improve future research and practical application of alternative reinforcement materials in TCC floor systems. A key recommendation is to conduct physical experiments, both to validate the design developed in this study and to generate additional data for use by other researchers. These tests can serve multiple purposes:

- **Enhance Methods for Assessing Structural Performance** Future studies should move beyond simplified mechanical property comparisons and focus on standardized testing of real structural behaviour. This includes compressive, tensile, and flexural capacity tests with clearly defined E-moduli. Such data would enable more accurate comparisons between reinforcement alternatives and support more reliable design decisions.

- **Develop Practical Design Tools for Fibre Reinforcement** To facilitate adoption in engineering practice, design tables or formulas should be developed that link commonly available fibre properties to structural performance. These tools should be based on standardized specimen testing and aligned with Eurocode requirements, making fibre-reinforced concrete more accessible and easier to specify.
- **Ensure Consistency in Material Properties for Fair Comparison** Comparative studies should use concrete mixes with equivalent compressive strength and E-modulus across all reinforcement types. This will ensure that differences in performance and environmental impact are due to the reinforcement itself, not variations in concrete composition.
- **Refine Modelling Approaches and Boundary Conditions** Numerical models should be improved by applying more accurate boundary conditions and selecting appropriate modelling software or element types. This is especially important for capturing shrinkage-induced cracking and diaphragm action realistically in TCC slabs.

In addition to laboratory testing and its applications, further progress can be made in the area of sustainability:

- **Expand Environmental Impact Assessment Scope** Environmental analyses should encompass all stages of the life cycle, with particular attention to end-of-life scenarios, as these can significantly influence the overall environmental impact. Future research should focus on addressing existing data gaps and re-evaluating the sustainability of reinforcement alternatives through a comprehensive life cycle perspective. Moreover, environmental impact assessments should extend beyond individual materials to include entire TCC floor systems. In particular, quantifying the environmental effects associated with the use of fibres would provide valuable insights for informed decision-making and should be prioritized in future investigations.
- **Explore Cross-Sectional Optimization** Given the overdesign observed in the basalt fibre alternative, future studies should investigate reducing concrete cross-sectional height to optimize material use. This could lower environmental impact while maintaining structural safety. However, vibration sensitivity must be considered as part of this optimization process.

References

[1] United Nations. *World Population Prospects: 2017, Revision, Key Findings and Advance Tables.* Report. United Nations, 2017.

[2] Clara H Mulder. "Population and housing: a two-sided relationship". In: *Demographic research* 15 (2006), pp. 401–412. ISSN: 1435-9871.

[3] Ahmad Faiz Abd Rashid and Sumiani Yusoff. "A review of life cycle assessment method for building industry". In: *Renewable and Sustainable Energy Reviews* 45 (2015), pp. 244–248. ISSN: 1364-0321.

[4] Michael Sansom and Roger J Pope. "A comparative embodied carbon assessment of commercial buildings". In: *The Structural Engineer* 90.10 (2012), pp. 38–49.

[5] Paolo Foraboschi, Mattia Mercanzin, and Dario Trabucco. "Sustainable structural design of tall buildings based on embodied energy". In: *Energy and Buildings* 68 (2014), pp. 254–269. ISSN: 0378-7788.

[6] David JM Flower and Jay G Sanjayan. "Green house gas emissions due to concrete manufacture". In: *The international Journal of life cycle assessment* 12 (2007), pp. 282–288. ISSN: 0948-3349.

[7] Ignacio Zabalza Bribián, Antonio Valero Capilla, and Alfonso Aranda Usón. "Life cycle assessment of building materials: Comparative analysis of energy and environmental impacts and evaluation of the eco-efficiency improvement potential". In: *Building and environment* 46.5 (2011), pp. 1133–1140. ISSN: 0360-1323.

[8] Hans-Martin Füssel. "Vulnerability: A generally applicable conceptual framework for climate change research". In: *Global environmental change* 17.2 (2007), pp. 155–167. ISSN: 0959-3780.

[9] Alireza Fadai and Wolfgang Winter. "Resource-efficient wood lightweight concrete composites in building constructions". In: *Structural Engineering International* 27.2 (2017), pp. 197–204. ISSN: 1016-8664.

[10] Ayesha Siddika et al. "Cross-laminated timber–concrete composite structural floor system: A state-of-the-art review". In: *Engineering Failure Analysis* 130 (2021), p. 105766. ISSN: 1350-6307.

[11] Md Abdul Hamid Mirdad et al. "Sustainability Design Considerations for Timber-Concrete Composite Floor Systems". In: *Advances in civil engineering* 2021.1 (2021), p. 6688076. ISSN: 1687-8094.

[12] Benjamin Kromoser and Philipp Holzhaider. "An innovative resource-efficient timber-concrete-composite ceiling system: Feasibility and environmental performance". In: *Civil Engineering Design* 3.5-6 (2021), pp. 179–191. ISSN: 2625-073X.

[13] Laura Corti and Giovanni Muciaccia. "Sustainability Optimization: Assessment of Recycling Scenarios for Timber-Concrete Hybrid Slabs". In: *RILEM Spring Convention and Conference*. Springer, 2024, pp. 349–356.

[14] Simon Lecours et al. "Optimizing composite floors for sustainability and efficiency: Cross laminated timber, concrete types, and ductile notch connectors with enhanced shape". In: *Cleaner Engineering and Technology* 14 (2023), p. 100635. ISSN: 2666-7908.

[15] Yannick Plüss and Daia Zwicky. "A case study on the eco-balance of a timber-concrete composite structure in comparison to other construction methods". In: *Concrete Innovation Conference CIC*. 2014, pp. 11–13.

[16] Mohammad Derikvand and Gerhard Fink. "Design for deconstruction: benefits, challenges, and outlook for timber–concrete composite floors". In: *Buildings* 13.7 (2023), p. 1754. ISSN: 2075-5309.

[17] Md Shahnewaz, Robert Jackson, and Thomas Tannert. "Reinforced cross-laminated timber-concrete composite floor systems". In: *Engineering Structures* 291 (2023), p. 116395. ISSN: 0141-0296.

[18] Klaus Holschemacher, Sven Klotz, and D Weibe. "Application of steel fibre reinforced concrete for timber-concrete composite constructions". In: *Lacer* 7 (2002), pp. 161–170.

[19] IEA. *World Energy Outlook 2008*. Report. IEA, 2008. URL: https://www.iea.org/reports/world-energy-outlook-2008.

[20] Anita Ogrin and Tomaž Hozjan. "Timber-concrete composite structural elements". In: *Engineered wood products for construction* (2021). ISSN: 1839627727.

[21] Marius Leonardus Robertus van der Linden. *Timber-concrete composite floor systems*. Journal Article. 1999.

[22] David Yeoh et al. "State of the art on timber-concrete composite structures: Literature review". In: *Journal of structural engineering* 137.10 (2011), pp. 1085–1095. ISSN: 0733-9445.

[23] F Nauta. *New Zealand Forest Service timber bridges*. Journal Article. 1984.

[24] U. Pynnonen. *The largest passable timber bridge in the world.* Report. Finnish National Road Administration, 1999.

[25] Techno Wood. *Looking to the future: Wooden-carbon bridge sets new standards*. 2023. URL: https://www.technowood.swiss/en/looking-to-the-future-wooden-carbon-bridge-sets-new-standards/.

[26] Osama AB Hassan, Fredrik Öberg, and Emil Gezelius. "Cross-laminated timber flooring and concrete slab flooring: A comparative study of structural design, economic and environmental consequences". In: *Journal of Building Engineering* 26 (2019), p. 100881. ISSN: 2352-7102.

[27] K Holschemacher, L Hoffmann, and B Heiden. "Environmental impact of timber-concrete composite slabs in comparison to other floor systems". In: *Santiago, Chile* (2021), p. 6.

[28] Leah Collins. "Timber-concrete composite: an alternative composite floor system". Master Thesis. 2020.

[29] Wendel Sebastian, Andrew Lawrence, and Andy Smith. *Commentary: The potential for multi-span continuous timber–concrete composite floors*. Generic 9. 2018, pp. 661–662.

[30] HoHo. *INFOS - BUSINESS-HOT SPOT GENAUSO WIE WOHLFÜHL-OASE - DIREKT AM SEE IM ZENTRUM DER SEESTADT*. 2021. URL: https://www.hoho-wien.at/infos/.

[31] HAUT. *Het gebouw*. 2025. URL: https://hautamsterdam.nl/nl/.

[32] Nationale Mileu Database. *Environmental data (LCA)*. 2025.

[33] Dat Tien Doan et al. "A critical comparison of green building rating systems". In: *Building and Environment* 123 (2017), pp. 243–260. ISSN: 0360-1323.

[34] BREEAM-NL. *Support*. 2025. URL: https://www.breeam.nl/support/downloads#nieuwbouw-en-renovatie.

[35] Duc Binh Tran et al. "A General Framework for Sustainability Assessment of Buildings: A Life-Cycle Thinking Approach". In: *Sustainability* 15.14 (2023), p. 10770. ISSN: 2071-1050.

[36] Walter Klöpffer. "Life cycle sustainability assessment of products: (with Comments by Helias A. Udo de Haes, p. 95)". In: *The International Journal of Life Cycle Assessment* 13 (2008), pp. 89–95. ISSN: 0948-3349.

[37] Mikko Viljakainen and Tero Lahtela. *Hiilijalanjäljen laskenta – rakentamistapojen vertailu*. Available at: https://proofer.faktor.fi/epaper/Puu319/. 2019.

[38] NEN. *NEN-EN-ISO 14040*. Standard. Stichting Koninklijk Nederlands Normalisatie Instituut, 2006.

[39] NEN. *NEN-EN 15978*. Standard. Stichting Koninklijk Nederlands Normalisatie Instituut, 2011.

[40] C Cao. "Sustainability and life assessment of high strength natural fibre composites in construction". In: *Advanced high strength natural fibre composites in construction*. Elsevier, 2017, pp. 529–544.

[41] Alemayehu Darge Dalbiso and Mohammad Haj Mohammadian Baghban. "Environmental Impact of Timber Concrete Composites: An Overview". In: *The International Conference on Net-Zero Civil Infrastructures: Innovations in Materials, Structures, and Management Practices (NTZR)*. Springer, 2024, pp. 623–634.

[42] Hooman Eslami et al. “Influence of different end-of-life cycle scenarios on the environmental impacts of timber-concrete composite floor systems”. In: *Proceedings of the 13th World Conference on Timber Engineering (WCTE), Oslo, Norway*. 2023, pp. 19–22.

[43] L Van Glabbeek. “Development of an innovative demountable floor system”. In: *Delft University of Technology]. http://resolver. tudelft. nl/uuid: 1ba2cd89-9b8e-469c-8cb0-9f8b5a21e803* (2019).

[44] CRSI. *Reinforcing basics*. 2015. URL: https://www.crsi.org/reinforcing-basics/reinforcing-steel/history-of-reinforcing-steel/.

[45] NEN. *NEN-EN 10080*. Standard. Stichting Koninklijk Nederlands Normalisatie Instituut, 2023.

[46] NEN. *NEN 6008:1968 nl*. Standard. Stichting Koninklijk Nederlands Normalisatie Instituut, 1968.

[47] NEN. *NEN-EN 1992-1-1+C2+A1*. Standard. Stichting Koninklijk Nederlands Normalisatie Instituut, 19 -01-2015 2015.

[48] Keehoon Kwon, Doyeong Kim, and Sunkuk Kim. “Cutting waste minimization of rebar for sustainable structural work: A systematic literature review”. In: *Sustainability* 13.11 (2021), p. 5929. ISSN: 2071-1050.

[49] World Steel Association. *About steel*. 2020.

[50] World Steel Association. *#steelfacts*. 2023.

[51] BoldData. *Bedrijven per regio*. 2025. URL: https://bolddata.nl/nl/bedrijven/nederland/staalbedrijven-nederland/.

[52] John Newman and Ban Seng Choo. *Advanced concrete technology 3: processes*. Elsevier, 2003.

[53] MS Khan et al. “Effects of incorporating fibres on mechanical properties of fibre-reinforced concrete: A review”. In: *Materials Today: Proceedings* (2023).

[54] Marco Di Prisco, Giovanni Plizzari, and Lucie Vandewalle. “Fibre reinforced concrete: new design perspectives”. In: *Materials and structures* 42.9 (2009), pp. 1261–1281.

[55] Antonio Nanni. *Fiber-reinforced-plastic for concrete structures: Properties and applications*. Amsterdam: Elsevier Science, 1993.

[56] Antonio Nanni, Antonio De Luca, and Hany Jawaheri Zadeh. *Reinforced Concrete with FRP Bars: Mechanics and Design*. Boca Raton, FL: CRC Press, Taylor & Francis Group, 2014. ISBN: 978-0-203-87429-5.

[57] W. P. Wu. “Thermomechanical properties of fiber reinforced plastic (FRP) bars”. PhD thesis. Morgantown, WV: West Virginia University, 1990.

[58] Lawrence C. Bank. *Fiber-Reinforced-Plastic (FRP) Reinforcement for Concrete Structures: Properties and Applications*. Ed. by Antonio Nanni. Vol. 42. Developments in Civil Engineering. Amsterdam: Elsevier, 1993, pp. 59–86.

[59] Antonio Nanni et al. “Characterization of GFRP ribbed rod used for reinforced concrete construction”. In: *Proceedings of the International Composites Exhibition (ICE-98)* (1998), 16A/1–6.

[60] T. Tamura. *Fiber-reinforced-plastic (FRP) reinforcement for concrete structures: Properties and applications*. Ed. by Antonio Nanni. Vol. 42. Developments in Civil Engineering. Amsterdam: Elsevier, 1993, pp. 291–303.

[61] Japan Society of Civil Engineering (JSCE). *Design Guidelines of FRP Reinforced Concrete Building Structures*. Tokyo, Japan, 1997.

[62] ACI Committee 440. *Guide for the Design and Construction of Structural Concrete Reinforced with FRP Bars*. Farmington Hills, MI, 2001.

[63] J. Plecnik and S. H. Ahmad. *Transfer of composite technology to design and construction of bridges*. 1988.

[64] Sanjay Gokul Venigalla et al. “Textile-reinforced concrete as a structural member: a review”. In: *Buildings* 12.4 (2022), p. 474.

[65] R Nivetha, A Vennila, and B Dharshini. “A review on various properties of textile reinforced concrete”. In: *Materials Today: Proceedings* (2023).

[66] Yongxiang Yang et al. “Recycling of composite materials”. In: *Chemical Engineering and Processing: Process Intensification* 51 (2012), pp. 53–68.

[67] CEN. *CEN/TC 259/SC 5*. Standard. the European Committee for Standardization, 2023.

[68] Marco Di Prisco, Giovanni Plizzari, and Lucie Vandewalle. “Fibre reinforced concrete: new design perspectives”. In: *Materials and structures* 42 (2009), pp. 1261–1281. ISSN: 1359-5997.

[69] MR LeBorgne and RM Gutkowski. “Effects of various admixtures and shear keys in wood–concrete composite beams”. In: *Construction and Building Materials* 24.9 (2010), pp. 1730–1738. ISSN: 0950-0618.

[70] Hubertus Kieslich and Klaus Holschemacher. “Composite constructions of timber and high-performance concrete”. In: *Advanced Materials Research* 133 (2010), pp. 1171–1176. ISSN: 1662-8985.

[71] BBR. *Nachhaltige Holz-Beton-Verbunddecken mit einer textilen Bewehrung aus Naturfasern zur Aktivierung der Zugtragfähigkeit des bewehrten Betonquerschnitts*. 2025. URL: https://www.zukunftbau.de/projekte/forschungsfoerderung/1008187-2210#eckdaten.

[72] Arup NEY-partners Besix. “Berekeningsnota-TCC-vloer bovenbouw”. These calculations are not open source, some parts have been added into the appendix.

[73] Arup. *Projects*. 2025. URL: https://www.arup.com/projects/mediavaert/.

[74] Stichting MRPI. *Environmental Product Declaration – VOBN Betonmortel*. Journal Article. 2012. URL: https://www.bouwoort.nl/Beton/userdata/uploads/MRPI-blad%20VOBN%20betonmortel_september2012.pdf.

[75] Stichting MRPI. *Environmental Product Declaration – Hoogovencement CEM III/B 42,5 N LH/SR*. Journal Article. 2025. URL: https://www.mrpi.nl/epd/hoogovencement-cem-iii-b-425-n-lh-sr/.

[76] Stichting MRPI. *Environmental Product Declaration – Cascade Zand 0-4 (industriezand)*. Report. 2020. URL: https://www.mrpi.nl/epd-files/epd/1.1.00A506.2024-cascade-zand-0-4-industriezand.pdf.

[77] Stichting MRPI. *Environmental Product Declaration – Cascade - Grind 4-32*. Report. 2024. URL: https://www.mrpi.nl/epd-files/epd/1.1.00A503.2024-cascade-grind-4-32.pdf.

[78] Swedish Wood. *Cross Laminated Timber Handbook - Swedish Version*. Available at: https://www.swedishwood.com/siteassets/5-publikationer/pdfer/clt-handbook-2019-eng-m-svensk-standard-2019.pdf. Stockholm, Sweden: Swedish Wood, 2019.

[79] IES. *Environmental Product Declaration: Reinforcing Steel electro-welded mesh - Gallega*. Report. EPD Number: S-P-13315, Valid until 2029-04-09. 2024. URL: https://www.environdec.com/library/epd13315.

[80] Rothoblaas. *KOP Coach Screw – Technical Data Sheet*. Tech. rep. Technical data sheet for KOP coach screws. Rothoblaas Timber Fastening Systems, 2023. URL: https://www.rothoblaas.com/products/fastening/screws/kop.

[81] Ecocem Benelux B.V. *Bestanddelen voor beton hydraulische bindmiddelen en toevoegsels: ATG 2609 Technical Approval*. Tech. rep. ATG 2609. Valid from 15-03-2025 to 14-03-2030. Certification by PROCERTUS, approval by SECO and Buildwise. Plaza 22, 4782 SK Moerdijk, Nederland: BUtgb (Belgische Unie voor de technische goedkeuring in de bouw), Mar. 2025. URL: https://www.butgb-ubatc.be.

[82] Peter O Akadiri, Paul O Olomolaiye, and Ezekiel A Chinyio. “Multi-criteria evaluation model for the selection of sustainable materials for building projects”. In: *Automation in construction* 30 (2013), pp. 113–125. ISSN: 0926-5805.

[83] Trevor Atkinson David Taylor Carsten Rieger. *CONCRETE SikaFiber® REINFORCED CONCRETE HANDBOOK*. Pamphlet. 2022.

[84] Stichting MRPI. *Environmental Product Declaration - Fibrofor High Grade*. Journal Article. 2021.

[85] Stichting MRPI. *Environmental Product Declaration - Plastic fiber*. Journal Article. 2024.

[86] Sika AG. *Construction*. 2025. URL: https://gbr.sika.com/en/construction/concrete/concrete-technology/fibre-reinforcedconcrete.html.

[87] Sika AG. *Construction Solutions*. 2025. URL: https://www.sika.com/en/construction/concrete-admixtures/fibers.html#types.

[88] Werken met Merken B.V. *Bouwstoffen*. 2025. URL: https://www.werkenmetmerken.nl/nl/sikacem_fibres/p/13665.

[89] Ha-Be. *Ha-Be PP-Fibre 18 µm FP - Technical data sheet*. Pamphlet. 2023. URL: https://www.ha-be.com/products_a-z/h/1805-ha-be-pp-fibre-18-m-fp.htm.

[90] Qianmin Ma et al. "Mechanical properties of concrete at high temperature—A review". In: *Construction and Building Materials* 93 (2015), pp. 371–383. ISSN: 0950-0618.

[91] Milind V Mohod. "Performance of polypropylene fibre reinforced concrete". In: *IOSR Journal of Mechanical and Civil Engineering* 12.1 (2015), pp. 28–36.

[92] Yassin A Ibrahim, Arsalan H Hasan, and Nyazi R Maroof. "Effects of polypropylene fiber content on strength and workability properties of concrete". In: *Polytechnic Journal* 9.1 (2019), p. 3. ISSN: 2707-7799.

[93] PwC—Sustainable Performance and Strategy. *Life Cycle Assessment of CFGF—Continuous Filament Glass Fibre Products*. Generic. Jan. 2023.

[94] Linder SE. *Glass Fibre Reinforced Concrete*. 2024. URL: https://www.lindner-group.com/en/products/glass-fibre-reinforced-concrete/application-areas-for-glass-fibre-concrete.

[95] Polycon. *Projects*. 2025. URL: https://www.lindner-group.com/en/products/glass-fibre-reinforced-concrete/application-areas-for-glass-fibre-concrete.

[96] International GRCA. *Uses of GRC*. 2025. URL: https://www.grca.online/uses-of-grc/grc-in-engineering.

[97] IN2-Concrete. *Brands*. 2025. URL: https://in2-concrete.com/en/product/merken/anti-crak/glass-fibre-for-concrete/.

[98] Chao Wu et al. "Effect of fiber content on mechanical properties and microstructural characteristics of alkali resistant glass fiber reinforced concrete". In: *Advances in Materials Science and Engineering* 2022.1 (2022), p. 1531570. ISSN: 1687-8442.

[99] B Krishna et al. "Determination of Strength Properties by using Glass Fibre in Concrete". In: *Int. J. Sci. Res. Dev* 5.2 (2017).

[100] Sayed Abolfazl Mirdehghan. "Fibrous polymeric composites". In: *Engineered polymeric fibrous materials*. Elsevier, 2021, pp. 1–58.

[101] Prathamesh Khorgade et al. "A comparative cradle-to-gate life cycle assessment of carbon fiber-reinforced polymer and steel-reinforced bridges". In: *Structural Concrete* 24.2 (2023), pp. 1737–1750. ISSN: 1464-4177.

[102] TV Muthukumarana et al. "A review on the variation of mechanical properties of carbon fibre-reinforced concrete". In: *Construction and Building Materials* 366 (2023), p. 130173. ISSN: 0950-0618.

[103] Composite-Envisions. *Clearance*. 2025. URL: https://compositeenvisions.com/product/precision-cut-chopped-carbon-fiber-epoxy-compatible-sizing-1lb/?srsltid=AfmBOorJV5aGYttPwSKfQthfQxfxTsqxwqFrMS1_c7M5yFRa3w1D-r68.

[104] Cristina Frazao et al. "Technical and environmental potentialities of recycled steel fiber reinforced concrete for structural applications". In: *Journal of building engineering* 45 (2022), p. 103579. ISSN: 2352-7102.

[105] M Yakhlaf. "Fresh and Mechanical Properties of Basalt Fiber Reinforced Concrete". In: *Intern. Civ. Eng. Archit. Symp. Acad*. 2023, pp. 50–55.

[106] Zongwen Li et al. "Properties and applications of basalt fiber and its composites". In: *IOP Conference Series: Earth and Environmental Science*. Vol. 186. IOP Publishing, 2018, p. 012052. ISBN: 1755-1315.

[107] Adeyemi Adesina. "Performance of cementitious composites reinforced with chopped basalt fibres–an overview". In: *Construction and Building Materials* 266 (2021), p. 120970. ISSN: 0950-0618.

[108] Dylmar Penteado Dias and Clelio Thaumaturgo. "Fracture toughness of geopolymeric concretes reinforced with basalt fibers". In: *Cement and concrete composites* 27.1 (2005), pp. 49–54. ISSN: 0958-9465.

[109] K. R and K. Ravande. "Influence of Different Lengths and Volumes of Basalt Fibre on Mechanical Properties of Concrete". In: *Civil Engineering And Architecture* 11(2) (2023), pp. 613–628. DOI: https://doi.org/10.13189/cea.2023.110207.

[110] Jan Fořt, Jan Kočí, and Robert Černý. "Environmental efficiency aspects of basalt fibers reinforcement in concrete mixtures". In: *Energies* 14.22 (2021), p. 7736. ISSN: 1996-1073.

[111] BE Ramachandran, V Velpari, and N Balasubramanian. "Chemical durability studies on basalt fibres". In: *Journal of Materials Science* 16 (1981), pp. 3393–3397. ISSN: 0022-2461.

[112] Benjamin Wolf et al. "Basalt reinforced concrete structures for retrofitting concrete surfaces". In: *MATEC Web of Conferences*. Vol. 199. EDP Sciences, 2018, p. 09014. ISBN: 2261-236X.

[113] Jun Zhi Zhang et al. "Bending resistance of short-chopped basalt fiber hydraulic concrete and RC element". In: *Advanced Materials Research* 261 (2011), pp. 407–410. ISSN: 1662-8985.

[114] Smriti Raj et al. "Basalt: Structural insight as a construction material". In: *Sādhanā* 42.1 (2017), pp. 75–84. ISSN: 0256-2499.

[115] James H Haido et al. "Effect of high temperature on the mechanical properties of basalt fibre self-compacting concrete as an overlay material". In: *Construction and Building Materials* 268 (2021), p. 121725. ISSN: 0950-0618.

[116] Zhihua Li, Chengfei Ma, and Xuan Guo. "Experimental and analytical study of the flexural behavior of basalt fiber-reinforced concrete beams". In: *Structural Concrete* 24.2 (2023), pp. 2342–2362. ISSN: 1464-4177.

[117] Deffner and Johann-GmbH. *Basalt Fibre, 4mm, 1kg*. Sept. 2025. URL: https://deffner-johann.de/en/basalt-fibre-4-mm.html.

[118] Vincenzo Fiore et al. "A review on basalt fibre and its composites". In: *Composites Part B: Engineering* 74 (2015), pp. 74–94. ISSN: 1359-8368.

[119] Wenjie Wang et al. "A critical review on the properties of natural fibre reinforced concrete composites subjected to impact loading". In: *Journal of Building Engineering* 77 (2023), p. 107497. ISSN: 2352-7102.

[120] JML Reis. "Fracture and flexural characterization of natural fiber-reinforced polymer concrete". In: *Construction and building materials* 20.9 (2006), pp. 673–678.

[121] D Grasselly et al. "Carbon footprint of coconut fibre (coir) substrates". In: *Infos-Ctifl* (2009).

[122] Konstantinos Tserpes and Vasileios Tzatzadakis. "Life-cycle analysis and evaluation of mechanical properties of a bio-based structural adhesive". In: *Aerospace* 9.2 (2022), p. 64. ISSN: 2226-4310.

[123] Mingli Gu et al. "Scientometric analysis and research mapping knowledge of coconut fibers in concrete". In: *Materials* 15.16 (2022), p. 5639. ISSN: 1996-1944.

[124] Jawad Ahmad et al. "Mechanical and durability performance of coconut fiber reinforced concrete: a state-of-the-art review". In: *Materials* 15.10 (2022), p. 3601. ISSN: 1996-1944.

[125] Conserv. *Lime plaster*. 2025. URL: https://www.lime-mortars.co.uk/lime-plaster/equipment/coir/250g.

[126] P Baruah and S Talukdar. "A comparative study of compressive, flexural, tensile and shear strength of concrete with fibres of different origins". In: *Indian concrete journal* 81.7 (2007), pp. 17–24. ISSN: 0019-4565.

[127] Majid Ali et al. "Mechanical and dynamic properties of coconut fibre reinforced concrete". In: *Construction and Building Materials* 30 (2012), pp. 814–825. ISSN: 0950-0618.

[128] Sanjay Mavinkere Rangappa et al. *Plant fibers, their composites, and applications*. Elsevier, 2022. ISBN: 0323852904.

[129] Sejal Sanjay Shanbhag, Manish K Dixit, and Petros Sideris. "Examining the global warming potential of hempcrete in the United States: A cradle-to-gate life cycle assessment". In: *Developments in the Built Environment* 20 (2024), p. 100572. ISSN: 2666-1659.

[130] Ildiko Merta. "Hemp fibres—a promising reinforcement for cementitious materials". In: *Natural Fibres: Advances in Science and Technology Towards Industrial Applications: From Science to Market*. Springer, 2016, pp. 291–303. ISBN: 9401775133.

[131] Md Azree Othuman Mydin et al. "Studies on durability properties of natural fibre-reinforced green lightweight foamed concrete employing industrial hemp fibres". In: *Journal of Advanced Research in Applied Mechanics* 101.1 (2023), pp. 36–52.

[132] Paulien De Bruijn. *Hemp concretes: mechanical properties using both shives and fibres*. Sveriges Lantbruksuniversitet, 2008. ISBN: 9185911879.

[133] Biobased-Bouwen. *Hennepbeton - Dunagro*. 2025. URL: https://www.biobasedbouwen.nl/producten/hempcal-hennepbeton/.

[134] Ribbonstore. *Natuurlijke touwen*. 2025. URL: https://www.ribbonstore.nl/a-53057234/hennep-draad/hennep-draad-2-mm-1-kilo/?srsltid=AfmBOor02eGSBMFDe5ddFDHEpIaXpMg_hUkFvGHPWsa_ch8dpUJZqqrF#description.

[135] Elie Antoine Awwad et al. "Sustainable concrete using hemp fibres". In: *Proceedings of the Institution of Civil Engineers-Construction Materials* 166.1 (2013), pp. 45–53. ISSN: 1747-6518.

[136] Basalt Fibertec GmbH. *Basalt Rebars - Product description*. Pamphlet. 2021. URL: https://www.basalt-fibertec.ch/images/pdf_data_sheets_en/060_tdb-basalt_rebars_en.pdf.

[137] Kevin van der Lingen. "Flexural Behaviour of Concrete Reinforced With Basalt Fibre Reinforcement Bars: An Experimental and Numerical Research". Master Thesis. 2024.

[138] Smarter Building Systems LLC. *Basalt Facts and Blogs - basalt.guru*. 2025. URL: https://basalt.guru/category/basalt-rebar/.

[139] Ahmed El Refai et al. "Shear performance of basalt fiber-reinforced concrete beams reinforced with BFRP bars". In: *Composite Structures* 288 (2022), p. 115443. ISSN: 0263-8223. DOI: https://doi.org/10.1016/j.compstruct.2022.115443. URL: https://www.sciencedirect.com/science/article/pii/S0263822322002379.

[140] Metal-Products. *Producten en Diensten*. 2025. URL: https://www.metalproductshorst.com/producten-en-diensten/staalvezels/.

[141] Stichting MRPI. *Environmental Product Declaration - Steel fibers for concrete, mortar and grout*. Journal Article. 2023.

[142] Cement Online. *Artikelen - Staalvezelbeton getoetst*. 2025. URL: https://www.cementonline.nl/artikelen/staalvezelbeton-getoetst.

[143] ArcelorMittal. *products - FE Flat End Steel Fibres – Wiresolutions*. 2025. URL: https://barsandrods.arcelormittal.com/wiresolutions/steelfibres/products/FE_Flat_End/EN.

[144] Sika Group. *Concrete - Concrete technologies - Steel Fibres for Fibre-Reinforced Concrete*. 2025. URL: https://gbr.sika.com/en/construction/concrete/concrete-technology/fibre-reinforcedconcrete/steel-fibres.html.

[145] Hectar B.V. *Staalvezelbeton – Kennisbank*. 2025. URL: https://www.hectar.nl/kennisbank/staalvezelbeton/.

[146] K Holschemacher, T Mueller, and Y Ribakov. "Effect of steel fibres on mechanical properties of high-strength concrete". In: *Materials and Design (1980-2015)* 31.5 (2010), pp. 2604–2615. ISSN: 0261-3069.

[147] Stichting MRPI. *Environmental Product Declaration - Reinforcing Mesh Plus*. Journal Article. 2023.

[148] IES. "Environmental Product Declaration - Reinforcing Steel electro-welded mesh". In: *The International EPD System (IES)* S-P-13315.EPD-IES-0013315:002 (2024).

[149] Betonstaal.nl. *Bouwstaalmatten*. 2022.

[150] Stichting MRPI. *Environmental Product - DeclarationEco2cem GGBS - Ecocem Benelux B.V.* Report. 2018. URL: https://www.mrpi.nl/epd/ecocem-benelux-b-v-eco2cem-ggbs/.

[151] ATG 2609. *Bestanddelen voor beton Hydrualische bindmiddelen en toevoegsels*. Report. 2025. URL: https://www.ecocemglobal.com/nl/downloads/.

[152] Chao Wu et al. "Effect of Fiber Content on Mechanical Properties and Microstructural Features of Concrete Containing Polypropylene Fibers". In: *Advances in Materials Science and Engineering* 2022 (2022). DOI: 10.1155/2022/1531570. URL: https://onlinelibrary.wiley.com/doi/full/10.1155/2022/1531570.

[153] IES. "Environmental Product Declaration - Superplasticizers Sika®ViscoCrete® and Sika®ViscoFlow®". In: *The International EPD System* S-P-06999.EPD-IES-0006999:001 (2022).

[154] Javier Oliver. "A consistent characteristic length for smeared cracking models". In: *International Journal for Numerical Methods in Engineering* 28.2 (1989), pp. 461–474.

[155] Ahmet B Kizilkanat et al. "Mechanical properties and fracture behavior of basalt and glass fiber reinforced concrete: An experimental study". In: *Construction and Building Materials* 100 (2015), pp. 218–224. ISSN: 0950-0618.

[156] Braam et al. *Concrete Structures under Temperature and Shrinkage Deformations – Theory and Practice*. Original Dutch edition, widely known as the "Pink Book". Delft: Delft University of Technology, 2-11.

[157] Tarek Alkhrdaji et al. "Guide for the design and construction of structural concrete reinforced with FRP bars". In: *Proceedings of the American Concrete Institute (ACI) Committee* 440 (2006).

[158] International Federation for Structural Concrete (fib). *Model code 2010*. Standard. fib, 2010.

[159] Stora Enso. *Environmental Product Declaration: Cross Laminated Timber (CLT)*. Report. EPD Number: S-P-09949, Valid until 2028-10-06. 2023. URL: https://www.environdec.com/library/epd4991.

[160] Adolf Würth GmbH & Co. KG. *Environmental Product Declaration: Stainless Steel Screws*. Report. EPD Number: EPD-AWU-20230569-CBA1-EN, Valid until 20.03.2029. 2024. URL: https://epd-online.com.

[161] João Paulo C Rodrigues, Luís Laím, and António Moura Correia. "Behaviour of fiber reinforced concrete columns in fire". In: *Composite Structures* 92.5 (2010), pp. 1263–1268. ISSN: 0263-8223.

[162] Shamsad Ahmad. "Reinforcement corrosion in concrete structures, its monitoring and service life prediction—a review". In: *Cement and concrete composites* 25.4-5 (2003), pp. 459–471. ISSN: 0958-9465.

[163] International Federation for Structural Concrete (fib). *Model code 2010*. Standard. fib, 2010.

[164] Arie van Wijngaarden. *Eigenschappen betonstaal B500A/B/C*. Pamphlet. 2016. URL: https://www.betonstaal.nl/kenniscentrum/betonstaal-b500abc-wat-is-het-verschil/.

[165] VWN. *wapned*. 2025. URL: https://www.wapned.nl/leden/overzicht.

[166] NMD. *Milieudata (LCA)*. 2024. URL: https://milieudatabase.nl/nl/milieudata-lca/milieu-impact-categorieen/rekenen-met-set-a1-en-set-a2/#accordion-item-1-wanneer-gaat-de-overgang-van-set-a1-naar-set-a2-plaatsvinden.

[167] IES. "Environmental Product Declaration - Processed steel: wire, mesh and truss girder". In: *The International EPD System (IES)* S-P-11654.EPD-IES-0011654:002 (2024).

[168] IES. "Environmental Product Declaration - Concrete Reinforcing Steel and Mesh Products". In: *The International EPD System (IES)* S-P-06079.EPD-IES-0006079:002 (2022).

[169] Stichting MRPI. *MRPI EPD-overzicht*. Web Page. 2025. URL: https://www.mrpi.nl/epd-overzicht/?_zoeken_epd_button_2=wapeningsstaal.

[170] IES. *Search the EPD Library*. 2025. URL: https://www.environdec.com/library.

[171] Michael Sansom and Nicholas Avery. "Briefing: Reuse and recycling rates of UK steel demolition arisings". In: *Proceedings of the Institution of Civil Engineers-Engineering Sustainability*. Vol. 167. Thomas Telford Ltd, 2014, pp. 89–94. ISBN: 1751-7680.

[172] Rademacher de Vries Architecten. *De verduurzaming van de staalindustrie in het Noordzeekanaalgebied*. Pamphlet. Den Haag, 2024. URL: https://www.collegevanrijksadviseurs.nl/adviezen-publicaties/publicatie/2024/06/27/de-verduurzaming-van-de-industrie.

[173] Stanislav Aidarov et al. "Cost-oriented analysis of fibre reinforced concrete column-supported flat slabs construction". In: *Journal of building engineering* 51 (2022), p. 104205. ISSN: 2352-7102.

[174] Luca Lanzoni, Andrea Nobili, and Angelo Marcello Tarantino. "Performance evaluation of a polypropylene-based draw-wired fibre for concrete structures". In: *Construction and building materials* 28.1 (2012), pp. 798–806. ISSN: 0950-0618.

[175] Jedidi Malek and Machta Kaouther. "Destructive and non-destructive testing of concrete structures". In: *Jordan journal of civil engineering* 8.4 (2014), pp. 432–441.

[176] Jim Bowyer et al. "Understanding steel recovery and recycling rates and limitations to recycling". In: *Dovetail Partners Inc.: Minneapolis, MN, USA* (2015), pp. 1–12.

[177] Munirah Hussein et al. "Heavy metals in leachate, impacted soils and natural soils of different landfills in Malaysia: An alarming threat". In: *Chemosphere* 267 (2021), p. 128874. ISSN: 0045-6535.

[178] Sushovan Sarkar and Debabrata Mazumder. "Solid waste management in steel industry-challenges and opportunities". In: *Eng. Technol. Int. J. Soc. Behav. Educ. Econ. Bus. Ind. Eng* 9.3 (2015), pp. 978–981.

[179] Miguel Alfonso Sellitto and Fábio Kazuhiro Murakami. "Destination of the waste generated by a steelmaking plant: a case study in Latin America". In: *Aestimum* (2020), pp. 127–144. ISSN: 1724-2118.

[180] Tata-Steel. *Hoe maken we staal*. 2025. URL: https://www.tatasteelnederland.com/staal-maken/wist-je-dit-al?_gl=1*6tyxfx*_up*MQ..*_ga*MTg4NTQ3MDAyOC4xNzQyMjIzMjg1*_ga_ZJG2C9ENNR*MTc0MjIyMzI4NC4xLjEuMTc0MjIyMzMzMS4wLjAuMA..

A

Detailed criteria list

In chapter 4 5 total criteria are used to assess the alternatives, in this appendix a more extensive description of the criteria that were not used given. In Figure A.1 an overview of example criteria that could be considered in a more extensive multi criteria analysis (MCA) is given.

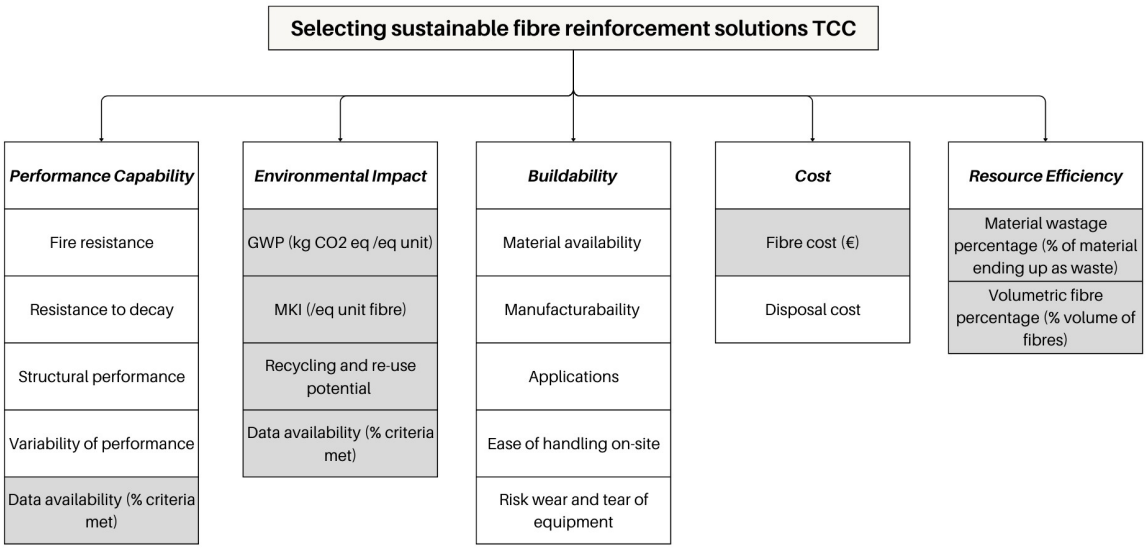

Figure A.1: Overview of criteria

A.1. Performance Capability

Performance capability evaluates the mechanical and durability properties of the alternative, including its tensile strength, stiffness, fatigue resistance, and long-term stability within the composite system. It also considers how well the alternative integrates with the TCC system to maintain composite action. Due to its direct influence on structural integrity and system reliability, this criterion weighs highly. Performance capability has several sub-criteria as follows:

- **Fire resistance**(quantitative): Assesses the alternative's ability to withstand high temperatures and resist ignition, flame spread, and structural failure under fire conditions. This includes compliance with fire safety standards (e.g., Euroclass ratings, ASTM E84) and the effectiveness of fire retardant treatments. For this sub-criterion, the alternatives will be put into order based on their thermal resistance.
- **Resistance to decay**(qualitative): Evaluates the alternatives durability against biological deterioration, such as fungal decay, insect attacks, and moisture-induced degradation. Highly resistant

alternatives enhance long-term performance and reduce maintenance needs.

- **Maintainability**(qualitative): Assesses the effort and resources needed to maintain the alternatives performance over time. This includes cleaning requirements, resistance to wear and tear, and ease of replacement or repair. Low-maintenance materials enhance cost-efficiency and user satisfaction.
- **Data availability**(quantitative): Examines the accessibility and reliability of performance-related data, including fire test reports, durability studies, thermal conductivity values, and maintenance guidelines. Comprehensive, third-party-verified data ensures informed decision-making and regulatory compliance.

A.2. Environmental impact

This criterion assesses the overall ecological footprint of the alternative, considering embodied carbon, energy consumption, pollution, and resource depletion across its life cycle. Sustainable sourcing, carbon sequestration potential, and low-impact processing methods are prioritized. Given the increasing focus on sustainability in construction, this factor holds substantial weight.

- **Toxicity**(quantitative): Examines whether the alternative contains or emits harmful substances that pose health or environmental risks. This includes volatile organic compounds (VOCs), heavy metals, and other hazardous chemicals that may leach during production, use, or disposal. Low-toxicity materials are prioritized to ensure safety for both workers and occupants.
- **Ozone depletion**(quantitative): Assesses the alternatives contribution to ozone layer degradation, primarily through the release of chlorofluorocarbons (CFCs) or other ozone-depleting substances during its production or disposal. Alternatives with negligible or zero ozone depletion potential are preferred.
- **Minimize pollution**(quantitative): Evaluates the extent to which the alternative contributes to environmental contamination. This includes water, soil, and air pollution during manufacturing, transportation, and end-of-life stages. Alternatives with minimal emissions, clean processing techniques, and reduced waste generation are more desirable.
- **Impact on air quality**(quantitative): Focuses on the A=lternative's effect on indoor and outdoor air quality, particularly through emissions of particulate matter, VOCs, or other pollutants. Materials that support healthier indoor environments by maintaining low emissions and avoiding off-gassing are favored.
- **Embodied energy**(quantitative): Measures the total energy consumption required for the alternatives extraction, processing, manufacturing, and transportation. Alternatives with lower embodied energy, particularly those utilizing renewable energy sources during production, are considered more sustainable.
- **Environmental impact during harvest**(quantitative): Examines the ecological effects of obtaining the raw material. For natural alternatives, this includes land use, deforestation risks, water consumption, and soil degradation. For synthetic or recycled alternatives, this considers the energy intensity and environmental cost of raw material sourcing. Alternatives that are responsibly sourced, certified sustainable, or derived from waste materials score higher in this category.
- **Data availability**(quantitative): The data availability criterion assesses the accessibility, reliability, and comprehensiveness of environmental data related to the alternative. A well-documented alternative allows for more accurate sustainability assessments, compliance with regulations, and informed decision-making.

A.3. Buildability

Resource efficiency measures how effectively raw materials are utilized in alternative production. This includes renewability, minimal energy-intensive processing, and optimized material usage to reduce excess consumption. Alternatives that require fewer resources while maintaining high performance are favoured, making this an important consideration.

- **Material availability**(quantitative): Examines the abundance and accessibility of raw materials required to produce the alternative. Considerations include geographical availability, supply

chain stability, reliance on rare or non-renewable resources, and potential competition with other industries. Easily sourced materials reduce supply disruptions and improve project feasibility.

- **Manufacturability**(qualitative): Evaluates the complexity of producing the alternative at an industrial scale. Factors include processing requirements (e.g., energy-intensive steps, specialized equipment), consistency in quality, and feasibility of mass production. A highly manufacturable alternative allows for cost-effective and reliable supply chains.
- **Ease of construction**(qualitative): Evaluates how straightforward it is to integrate the alternative into building systems, considering factors like workability, compatibility with adhesives/binders, and required construction techniques. Materials that simplify construction can reduce costs and errors.
- **Risk wear and tear of equipment**(qualitative): Assesses the potential impact of alternative processing on machinery and tools. Some alternatives may cause excessive wear due to abrasiveness, hardness, or clogging tendencies, leading to increased maintenance costs and reduced efficiency in manufacturing and installation.

A.4. Life Cycle Cost

The life cycle cost criterion accounts for the total financial impact of the alternative, including production, installation, maintenance, and end-of-life disposal or reuse. A cost-effective alternative must balance affordability with durability to minimize long-term expenses. Since cost efficiency is crucial for large-scale implementation, this criterion receives significant weighting.

- **Initial cost**(quantitative): Assesses the upfront expenses associated with material procurement and processing, from when the alternative would be ready to use in a concrete mixture. Lower initial costs improve the economic feasibility of a alternative.
- **Maintanance cost**(qualitative): Evaluates the ongoing expenses required to maintain the alternatives performance over its lifespan. This includes durability, susceptibility to wear and tear, resistance to environmental degradation (e.g., moisture, UV exposure), and the need for repairs or replacements. A low-maintenance alternative reduces operational costs over time.
- **Disposal cost**(qualitative): Examines the financial implications of managing the alternative at the end of its life cycle. Considerations include ease of recycling, landfill fees, potential for repurposing, and adherence to waste management regulations. Sustainable disposal solutions can mitigate costs and environmental impact.

A.5. Resource efficiency

Resource efficiency measures how effectively raw materials are utilized in alternative production. This includes renewability, minimal energy-intensive processing, and optimized material usage to reduce excess consumption. alternatives that require fewer resources while maintaining high performance are favoured, making this an important practical consideration.

- **Amount of wastage during production**(quantitative): Evaluates how much material is lost or wasted during manufacturing. A alternative with a high production yield and minimal scrap contributes to a more efficient and cost-effective process. Efficient production techniques, such as recycling by-products, improve sustainability.
- **Reinforcement ratio** (quantitative): Examines how much alternative is required within a concrete mix to achieve the desired performance. A lower volumetric percentage with high effectiveness enhances efficiency, reduces material consumption, and minimizes added weight in structural applications.
- **Use of local materials**(qualitative): Prioritizes the availability and sourcing of alternatives from local or regional suppliers to minimize transportation emissions, lower costs, and support local economies. Locally sourced alternatives improve supply chain sustainability and reduce the carbon footprint of production.

A.6. Waste minimization

This criterion evaluates the potential for alternative reuse, recycling, and biodegradability at the end of its life cycle. Materials that contribute to a circular economy by reducing construction and demolition waste are preferred. Since waste management is a growing concern in sustainable design, this criterion plays a key role in alternative selection.

- **Environmental sound disposal option**(qualitative): Assesses the availability and implementation of disposal methods that minimize environmental harm. This includes evaluating whether the material can be safely decomposed, incinerated with energy recovery, or disposed of in a manner that prevents soil and water contamination. Environmentally responsible disposal practices help conserve landfill space and protect ecosystems.
- **Recycling and reuse potential**(qualitative): Evaluates the alternative's capacity to be recycled or repurposed at the end of its useful life. Materials with high recycling and reuse potential can be transformed into new products or applications, reducing the demand for virgin resources and lowering environmental impact. For example, certain construction materials can be recycled into aggregate for new concrete or repurposed for other structural applications.

B

Baseline for a more detailed assessment of criteria

In chapter 4.3, figure A.1, an overview is given of criteria to assess for a full assessment in A. An overview of values and explanations of the process involving regular reinforcement mesh for these criteria is given in this appendix.

Fire resistance: Steel and concrete have the same coefficient of expansion when heated. The minimum thickness is not specified, but assumed at 10 mm as this is the c_{min} given by the Eurocode 2 , section 4.2 [47]. In FRC it says that replacing the rebar by steel fibres is good until a certain level, after which they behave worse (Joao Paulo C., 2010) [161]. The concrete protects most of the rebar, the melting point of steel reinforcement lies between 1200 and 1300 degrees Celsius [4].

Resistance to decay: Steel is corrosion sensitive due to (i) carbonation of concrete, and (ii) presence of chloride ions. The permeability, nature and intensity of cracks, and the cover thickness, of concrete, have a great bearing upon the initiation and sustenance of reinforcement corrosion. Once reinforcement corrosion is initiated, it progresses almost at a steady rate and shortens the service life of the structure, by causing surface cracking and subsequently spalling of the cover concrete due to expansion of the corroding steel. The rate of corrosion directly affects the extent of the remaining service life of a corroding RC structure [162].

Structural performance: The requirements and design with fibres can be found in fib 2010, volume 1 and 2 [158, 163]. With most alternatives in literature, it is mentioned by how well they could replace regular steel rebar. The rebar type used in the original design is Comparable parameters:

- Yield strength Strength (MPa) – Point that plastic deformation starts.
- Steel rebar benchmark: The characteristic values of reinforcement steel can be found in Appendix C of NEN-1992-1-1 where the characteristic yield strength has a value between 400 and 600 Mpa [47]. **Better if:**Alternative has comparable or higher tensile strength. Elastic Modulus (GPa) – Stiffness and ability to resist deformation.
- Steel rebar benchmark: In NEN-EN 1992-1-1 in section 3.2.7 the elastic modules is defined with a calculation value of 200 GPa [47]. **Better if:** Alternative has similar or higher modulus; worse if it is significantly lower, leading to excessive deflection.
- Bond Strength with Concrete (MPa or pull-out force in kN) – Determines composite action efficiency. Steel rebar benchmark: For reinforcement bars with a diameter of 5-6 mm the minimum relative rib area fR,min is equal to 0.035, according to Eurocode 2 Appendix C[47]. **Better if:** Alternative has superior interfacial bonding and does not pull out easily.
- Ductility and Energy Absorption (%) – Ability to deform before failure. Steel rebar benchmark: High ductility when Rm/Re factor 1.05-1.35 and characteristic deformation at maximum strength

ϵ_{uk} has a value between 2.5 and 7.5 %, according to Eurocode 2 Appendix C [47, 164]. **Better if:** Alternative prevents brittle failure and provides residual strength after cracking.

Variability of performance: Very consistent, as it is made in a factory, set guidelines in place for fabrication. In line with design codes, NEN-EN 10080, section 7.2.1: "In the context of this European Standard the characteristic value of an essential characteristic is (unless otherwise indicated) the lower or upper limit (fractile p) of the confidence interval at which there is a 90 % probability (1 - α = 0, 90) that 95 % (p = 0, 95) or 90 % (p = 0, 90) of the individual measured values are at or above this lower limit, or are at or below this upper limit respectively" [45]. From section 7.3.3 the density of reinforcement steel can be found as 7850 kg/m^3.

Data availability: As there are many producers and there is a lot of research into rebar, mechanical data (characteristic values) for standard rebar is widely available. In the Netherlands alone, there are 45 members of the Dutch association for reinforcement. This number of producers in such a small country showcases the widespread availability of data besides the numerous research topics related to reinforcement steel [165].

Global Warming Potential (GWP): For A1-A3 the EPD of van Merksteijn International B.V., accessed through the MRPI database, gives the following value for the GWP per tonne of reinforcement steel mesh, 455 kg CO_2 equivalent/tonne of rebar mesh (made out of sustainably produced steel) [147]. For another rebar mesh, made of virgin materials, the GWP is equal to 2320 kg CO_2 equivalent/tonne rebar mesh, accessed through the International EPD System library. The keywords steel mesh, with Product Category – Construction Products, PCR – Being updated – Construction products (EN 15804 +A2), in the Geographical scope of Europe were used to look for reinforcement mesh EPD's [148]. For this analysis, the average of these two GWP values will be used.

Millieu Kosten Indicator (MKI): In the Netherlands, the values used to get the shadow costs are as follows, there is a table with the monetary value per environmental impact category (per functional unit). From EPD's the amount in units of that category is calculated based on the amount needed (converted from the declared functional unit) in a project/element. Each category has a different cost attached to it, based on how much it would cost to undo the impact in that category. The values used to convert the impact to a monetary value in the Netherlands can be found in Figure B.1 [166].

Milieu effect	Eenheid	Weegfactor
Klimaatverandering*	€/kg CO2	0,116
Klimaatverandering: fossiel	€/kg CO2	0,116
Klimaatverandering: biogeen	€/kg CO2	0,116
Klimaatverandering: landgebruik en landgebruiksveranderingen	€/kg CO2	0,116
Ozonlaagaantasting	€/kg CFK11-eq	32
Verzuring	€/Mol H+-eq.	0,39
Vermesting: zoetwater	€/kg P-eq	1,96
Vermesting: zoutwater	€/kg N	3,28
Vermesting: land	€/Mol N-eq.	0,36
Smogvorming	€/kg NMVOC-eq.	1,22
Grondstofuitputting: metalen en mineralen	€/kg Sb-eq	0,3
Grondstofuitputting: energiedragers	€/MJ	0,00033
Waterschaarste	m3 water eq	0,00506
Fijnstofvorming	€/kg ziektegevallen	549.750
Straling	€/kg kBq U235-eq	0,049
Ecotoxiciteit: aquatisch zoetwater	€/CTUe	0,00013
Humane toxiciteit: kankerverwekkend effect	€/CTUh	1.096.368
Humane toxiciteit: niet-kankerverwekkend effect	€/CTUh	147.588
Landgebruik	Pt/m2 .jaar	0,000087

Figure B.1: Conversion factors, environmental impact to euros [166]

For the steel reinforcement mesh two EPD's from Spain has been considered as this is relatively close to the Netherlands and the Dutch EPD used for the GWP was incomplete for a full shadow cost calculation. The EPD made of virgin materials results in a shadow cost of 364,21 euros per tonne of steel rebar mesh and the 99.99% recycled mesh results in 86,94 euros per tonne steel rebar mesh [148, 167]
Data availability: For EPD's available, the MRPI has one EPD available for steel reinforcement meshes, in the international EPD library three EPD's for steel reinforcement meshes were available in the Europe region [147, 148, 167, 168]. When looking at just reinforcement bars, there are six EPD's available in the

MRPI database and three were found in the international EPD database (keyword: reinforcement bar) in the Europe region [169, 170].
The specific mesh reinforcement had data for the life cycle stages A1-A3 and was missing data for 6 of the environmental impact categories (human health, toxicity and soil quality) [147].
All the EPD's from the internation EPD library had data from the life cycle stages A1-A4, C1-C4 and stage D. The Hellenic Halyvourgia S.A. – Concrete Reinforcing Steel and Mesh Products contains data on 14 environmental impact categories and the other two have data on all the 19 environmental impact categories [148, 167, 168].

Recycling and re-use options: Steel in itself is a material that is recycled often. Within the construction industry, most reinforcement steel from demolition of buildings gets recycled. Thus reinforcement alternatives will score better if they are easier to recycle [171].

Material availability: As mentioned previously, there are 45 members of the reinforcement steel association in the Netherlands alone. On top of the steel reinforcement industry the Netherlands is host country to Tata steel Ijmuiden, the largest steel factory. These two factors show the wide availability of both steel as a material and reinforcement steel as a product readily available [165, 172].

Manufacturability: Steel is a material that is widely processed into various products. The process is quite energy intensive due to the high temperatures needed to process the raw materials and there are various steps involved before semi-finished products are acquired. Yet, there is a big industry in place to process and produce steel products, in 2023 the crude steel production globally was 1.892 mega tons. In the Netherlands roughly 88% of steel companies focus on braiding concrete reinforcement, showing the manufacturing of steel reinforcement is a significant part of the Dutch steel sector and shows the relative ease of steel reinforcement compared to other reinforcement methods [49–51].

Applications: Concrete reinforcement is a widely used application of steel as a component in the construction industry with K. Kwon (2021) estimating a use of roughly 950 million tonnes in 2019 [48]. There are design codes in place that ensure safe design of structures using steel reinforcement, the lack of design codes for materials such as fibre reinforcement can make it difficult to apply them on a bigger scale in projects. Reinforcement steel has been used for over a century, with the first specifications related to reinforcement steel dating back to the 1910's [44]. In the Netherlands the first guidelines for quality of steel rebar date back to 1968 and currently can be found in NEN-EN 10080 [45, 46]. The guidelines related to designing with reinforcement steel can be found in Eurocode 2 for concrete structures [47].

Ease of handling on-site: In general, it expected that by replacing the reinforcement steel meshes with fibre, the time on site will be reduced and thus all fibres are expected to be easier to handle than reinforcement steel. The parameters for the assessment of the construction period used by Aidarov et al. in 2022 were the following [173]:

- Number of steel fixers in the crew,
- Amount of labour hours in a shift,
- Number of shifts per a day.

As can be seen in Figure B.2[173], the shore positioning, beam placement of the shoring system and concrete compacting and finishing are activities that do not change when replacing standard reinforcement meshes with alternatives. What does change is the reinforcement fixing (which is completely eliminated in a comparison) and the concrete pumping (depending on the influence of the alternative on the workability) In this assessment, the weight of the alternatives to put into the concrete mixture and influence on workability of the concrete mixture will be the factors that influence the ease of handling on site the most, as moving heavier materials will be more labour intensive and if the workability decreases the pouring of concrete might take longer. Risk wear and tear of equipment: As mentioned by Lanzoni et al. (2012) some alternatives, for example steel fibres, might increase the wear and tear of the machinery used for mixing and pouring/pumping of the concrete [174]. Thus if a alternative contributes to the wear and tear of the equipment in a significant way, this alternative performs worse

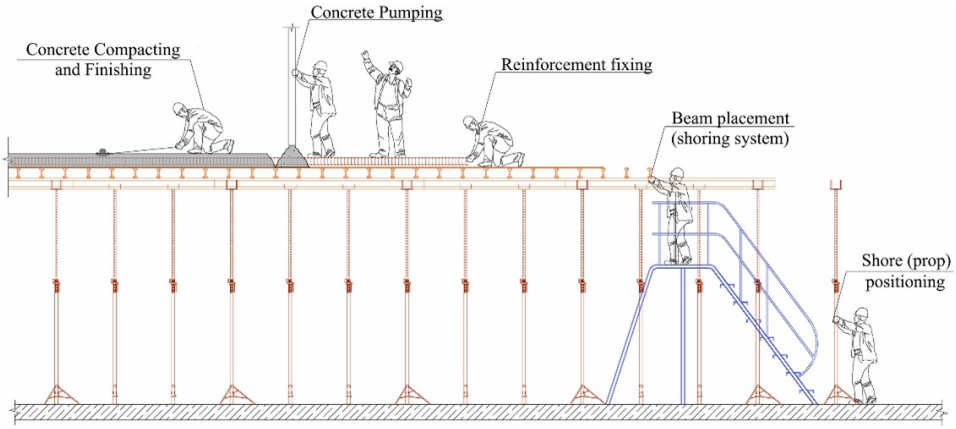

Figure B.2: Construction action influencing construction time [173].

in comparison

Reinforcement cost from supplier: The specific cost of reinforcement is dependent on the supplier. The supplier for the reinforcement meshes in the DPG building is unknown, data for the price reinforcement meshes has been taken from betonstaal. From their website, the price per tonne of mesh is roughly equal to 900,50 euros (assuming between more than 30 meshes were used for the whole building, 1 mesh $\approx$ 10 m^2 and the drawings show 1368.8 m^2 in rebar meshes) [149].

Maintainability: As the maintainability of reinforcements is dependent on their long-term performance, the maintainability also depends heavily on how well one can assess the performance of the reinforcement in real time. For existing concrete structures, there are various methods in place to assess the state of the reinforcement both destructive and non-destructive [175]. The more methods and research there are available for the assessment of (fibre) reinforcement, the more likely it is to be cheaper.

Disposal costs: In 2015, Bowyer et al. Mentioned that in 2013, 81% steel ended up getting recycled, with the construction sector recycling roughly 97.5% of steel in North America the remaining is disposed of as old scrap steel [176]. The disposal of steel is usually done by disposing it in a landfill, however if done improperly the leakage of metal can have a negative impact on the environment [177]. Considering the possible shadow costs of waste, the more harmful substances it contains the more it will cost.

Volumetric wastage percentage: The production of steel results in 0.55 -0.6 tons of waste [178, 179]. In the Netherlands, some of the waste products can be used in a different application, according to TATA steel 98% of all the waste- and bi-products gets a new life. These products can be either used directly or be used in another process [180].

Reinforcement ratio The volumetric reinforcement percentage has a set limit in reinforced concrete. For reinforcement bars this is equal to 0,04 Ac, which, if the concrete cross-section is considered to be 100%, results in 4% maximum of reinforcement steel, according to Eurocode 2 section 9.2.1.1 [47]. In the DPG floor type 1 the reinforcement ratio was found to be $\approx$ 0.38%, as can be seen in C.

–> add the whole part above this to the appendix and bring the appendix of the alternatives to the main report, makea similar summary for the origina design mesh.

C

Environmental impact and Cost MCA - Calculation examples

C.1. Concrete values

The calculation for the regular concrete mixture can be found in the main report, the computation of the FRC mixes can be found in this appendix.

For the concrete mix used for the FRC, the values can be found in table C.1, the mixture components and amounts are taken from literature [74–77, 152, 153]. This mixture results in a total of 188.21 kg CO_2 equivalent per m^3 of concrete, without the fibres being included. The resulting concrete density is equal to 2498 kg/m^3.

Table C.1: Fibre concrete mix values (C30/37)[74–77, 152, 153]

Component	kg CO_2 eq/ func unit	func unit	Amount[kg]/ m^3 concrete	kg CO_2 eq/ m^3
Cement (Hoogovencement CEMIII - 42.5 N)	500	metric tons	330	$0.364 \cdot 500 = 182.00$
Stone (River stone)	1.74	metric tons	1045	$1.74E\text{-}3 \cdot 1045 = 1.82$
River sand	2.39	metric tons	750	$0.00239 \cdot 750 = 1.79$
Water	-	-	200	-
Water reducing agent	0.867	kg	3	$0.867 \cdot 3 = 2.601$

Using eco$_2$cem instead of CEM II for 50% of the cement, results in a strength class of 42.5 N which is comparable to that used for C30/37 in the first concrete mix. Eco$_2$cem has a GWP of 3.39E-2 kg CO_2 eq/kg material. Replacing the original cement content with 50% eco$_2$cem results in the following environmental impacts of concrete mixtures, as can be seen in table C.2 [150, 151].

For the concrete mix used for the regular reinforcement mesh, the GWP of the concrete mix results in 69.31 kg CO_2 eq/m^3 concrete. The density is equal to 2325 kg/ m^3 - the sum of kg material per m^3 of concrete. For the fibre reinforcement mix the GWP of the concrete mix results in 105.69 kg CO_2 eq/m^3 concrete, as can be seen in table C.3. The density is equal to 2498 kg/ m^3 - the sum of kg material

per m^3 of concrete.

Table C.2: Regular concrete mix values (C30/37) - 50% eco_2cem [74–77, 150]

Component	kg CO_2 eq/ func unit	func unit	Amount[kg]/ m^3 concrete	kg CO_2 eq/ m^3
Regular cement (42.5N)	364.00	metric tons	165	$0.364 \cdot 165 = 60.06$
Eco_2cem	33.9	metric tons	165	3.39E-2 ·165 = 5.59
Stone (River stone)	1.74	metric tons	1070	1.74E-3 ·1070= 1.86
River sand	2.39	metric tons	750	$0.00239 \cdot 750 = 1.79$
Water	-	-	175	-

Table C.3: Fibre concrete mix values (C30/37) - 50% eco_2cem [74–77, 150, 152, 153]

Component	kg CO_2 eq/ func unit	func unit	Amount[kg]/ m^3 concrete	kg CO_2 eq/ m^3
Regular cement (42.5N)	364.00	metric tons	250	$0.364 \cdot 250 = 91.00$
Eco_2cem	33.9	metric tons	250	3.39E-2 ·250= 8.48
Stone (River stone)	1.74	metric tons	1045	1.74E-3 ·1045= 1.82
River sand	2.39	metric tons	750	2.39E-3 ·750= 1.79
Water	-	-	200	-
Water reducing agent	0.867	kg	3	$0.867 \cdot 3 = 2.601$

C.2. Reinforcement bars emissions - example steel mesh - regular concrete

To determine the impact of this reinforcement alternative, firstly, the reinforcement ratio needs to be calculated. The rebar in the original TCC floor design is spaced every 150 mm - spanning in both directions - with a diameter of 6mm. The reinforcement ratio can be calculated as follows:

$$A_S \cdot n \cdot l_s/(l_c \cdot b_c \cdot h_c)$$

Where:
A_s is equal to the cross-section of the reinforcement bar;
n is equal to the amount of bars in the analysed cross-section;
l_s is equal to the length of the rebar in the analysed cross-section;
l_c is equal to the length of the concrete cross-section;
b_c is equal to the width of the concrete cross-section;
h_c is equal to the height of the concrete cross-section.
The cross-section of one bars is equal to 28.27 mm^2, with a total of 13 1/3 bars per m^2 of the slab.
With a concrete slab of 100 mm thick, this then results in a reinforcement ratio of:

$$28,27 \cdot 13_{1/3} \cdot 1000/(1000 \cdot 1000 \cdot 100 = 0.38\%$$

Using the density, GWP and cost values from chapter 4 and the concrete GWP data from table **??**, the

cost and GWP for this specific application is calculated. These calculations leave out the overlap length - including this would result in extra material and thus extra cost and higher GWP.

Example calculation: GWP - regular cement
Using the density of steel - $\rho = 7850 kg/m^3$ [45] - and the reinforcement ratio of 0.38%, this would then result in a specific amount - in kg - of the amount of reinforcement applied per m^3 concrete.

$$\rho \cdot \ v\%/100 = 7850 \cdot 0.38/100 = 29.83 kg$$

With a GWP of 1372.5 kg CO_2 eq/tonne reinforcement, average of two EPD's [79, 147]. The total GWP in life cycle stages A1-A3 of regular reinforced concrete results in - just for the reinforcement in one cubic meter of concrete- 40.94 kg CO_2 eq/m^3 of reinforced concrete.
With 99.68 % of the volume being concrete, for the concrete portion, using the data from table **??**,this then results in 136.461 kg CO_2 eq/m^3 of reinforced concrete.
For this specific application the GWP of reinforced concrete is the equal to 177.40 kg CO_2 eq/m^3 of reinforced concrete.

Example calculation: GWP - 50 % for the cement eco$_2$cem
This section shows examples of the calculations, using 50 % for the cement eco$_2$cem.
With a GWP of 1372.5 kg CO_2 eq/tonne reinforcement this results in - just for the reinforcement in one cubic meter of concrete - 40.94 kg CO_2 eq/m^3 of reinforced concrete.
With 99.68 % of the volume being concrete, for the concrete portion, using the data from table C.2,this then results in 77.11 kg CO_2 eq/m^3 of reinforced concrete.
For this specific application the GWP of reinforced concrete is the equal to 118.05 kg CO_2 eq/m^3 of reinforced concrete.

Example calculation: Cost
From chapter 4, the cost per kg of steel mesh reinforcement is found to be equal to 0.9005 €/kg. The cost of the reinforcement is then equal to 26.86 €/m^3 reinforced concrete.

C.3. Fibre reinforcement calculations- example PP fibres

Using the density, GWP and cost values from chapter 4 and the concrete GWP data from table C.1, the cost and GWP for this specific application is calculated. These calculations leave out the overlap length - including this would result in extra material and thus extra cost and higher GWP.

Example calculation: GWP
Using the density of PP-fibre - $\rho = 900 kg/m^3$ - and the reinforcement ratio of 0.43%, this would then result in a specific amount - in kg - of the amount of reinforcement applied per m^3 concrete.

$$\rho \cdot \ v\%/100 = 900 \cdot 0.43/100 = 3.87 kg$$

With a GWP of 4600 kg CO_2 eq/tonne reinforcement this results in - just for the reinforcement in one cubic meter of concrete - 17.80 kg CO_2 eq/m^3 of reinforced concrete.
With 99.57 % of the volume being concrete, for the concrete portion, using the data from table C.1, this then results in 199.60 kg CO_2 eq/m^3 of reinforced concrete.
For this specific application the GWP of reinforced concrete is equal to 217.40 kg CO_2 eq/m^3 of PP-fibre reinforced concrete.

Example calculation: GWP - 50 % for the cement eco$_2$cem
Using the density, GWP and cost values from chapter 4 and the concrete GWP data from table C.3, the cost and GWP for this specific application is calculated. This section shows examples of the calculations, using 50 % for the cement eco$_2$cem.
With a GWP of 4600 kg CO_2 eq/tonne reinforcement this results in - just for the reinforcement in one cubic meter of concrete - 17.80 kg CO_2 eq/m^3 of reinforced concrete.
With 99.57 % of the volume being concrete, for the concrete portion, using the data from table C.3, this then results in 117.42 kg CO_2 eq/m^3 of reinforced concrete.
For this specific application the GWP of reinforced concrete is the equal to 135.22 kg CO_2 eq/m^3 of PP-fibre reinforced concrete.

Example calculation: Cost
From chapter B, the cost per kg of PP-fibre mesh reinforcement is found to be equal to 35.- €/kg. The cost of the reinforcement is then equal to 135.45 €/m^3 reinforced concrete.

D

Sensitivity analysis

The multi criteria analysis (MCA) performed in chapter 4 gave one variable as the best in all scenario. It is worth noting that though the values and methods used in the MCA were chosen with care and based on literature, they were chosen by one person and with a small set of data, thus it is of interest to check how sensitive the MCA is to certain changes in approach or variables. In this paragraph multiple sensitivity checks are performed.

D.1. Interpolation method

The current method used is a linear interpolation between the 'best' and the 'worst' value, scored 100.00 and 0.00 respectively. Another way of calculating the scores of the alternatives between these would be logarithmic and exponential. These can be seen below in figures D.6 D.8 D.2 D.4 D.5 D.7 D.1 D.3. Each interpolation method has two variants:

1. In the first variant, the linear scores per alternative were transformed either logarithmic or exponential.
2. With the second variant the original values were transformed either logarithmic or exponential and then calculated linearly between the maximum and minimum of these transformed values.

log	A1	A2	A3	A4	A5	A6	A7	Sm1	Sm2	FRP
C11 (Mpa)	1,02779	1,68456	2	1,8666691	0	1,048975	1,58026	0,849	0,849	1,3532
C12 (m/m%)	1,852198	1,12909	0	0,6905368	2	0,69897	0,88606	1,12909	1,12909	0,48812
C21 (kg CO2	1,907281	1,91465	0	1,9326578	1,930846	1,967192	1,76488	1,97075	1,97075	2
C31	1,875061	1,69897	1,544068	1,1760913	0	0	1,87506	2	2	1,69897
C41 (€/kg)	1,867671	0	0,674308	1,9625251	1,521027	1,899094	1,96263	1,99427	1,99427	2
weighteds	2,74	2,48	0,53	2,64	2,37	2,42	2,55	2,72	2,72	2,69

Figure D.1: Logarithmically transformed linear scores variant, regular cement

log	A1	A2	A3	A4	A5	A6	A7	Sm1	Sm2	FRP
C11 (Mpa)	0,668122	1,68456	2	1,86666913	0	1,048975	1,58026	0,849	0,849	1,3532
C12 (m/m%)	1,852198	1,12909	0	0,69053684	2	0,69897	0,88606	1,12909	1,12909	0,48812
C21 (kg CO2	1,937809	1,94522	0	1,96343801	1,9606	1,997296	1,79488	1,96619	1,96619	2
C31	1,875061	1,69897	1,54406804	1,17609126	0	0	1,87506	2	2	1,69897
C41 (€/kg)	1,867671	0	0,674308	1,96252511	1,521027	1,899094	1,96263	1,99427	1,99427	2
weighteds	2,72	2,51	0,53	2,68	2,40	2,45	2,58	2,71	2,71	2,69

Figure D.2: Logarithmically transformed linear scores variant, eco$_2$cem cement

The methods influence the results, as seen in figures D.6 D.8 D.2 D.4 D.5 D.7 D.1 D.3. In D.1 D.2 it can be seen that alternative A1, polypropylene (PP) fibres, score best, followed by regular mesh reinforcement

log2	A1	A2	A3	A4	A5	A6	A7	Sm1	FRP
C11 (Mpa)	25,668531	79,93551931	100	91,439981	0	43,087075	73,476199	33,347238	59,871039
C12 (m/m%	89,05176	41,39182985	0	21,149696	100	21,458034	29,129569	41,39183	14,695257
C21 (kg CO2	70,36684	72,20340363	0	76,996063	76,492992	87,621992	44,667397	88,843012	100
C31	93,753063	84,94850022	77,20340222	58,804563	0	0	93,753063	100	84,9485
C41 (€/kg)	39,547477	0	1,500940067	67,65579	12,391729	45,919749	67,709694	92,22847	100
weighteds	101,37	97,99	22,34	106,88	90,54	101,43	77,68	122,21	132,44

Figure D.3: Logarithmically transformed values variant, linearly interpolated, regular cement

log2	A1	A2	A3	A4	A5	A6	A7	Sm1	FRP
C11 (Mpa)	25,6685307	79,93551931	100	91,43998142	0	43,0870751	73,4761993	33,3472379	59,8710386
C12 (m/m%	89,0517605	41,39182985	0	21,14969641	100	21,4580337	29,129569	41,3918299	14,6952571
C21 (kg CO2	113,515117	116,5034748	17,36658151	124,5482617	123,2244018	142,876246	75,0216859	125,857613	144,583481
C31	93,7530632	84,94850022	77,20340222	58,80456295	0	0	93,7530632	100	84,9485002
C41 (€/kg)	39,5474775	0	1,500940067	67,65579029	12,39172873	45,9197487	67,7096937	92,2284704	100
weightedsc	144,52	142,29	39,70	154,43	137,27	156,68	108,03	159,23	177,02

Figure D.4: Logarithmically transformed variant, linearly interpolated, eco$_2$cem cement

and Basalt fibre reinforcement polymer bars (refered to as FRP in the figures).
In D.3 it can be seen that alternative FRP, score best, followed by regular mesh reinforcement and alternative A4, basalt fibre. Whereas in D.4 the steel mesh is followed by A6, hemp fibres.

exp	A1	A2	A3	A4	A5	A6	A7	Sm1	Sm2	FRP
C11 (Mpa)	42651,0612	1,01E+21	2,688E+43	8,886E+31	1	72672,74	3,32E+16	1168,174	1168,174	6,23E+09
C12 (m/m%	7,9749E+30	701894,6	1	134,80727	2,69E+43	148,4132	2191,426	701894,6	701894,6	21,69156
C21 (kg CO2	1,2036E+35	4,79E+35	1	1,554E+37	1,09E+37	1,86E+40	1,88E+25	3,99E+40	3,99E+40	2,69E+43
C31	3,7332E+32	5,18E+21	1,586E+15	3269017,4	1	1	3,73E+32	2,69E+43	2,69E+43	5,18E+21
C41 (€/kg)	1,0533E+32	1	112,61552	6,904E+39	2,6E+14	2,66E+34	7,06E+39	7,25E+42	7,25E+42	2,69E+43
weightedsc	1,20E+35	4,79E+35	3,36E+42	8,79E+38	3,36E+42	1,86E+40	8,82E+38	4,31E+42	4,31E+42	3,02E+43

Figure D.5: Exponentially transformed linear scores variant, regular cement

exp	A1	A2	A3	A4	A5	A6	A7	Sm1	Sm2	FRP
C11 (Mpa)	105,3372	1,01E+21	2,6881E+43	8,8862E+31	1	72672,74	3,32E+16	1168,174	1168,174	6,23E+09
C12 (m/m%	7,97E+30	701894,6	1	134,807273	2,69E+43	148,4132	2191,426	701894,6	701894,6	21,69156
C21 (kg CO2	4,32E+37	1,92E+38	1	8,3738E+39	4,6E+39	1,44E+43	1,2E+27	1,5E+40	1,5E+40	2,69E+43
C31	3,73E+32	5,18E+21	1,586E+15	3269017,37	1	1	3,73E+32	2,69E+43	2,69E+43	5,18E+21
C41 (€/kg)	1,05E+32	1	112,615516	6,9039E+39	2,6E+14	2,66E+34	7,06E+39	7,25E+42	7,25E+42	2,69E+43
weightedsc	4,32E+37	1,92E+38	3,36E+42	9,24E+39	3,36E+42	1,44E+43	8,82E+38	4,28E+42	4,28E+42	3,02E+43

Figure D.6: Exponentially transformed linear scores variant, eco$_2$cem cement

exp2	A1	A2	A3	A4	A5	A6	A7	Sm1	FRP
C11 (Mpa)	0,201196243	7,478388161	100	27,22947926	0	0,572246067	4,222905288	0,324333478	1,575078357
C12 (m/m%)	0,055308437	1,64081E-08	0	1,31748E-09	100	1,36377E-09	3,26423E-09	1,64081E-08	6,2614E-10
C21 (kg CO2 e	100	100	0	100	100	100	100	100	100
C31	1,38879E-09	1,92875E-20	5,90009E-27	1,2161E-35	0	0	1,38879E-09	100	100
C41 (€/kg)	100	0	99,99999988	100	100	100	100	100	100
weightedscor	112,53	100,93	25,00	115,90	125,00	112,57	113,03	125,04	125,20

Figure D.7: Exponentially transformed values variant, linearly interpolated, regular cement

From the exponential variants an influence on the best scoring alternative reinforcement is also found. First the influence of scoring variant 1. In D.3 it can be seen that alternative FRP, score best, followed by

exp2	A1	A2	A3	A4	A5	A6	A7	Sm1	FRP
C11 (Mpa)	0,20119624	7,478388161	100	27,22947926	0	0,57224607	4,22290529	0,32433348	1,57507836
C12 (m/m%	0,05530844	1,64081E-08	0	1,31748E-09	100	1,3638E-09	3,2642E-09	1,6408E-08	6,2614E-10
C21 (kg CO2	100	100	0	100	100	100	100	100	100
C31	1,3888E-09	1,92875E-20	5,90009E-27	1,2161E-35	0	0	1,3888E-09	100	100
C41 (€/kg)	100	0	99,99999988	100	100	100	100	100	100
weightedsc	112,53	100,93	25,00	115,90	125,00	112,57	113,03	125,04	125,20

Figure D.8: Exponentially transformed variant, linearly interpolated, eco$_2$cem cement

regular mesh reinforcement and alternative A5, coir fibre. Whereas in D.4 A6, hemp fibre, is followed by the steel mesh.
With scoring variant 2, in **??** it can be seen that alternative FRP, score best, followed by regular mesh reinforcement and alternative A4, basalt fibre.

D.2. Ranking

Instead of attaching a score to each value of the criteria, the alternatives can be ranked based on their values for a criterion. Resulting in a score between 1.0 and 9.0. In the figures D.9 D.10 below the result of the ranking can be seen. The ranking results in a smaller spread of scores, but also shifts some

	A1	A2	A3	A4	A5	A6	A7	Sm1	FRP
C11 (Mpa)	2	7	9	8	1	4	6	3	5
C21 (kgCO2 eq/m3 conc	3	4	1	6	5	7	2	8	9
C31	7	5	4	3	1	1	7	9	5
C41 (€/m3 concrete)	4	1	2	7	3	6	5	8	9
C12 (m/m - %)	8	5	1	3	9	4	7	5	2
total score (no weight)	24	22	17	27	19	22	27	33	30
total score (weighted)	6,875	7,75	4,25	10	8	9,875	6,75	12,125	12,5

Figure D.9: Ranked scores for regular cement

	A1	A2	A3	A4	A5	A6	A7	Sm1	FRP
C11 (Mpa)	2	7	9	8	1	4	6	3	5
C21 (kgCO2 eq/m3 conc	3	4	1	6	5	8	2	7	9
C31	7	5	4	3	1	1	7	9	5
C41 (€/m3 concrete)	4	1	2	7	3	6	5	8	9
C12 (m/m - %)	8	5	1	3	9	4	7	5	2
total score (no weight)	24	22	17	27	19	23	27	32	30
total score (weighted)	6,875	7,75	4,25	10	8	10,875	6,75	11,125	12,5

Figure D.10: Ranked scores for partial eco$_2$cem cement

alternatives in term of how well they do for the final scores. It shows that for both the regular cement and the partial eco$_2$cem the same reinforcement materials get the same scoring and that these are very close to each other. The basalt fibre reinforced polymer (BFRP) scores best. When not looking at BFRP reinforcement or regular reinforcement mesh, the basalt fibre get the highest score.

D.3. Weights

The main-criteria and sub-criteria both have weights attached to them in chapter 4 which contribute to the final reinforcement alternative. In this paragraph, the influence of the weights on the chosen final reinforcement is investigated. For reference, figures D.11 and D.12 show the total scores of the alternative reinforcements without weight attached to the main- and/or sub-criteria.

	A1	A2	A3	A4	A5	A6	A7	Sm1	FRP
C11 (Mpa)	4,66	48,37	100,00	73,56	0,00	11,19	38,04	7,06	22,55
C12 (m/m%)	71,15	13,46	0,00	4,90	100,00	5,00	7,69	13,46	3,08
C21 (kg CO2 eq/m3 con	80,78	82,16	0,00	85,64	85,28	92,72	58,19	93,49	100,00
C31	75	50	35	15	0	0	75	100	50
C41 (€/kg)	73,73	0,00	4,72	91,73	33,19	79,27	91,75	98,69	100,00
total	305,32	193,99	139,72	270,84	218,47	188,18	270,68	312,70	275,63

Figure D.11: Unweighted scores regular cement

	A1	A2	A3	A4	A5	A6	A7	Sm1	FRP
C11 (Mpa)	4,66	48,37	100,00	73,56	0,00	11,19	38,04	7,06	22,55
C12 (%)	71,15	13,46	0,00	4,90	100,00	5,00	7,69	13,46	3,08
C21 (kg CO2 eq/m3 con	86,66	88,15	0,00	91,93	91,33	99,38	62,36	92,51	100,00
C31	75,00	50,00	35,00	15,00	0,00	0,00	75,00	100,00	50,00
C41 (€/kg)	73,73	0,00	4,72	91,73	33,19	79,27	91,75	98,69	100,00
total	311,20	199,98	139,72	277,13	224,52	194,84	274,85	311,72	275,63

Figure D.12: Unweighted scores partial eco$_2$cem cement

D.3.1. Weights sub-criteria

For the sensitivity analysis of the sub criteria, the following weights are given to the sub criteria:

A. All sub-criteria 0.5;

B. Each sub-criteria weighted 1 and C1 0.5;

C. Sub-criteria of C1 together 1 the others already 1 (varying the values of weights w_{11} and w_{12}).

	A1	A2	A3	A4	A5	A6	A7	Sm1	FRP	sub criteria weight
C11 (Mpa)	4,66	48,37	100,00	73,56	0,00	11,19	38,04	7,06	22,55	0,50
C12 (m/m%)	71,15	13,46	0,00	4,90	100,00	5,00	7,69	13,46	3,08	0,50
C21 (kg CO2 eq/m3 con	80,78	82,16	0,00	85,64	85,28	92,72	58,19	93,49	100,00	0,50
C31	75	50	35	15	0	0	75	100	50	0,50
C41 (€/kg)	73,73	0,00	4,72	91,73	33,19	79,27	91,75	98,69	100,00	0,50
Weighted score	152,66	96,99	69,86	135,42	109,24	94,09	135,34	156,35	137,81	

Figure D.13: Weighted sub-criteria scores A. regular cement

	A1	A2	A3	A4	A5	A6	A7	Sm1	FRP	sub criteria weight
C11 (Mpa)	4,66	48,37	100,00	73,56	0,00	11,19	38,04	7,06	22,55	0,50
C12 (m/m%)	71,15	13,46	0,00	4,90	100,00	5,00	7,69	13,46	3,08	0,50
C21 (kg CO2 eq/m3 con	86,66	88,15	0,00	91,93	91,33	99,38	62,36	92,51	100,00	0,50
C31	75	50	35	15	0	0	75	100	50	0,50
C41 (€/kg)	73,73	0,00	4,72	91,73	33,19	79,27	91,75	98,69	100,00	0,50
Weighted score	155,60	99,99	69,86	138,56	112,26	97,42	137,42	155,86	137,81	

Figure D.14: Weighted sub-criteria scores A. eco$_2$cem cement

From figures D.13 and D.14 it can be seen that regular steel mesh reinforcement is the best scoring of the considered alternatives when the sub-crietria get a weight of 0.5, followed by Alternative 1, PP-fibres.
From figures D.15 and D.16 it can be seen that regular steel mesh reinforcement is the best scoring of

	A1	A2	A3	A4	A5	A6	A7	Sm1	FRP	sub criteria weight
C11 (Mpa)	4,66	48,37	100,00	73,56	0,00	11,19	38,04	7,06	22,55	0,50
C12 (m/m%)	71,15	13,46	0,00	4,90	100,00	5,00	7,69	13,46	3,08	0,50
C21 (kg CO2 eq/m3 con	80,78	82,16	0,00	85,64	85,28	92,72	58,19	93,49	100,00	1,00
C31	75	50	35	15	0	0	75	100	50	1,00
C41 (€/kg)	73,73	0,00	4,72	91,73	33,19	79,27	91,75	98,69	100,00	1,00
Weighted score	267,42	163,07	89,72	231,60	168,47	180,09	247,82	302,44	262,81	

Figure D.15: Weighted sub-criteria scores B. regular cement

the considered alternatives when the sub-crietria get a weight of 0.5, followed by Alternative 1, PP-fibres.
From figures D.17 and D.18 it can be seen that regular steel reinforcement scores the best in both cases.

	A1	A2	A3	A4	A5	A6	A7	Sm1	FRP	sub criteria weight	
C11 (Mpa)	4,66	48,37	100,00	73,56	0,00	11,19	38,04	7,06	22,55	0,50	
C12 (m/m%)	71,15	13,46	0,00	4,90	100,00	5,00	7,69	13,46	3,08	0,50	
C21 (kg CO2 eq/m3 con	86,66	88,15	0,00	91,93	91,33	99,38	62,36	92,51	100,00	1,00	
C31	75	50	35	15	0	0	75	100	50	1,00	
C41 (€/kg)	73,73	0,00	4,72	91,73	33,19	79,27	91,75	98,69	100,00	1,00	
Weighted score	273,30	169,06	89,72	237,89	174,52	186,74	251,98	301,46	262,81		

Figure D.16: Weighted sub-criteria scores B. eco$_2$cem cement

	A1	A2	A3	A4	A5	A6	A7	Sm1	FRP	sub criteria weight	
C11 (Mpa)	4,66	48,37	100,00	73,56	0,00	11,19	38,04	7,06	22,55	0,25	0,75
C12 (m/m%)	71,15	13,46	0,00	4,90	100,00	5,00	7,69	13,46	3,08	0,75	0,25
C21 (kg CO2 eq/m3 con	80,78	82,16	0,00	85,64	85,28	92,72	58,19	93,49	100,00	1,00	1,00
C31	75	50	35	15	0	0	75	100	50	1,00	1,00
C41 (€/kg)	73,73	0,00	4,72	91,73	33,19	79,27	91,75	98,69	100,00	1,00	1,00
Weighted score	284,04	154,35	64,72	214,44	193,47	178,54	240,23	304,04	257,95		
Weighted score	250,79	171,80	114,72	248,77	143,47	181,64	255,40	300,84	267,68		

Figure D.17: Weighted sub-criteria scores C. regular cement

	A1	A2	A3	A4	A5	A6	A7	Sm1	FRP	sub criteria weight	
C11 (Mpa)	4,66	48,37	100,00	73,56	0,00	11,19	38,04	7,06	22,55	0,25	0,75
C12 (m/m%)	71,15	13,46	0,00	4,90	100,00	5,00	7,69	13,46	3,08	0,75	0,25
C21 (kg CO2 eq/m3 con	86,66	88,15	0,00	91,93	91,33	99,38	62,36	92,51	100,00	1,00	1,00
C31	75	50	35	15	0	0	75	100	50	1,00	1,00
C41 (€/kg)	73,73	0,00	4,72	91,73	33,19	79,27	91,75	98,69	100,00	1,00	1,00
Weighted score	289,92	160,34	64,72	220,73	199,52	185,19	244,39	303,06	257,95		
Weighted score	256,67	177,79	114,72	255,06	149,52	188,29	259,57	299,86	267,68		

Figure D.18: Weighted sub-criteria scores C. eco$_2$cem cement

It is also worth noting that when sub-criteria C_{11} has a weight of 0.25 and C_{12} 0.75, the runner up is alternative 1, PP fibres. But when C_{11} has a weight of 0.75 and C_{12} 0.25, the runner up becomes FRP.

D.3.2. Weights of main-criteria

A. C1 gets a weight of 0.5, C2 a weight 1.0 and C3 and C4 get a weight of 0.25;

B. C1 gets a weight of 0.5, C2 a weight 1.0 and C3 and C4 get a weight of 0.125;

C. C1 gets a weight of 0.25, C2 a weight 1.0 and C3 and C4 get a weight of 0.125.

	A1	A2	A3	A4	A5	A6	A7	Sm1	FRP	sub criteria weight		
C11 (Mpa)	4,66	48,37	100,00	73,56	0,00	11,19	38,04	7,06	22,55	0,50	0,5	0,25
C12 (m/m%)	71,15	13,46	0,00	4,90	100,00	5,00	7,69	13,46	3,08	0,50	0,5	0,25
C21 (kg CO2 eq/m3 con	80,78	82,16	0,00	85,64	85,28	92,72	58,19	93,49	100,00	1,00	1,00	1,00
C31	75	50	35	15	0	0	75	100	50	0,25	0,125	0,125
C41 (€/kg)	73,73	0,00	4,72	91,73	33,19	79,27	91,75	98,69	100,00	0,25	0,125	0,125
Weighted score	155,86	125,57	59,93	151,55	143,58	120,64	122,75	153,42	150,31			
Weighted score	137,27	119,32	54,97	138,21	139,43	110,73	101,91	128,59	131,56			
Weighted score	118,32	103,87	29,97	118,60	114,43	106,68	90,47	123,45	125,16			

Figure D.19: Weighted criteria scores A. (white), B. (grey) and C. (blue) regular cement

	A1	A2	A3	A4	A5	A6	A7	Sm1	FRP	sub criteria weight		
C11 (Mpa)	4,66	48,37	100,00	73,56	0,00	11,19	38,04	7,06	22,55	0,50	0,5	0,25
C12 (m/m%)	71,15	13,46	0,00	4,90	100,00	5,00	7,69	13,46	3,08	0,50	0,5	0,25
C21 (kg CO2 eq/m3 con	86,66	88,15	0,00	91,93	91,33	99,38	62,36	92,51	100,00	1,00	1,00	1,00
C31	75	50	35	15	0	0	75	100	50	0,25	0,125	0,125
C41 (€/kg)	73,73	0,00	4,72	91,73	33,19	79,27	91,75	98,69	100,00	0,25	0,125	0,125
Weighted score	161,75	131,56	59,93	157,84	149,62	127,29	126,91	152,44	150,31			
Weighted score	143,16	125,31	54,97	144,50	145,48	117,38	106,07	127,61	131,56			
Weighted score	124,20	109,86	29,97	124,88	120,48	113,34	94,63	122,48	125,16			

Figure D.20: Weighted criteria scores A. (white), B. (grey) and C. (blue), eco$_2$cem cement

In figures D.19 D.20 A. is not coloured, B. is grey and C. is blue. It can be seen for A. that for both regular and eco$_2$cem cement, Alternative 1 , PP-fibres, scores best followed by regular steel mesh for regular

cement and basalt fibre for eco$_2$cem cement. For scenario B. for both regular and eco$_2$cem alternative 5, coir fibres scores best, followed by basalt fibres. In scenario C. FRP scores best, followed by regular rebar mesh in the case of regular cement and followed by basalt fibre in case of eco$_2$cem.

D.3.3. Combined weights

Combining B. from the sub-criteria with B. form the main criteria, this results in C. from the main criteria. This then results in the chosen alternative as argued in 4.5.

D.4. Excluding alternatives

Looking at the results in chapter 4 it can be noted that BFRP comes out on top and carbon scores the lowest. By then removing these two alternatives, a different scoring start to show. In the regular cement scenario, the regular reinforcement mesh scores best and in the partial eco$_2$cem scenario the basalt fibre scores the best, as can be seen in figures D.21 D.22 D.23 D.24.

	A1	A2	A3	A4	A5	A6	A7	Sm1
C11 (Mpa)	4,66	48,37	100,00	73,56	0,00	11,19	38,04	7,06
C12 (%)	71,15	13,46	0,00	4,90	100,00	5,00	7,69	13,46
C21 (kg CO2 eq/m3 con	86,40	87,88	0,00	91,60	91,22	99,18	62,25	100,00
C31	75	50	35	15	0	0	75	100
C41 (€/kg)	74,71	0,00	4,79	92,95	33,63	80,32	92,97	100,00
weightedscore	124,07	109,59	29,97	124,71	120,43	113,27	94,68	130,13

Figure D.21: Excluding BFRP, regular cement

	A1	A2	A3	A4	A5	A6	A7	Sm1
C11 (Mpa)	4,66	48,37	100,00	73,56	0,00	11,19	38,04	7,06
C12 (%)	71,15	13,46	0,00	4,90	100,00	5,00	7,69	13,46
C21 (kg CO2 eq/m3 con	87,20	88,70	0,00	92,50	91,90	100,00	62,75	93,09
C31	75	50	35	15	0	0	75	100
C41 (€/kg)	74,71	0,00	4,79	92,95	33,63	80,32	92,97	100,00
weightedscore	124,87	110,41	29,97	125,61	121,10	114,09	95,18	123,22

Figure D.22: Excluding BFRP, eco$_2$cem cement

	A1	A2	A4	A5	A6	A7	Sm1
C11 (Mpa)	6,33	65,75	100,00	0,00	15,22	51,71	9,60
C12 (%)	69,67	9,00	0,00	100,00	0,10	2,93	9,00
C21 (kg CO2 eq/m3 con	63,98	67,90	77,76	76,75	97,84	0,00	100,00
C31	75	50	15	0	0	75	100
C41 (€/kg)	74,71	0,00	92,95	33,63	80,32	92,97	100,00
weightedscore	101,70	92,84	116,25	105,95	111,71	34,66	129,65

Figure D.23: Excluding BFRP and carbon fibre reinforcement, regular cement

	A1	A2	A4	A5	A6	A7	Sm1
C11 (Mpa)	6,33	65,75	100,00	0,00	15,22	51,71	9,60
C12 (%)	69,67	9,00	0,00	100,00	0,10	2,93	9,00
C21 (kg CO2 eq/m3 con	65,64	69,67	79,87	78,25	100,00	0,00	81,45
C31	75	50	15	0	0	75	100
C41 (€/kg)	74,71	0,00	92,95	33,63	80,32	92,97	100,00
weightedscore	103,35	94,60	118,36	107,46	113,87	34,66	111,10

Figure D.24: Excluding BFRP and carbon fibre reinforcement eco$_2$cem cement

D.5. Setting the min and max values outside of the ranges of variables

For this check, the maximum and minimum were increased/decreased by 10 % on each side of the range. This results in the figures and scores as seen in figure D.26 D.25.

	A1	A2	A3	A4	A5	A6	A7	Sm1	FRP
C11 (Mpa)	4,50	44,01	90,67	66,78	0,29	10,41	34,67	6,68	20,68
C12 (m/m%)	64,53	12,63	0,52	4,93	90,48	5,02	7,44	12,63	3,29
C21 (kg CO2 eq/m3 con	79,82	80,97	12,49	83,87	83,57	89,78	61,00	90,41	95,84
C31	75	50	35	15	0	0	75	100	50
C41 (€/kg)	75,89	9,45	13,71	92,11	39,36	80,88	92,13	98,38	99,56
weighteds	107,31	95,48	29,98	106,22	99,84	101,82	87,15	117,63	117,53

Figure D.25: Extended range, regular cement

	A1	A2	A3	A4	A5	A6	A7	Sm1	Sm2	FRP
C11 (Mpa)	4,50	44,01	90,67	66,78	0,29	10,41	34,67	6,68	6,68	20,68
C12 (m/m%)	64,53	12,63	0,52	4,93	90,48	5,02	7,44	12,63	12,63	3,29
C21 (kg CO2 eq/m3 con	85,74	87,02	11,39	90,26	89,75	96,66	64,89	90,76	90,76	97,19
C31	75,00	50,00	35,00	15,00	0,00	0,00	75,00	100,00	100,00	50,00
C41 (€/kg)	75,89	9,45	13,71	92,11	39,36	80,88	92,13	98,38	98,38	99,56
weighteds	121,86	108,61	40,27	121,58	117,36	110,63	96,31	120,39	120,39	121,88

Figure D.26: Extended range, eco_2cem cement

The figure D.26 shows that regular mesh reinforcement, scores best, followed by alternative FRP and alternative A1, PP-fibre.
Figure D.25 shows that regular mesh reinforcement, scores best, followed by alternative FRP and alternative A1, PP-fibre.

D.6. Conclusion of sensitivity analysis

An overview of the ranking per method used in the sensitivity analysis can be seen in table D.1. In this table nr.1 comes best in the ranking of a specific analysis method and nr. 9 is the worst variant according to the same method.

The sensitivity analysis highlights that the outcome of the MCA is significantly influenced by the choice of analysis method, scoring approach, and weighting of criteria. While the top-performing alternatives tend to remain within a narrow score range across methods, their relative rankings can shift depending on these parameters. Notably, alternatives A2 and A3 – glass and carbon fibre – consistently rank lower and do not lead in any of the scenarios studied. This demonstrates that although the MCA offers a structured framework for decision-making, it is sensitive to methodological choices. Therefore, when applying this approach in practice, it is essential to clearly justify the selected weights and scoring systems to ensure transparency and reproducibility in the decision process.

[1] A1: Polypropylene Fibres
[2] A2: Glass Fibres
[3] A3: Carbon Fibres
[4] A4: Basalt Fibres
[5] A5: Coir Fibres
[6] A6: Hemp Fibres
[7] A7: Steel Fibres
[8] A8: Basalt fibre reinforced polymer (BFRP) bars
[9] A9: Standard steel mesh

Table D.1: Ranking of sensitivity analysis

	nr. 1	nr. 2	nr. 3	nr. 4	nr. 5	nr. 6	nr. 7	nr. 8	nr. 9
Logarithmic linear interpolation regular cement version 1	A1[1]	A9[9]	A8[8]	A4[4]	A7[7]	A2[2]	A6[6]	A5[5]	A3[3]
Logarithmic linear interpolation eco$_2$cem cement version 1	A1	A9	A8	A4	A7	A2	A6	A5	A3
Logarithmic linear interpolation regular cement version 2	A8	A9	A4	A6	A1	A2	A5	A7	A3
Logarithmic linear interpolation eco$_2$cem cement version 2	A8	A9	A6	A4	A1	A2	A5	A7	A3
Exponential linear interpolation regular cement version 1	A8	A9	A5	A3	A6	A7	A4	A2	A1
Exponential linear interpolation eco$_2$cem cement version 1	A8	A6	A9	A5	A3	A4	A7	A1	A2
Exponential linear interpolation regular cement version 2	A8	A9	A5	A4	A7	A6	A1	A2	A3
Exponential linear interpolation eco$_2$cem cement version 2	A8	A9	A5	A4	A7	A6	A1	A2	A3
Ranking method regular cement	A8	A9	A4	A6	A5	A2	A1	A7	A3
Ranking method eco$_2$cem cement	A8	A9	A6	A4	A5	A2	A1	A7	A3
Weights sub-criteria regular cement version A	A9	A1	A8	A4	A7	A5	A2	A6	A3
Weights sub-criteria eco$_2$cem cement version A	A9	A1	A4	A8	A7	A5	A2	A6	A3
Weights sub-criteria regular cement version B	A9	A1	A8	A7	A4	A6	A5	A2	A3
Weights sub-criteria eco$_2$cem cement version B	A9	A1	A8	A7	A4	A6	A5	A2	A3
Weights sub-criteria regular cement version C.1	A9	A1	A8	A7	A4	A5	A6	A2	A3
Weights sub-criteria eco$_2$cem cement version C.1	A9	A1	A8	A7	A4	A5	A6	A2	A3
Weights sub-criteria regular cement version C.2	A9	A8	A7	A1	A4	A6	A2	A5	A3
Weights sub-criteria eco$_2$cem cement version C.2	A9	A8	A7	A1	A4	A6	A2	A5	A3

Weights main-criteria regular cement version A	A1	A9	A4	A8	A5	A2	A7	A6	A3
Weights main-criteria eco_2cem cement version A	A1	A4	A8	A9	A5	A2	A6	A7	A3
Weights main-criteria regular cement version B	A5	A4	A1	A8	A9	A2	A6	A7	A3
Weights main-criteria eco_2cem cement version B	A5	A4	A1	A8	A9	A2	A6	A7	A3
Weights main-criteria regular cement version C	A8	A9	A4	A1	A5	A6	A2	A7	A3
Weights main-criteria eco_2cem cement version C	A8	A4	A1	A9	A5	A6	A2	A7	A3
Final weights criteria regular cement	A8	A9	A1	A4	A6	A5	A2	A7	A3
Final weights criteria eco_2cem cement	A8	A4	A1	A9	A5	A6	A2	A7	A3
Excluding BFRP regular cement	A9	A4	A1	A5	A6	A2	A7	A3	-
Excluding BFRP eco_2cem cement	A4	A1	A9	A5	A6	A2	A7	A3	-
Excluding BFRP and carbon fibre regular cement	A9	A4	A6	A5	A1	A2	A7	-	-
Excluding BFRP and carbon fibre eco_2cem cement	A4	A6	A9	A5	A1	A2	A7	-	-
Extended range regular cement	A9	A8	A1	A4	A6	A5	A2	A7	A3
Extended range eco_2cem cement	A8	A1	A4	A9	A5	A6	A2	A7	A3

E

LS-Dyna results

E.1. SLS models

The material models were verified by comparing hand calculations for sag to model computations of vertical displacement, using the same load. The hand calculation was computed for a non-reinforced slab and a regular reinforced slab. The sag was also computed for the fibre reinforced concrete model, even though no hand calculations were performed for that model. The hand calculations, using the following formula

$$w = \frac{5}{384} \cdot \frac{q \cdot l^4}{EI} \tag{E.1}$$

with;

- E = 33 GPa
- I = $\frac{1}{12(1-v^2) \cdot b \cdot h^3}$
- l = 2.4 m
- q = 9.9525 kN/m^2

The sag was found to be equal to 1.51 mm, which differs from the model outcome of the steel reinforced model roughly 0.15 mm.

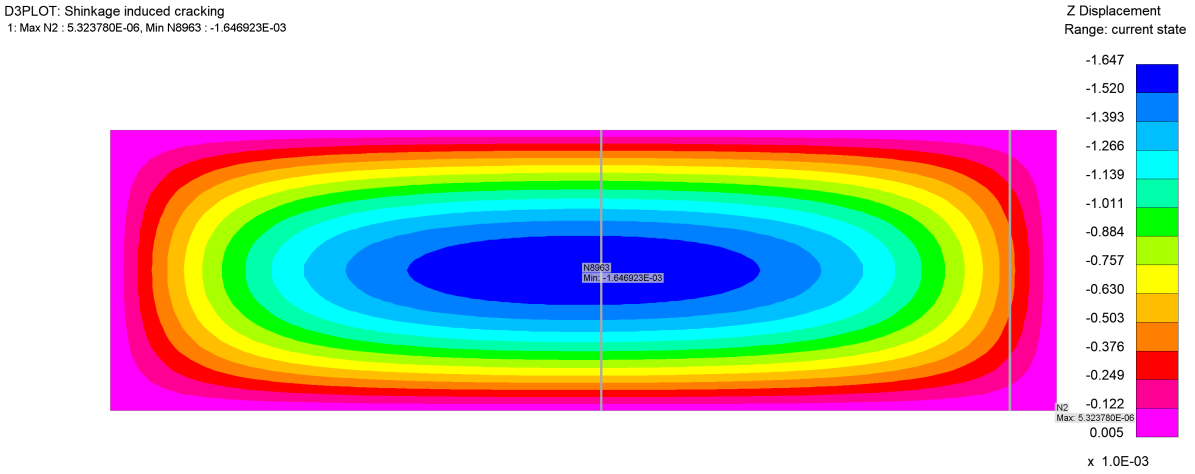

Figure E.1: SLS, model without reinforcement

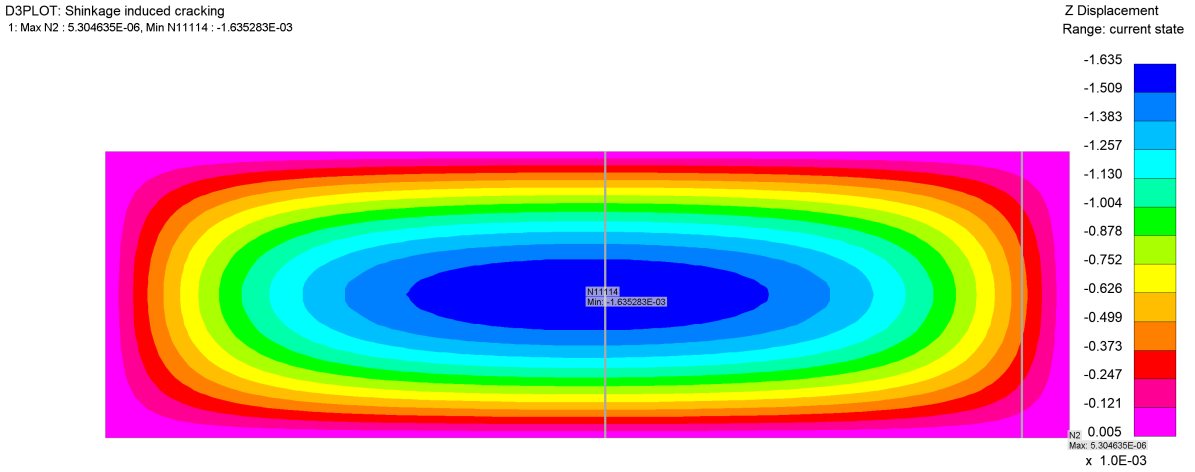

Figure E.2: SLS, model witt steel mesh reinforcement

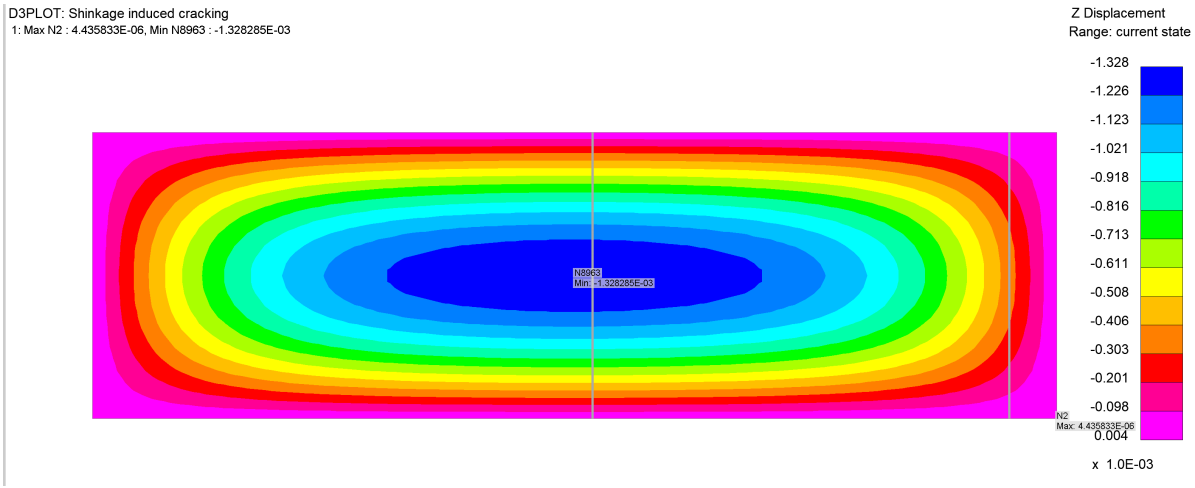

Figure E.3: SLS, model with basalt fibre reinforcement

E.2. Crack width development, shrinkage without discrete beams

E.2.1. Non-reinforced model

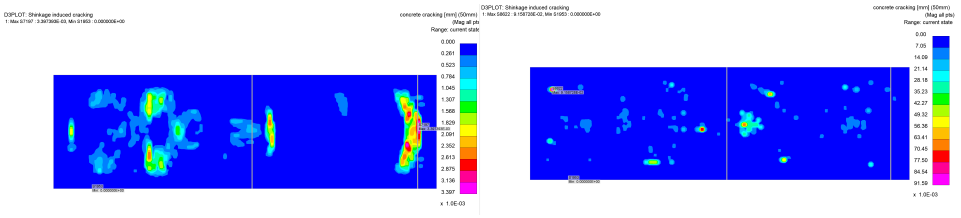

(a) Shrinkage cracks at t=0.51 **(b)** Shrinkage cracks at t=2.23

Figure E.4: Resultants from LS-Dyna for model without reinforcement

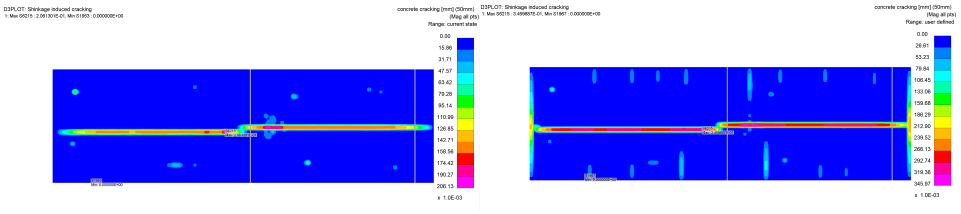

(a) Shrinkage cracks at t=2.24 **(b)** Shrinkage cracks at t=3.0

Figure E.5: Resultants from LS-Dyna for model without reinforcement

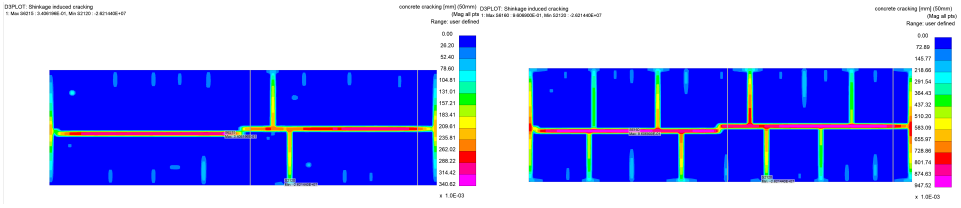

(a) Shrinkage cracks at t=3.01 **(b)** Shrinkage cracks at t=8.0

Figure E.6: Resultants from LS-Dyna for model without reinforcement

E.2.2. Steel mesh reinforced model

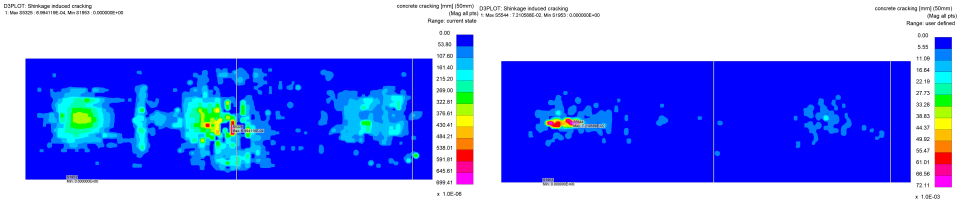

(a) Shrinkage cracks at t=0.51 **(b)** Shrinkage cracks at t=2.2

Figure E.7: Resultants from LS-Dyna for model with reinforcement

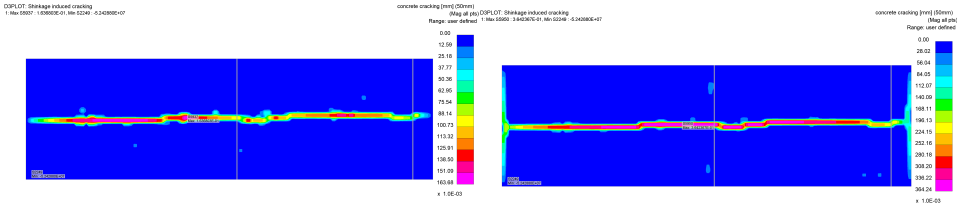

(a) Shrinkage cracks at t=2.36 **(b)** Shrinkage cracks at t=2.69

Figure E.8: Resultants from LS-Dyna for model with reinforcement

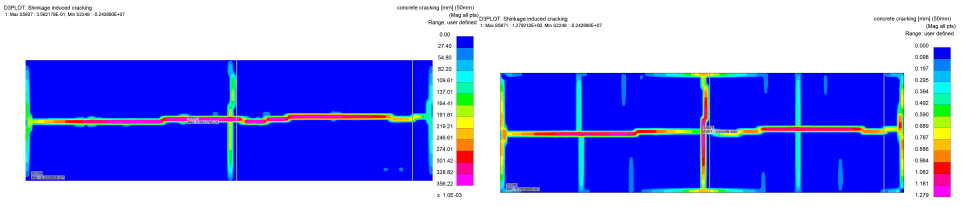

(a) Shrinkage cracks at t=2.70 **(b)** Shrinkage cracks at t=8.0

Figure E.9: Resultants from LS-Dyna for model with reinforcement

E.2.3. Basalt fibre reinforced model

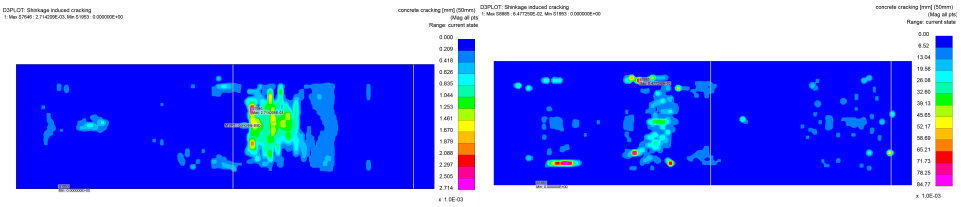

(a) Shrinkage cracks at t=0.51 **(b)** Shrinkage cracks at t=2.24

Figure E.10: Resultants from LS-Dyna for model with fibre reinforcement

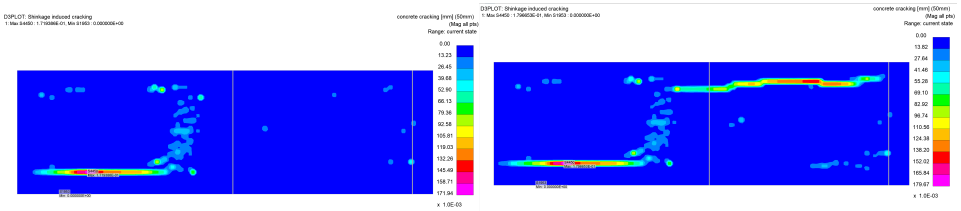

(a) Shrinkage cracks at t=2.25 **(b)** Shrinkage cracks at t=2.33

Figure E.11: Resultants from LS-Dyna for model with fibre reinforcement

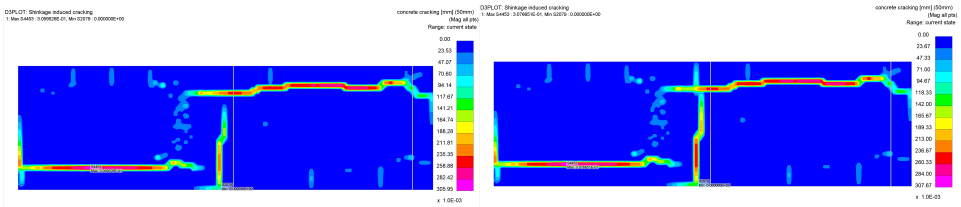

(a) Shrinkage cracks at t=2.93 **(b)** Shrinkage cracks at t=2.94

Figure E.12: Resultants from LS-Dyna for model with fibre reinforcement

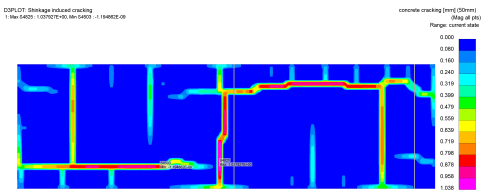

Figure E.13: Resultants from LS-Dyna for model with fibre reinforcement, Shrinkage cracks at t=8.0

E.3. Crack width development, shrinkage with discrete beams

E.3.1. Non-reinforced model

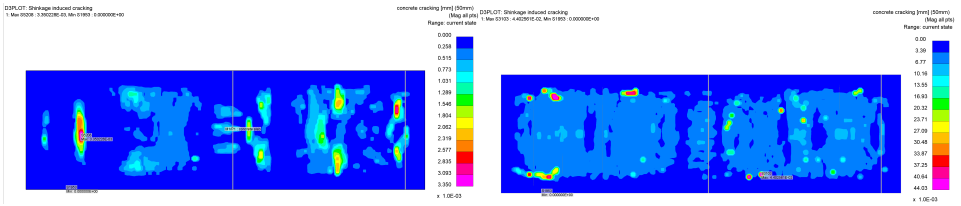

(a) Shrinkage cracks at t=0.51 **(b)** Shrinkage cracks at t=2.23

Figure E.14: Resultants from LS-Dyna for model without reinforcement

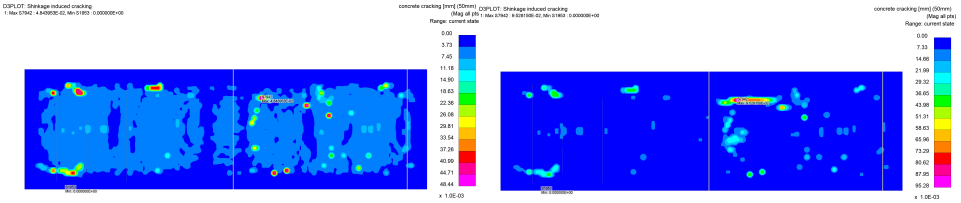

(a) Shrinkage cracks at t=2.27 **(b)** Shrinkage cracks at t=2.28

Figure E.15: Resultants from LS-Dyna for model without reinforcement

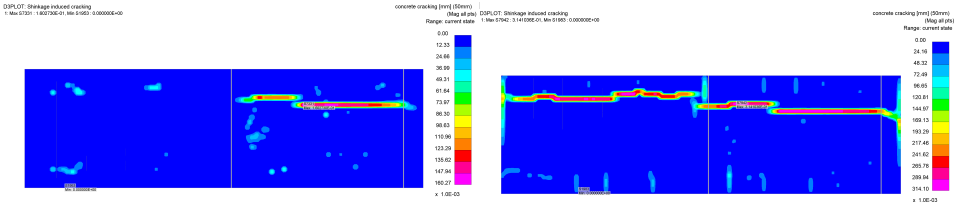

(a) Shrinkage cracks at t=2.29 **(b)** Shrinkage cracks at t=3.01

Figure E.16: Resultants from LS-Dyna for model without reinforcement

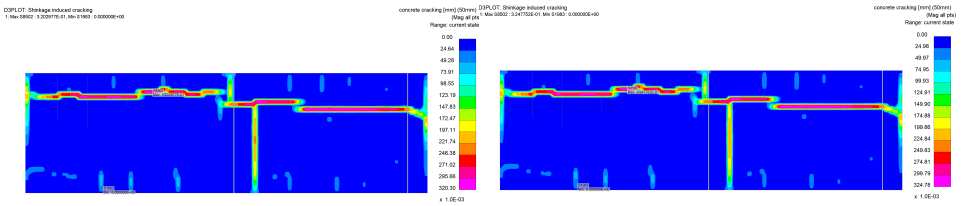

(a) Shrinkage cracks at t=3.06 **(b)** Shrinkage cracks at t=3.07

Figure E.17: Resultants from LS-Dyna for model without reinforcement

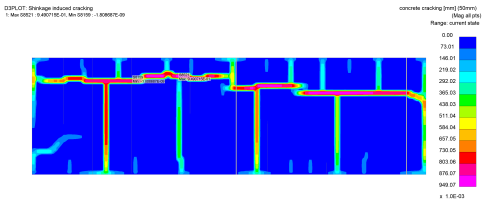

Figure E.18: Resultants from LS-Dyna for model with fibrereinforcement, Shrinkage cracks at t=8.0

E.3.2. Steel mesh reinforced model

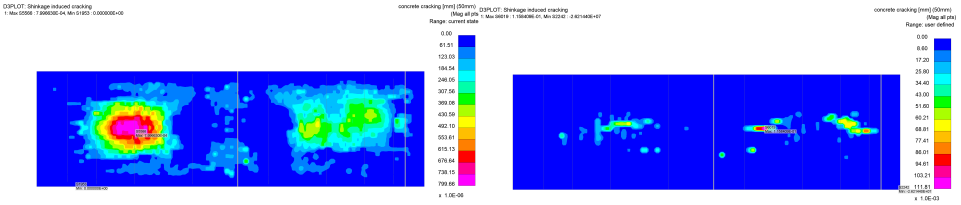

(a) Shrinkage cracks at t=0.51 **(b)** Shrinkage cracks at t=2.29

Figure E.19: Resultants from LS-Dyna for model with reinforcement

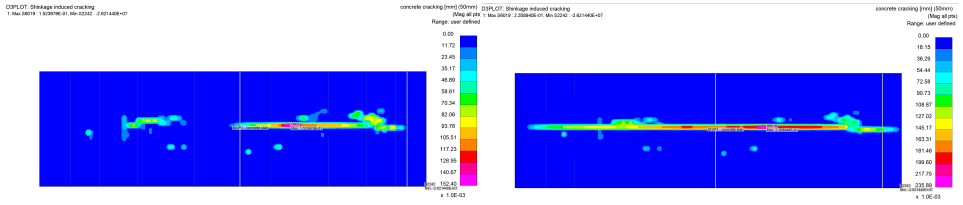

(a) Shrinkage cracks at t=2.32 **(b)** Shrinkage cracks at t=2.33

Figure E.20: Resultants from LS-Dyna for model with reinforcement

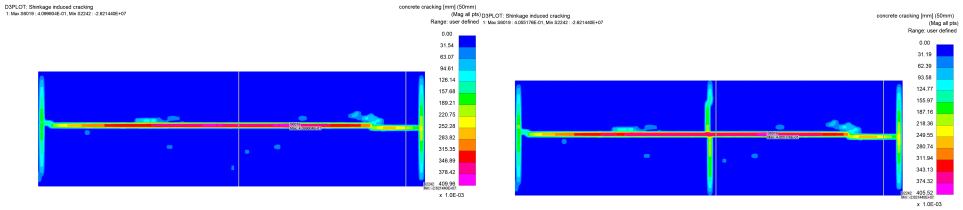

(a) Shrinkage cracks at t=2.70 **(b)** Shrinkage cracks at t=2.71

Figure E.21: Resultants from LS-Dyna for model with reinforcement

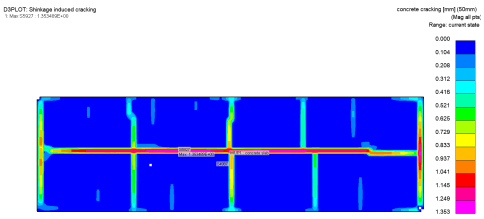

Figure E.22: Resultants from LS-Dyna for model with fibrereinforcement, Shrinkage cracks at t=8.0

E.3.3. Basalt fibre reinforced model

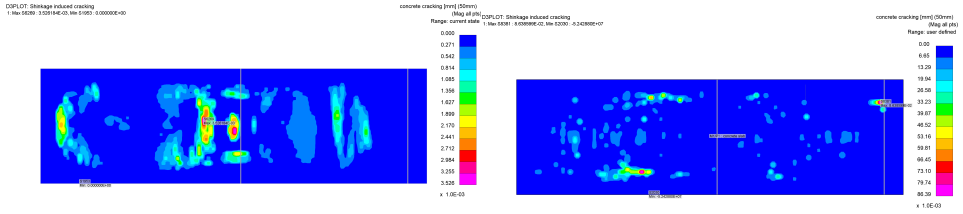

(a) Shrinkage cracks at t=0.51 **(b)** Shrinkage cracks at t=2.28

Figure E.23: Resultants from LS-Dyna for model with fibre reinforcement

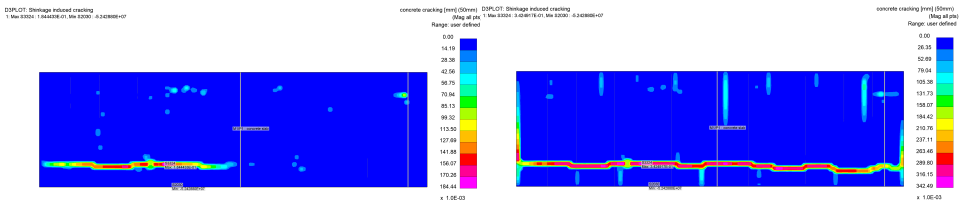

(a) Shrinkage cracks at t=2.29 **(b)** Shrinkage cracks at t=3.12

Figure E.24: Resultants from LS-Dyna for model with fibre reinforcement

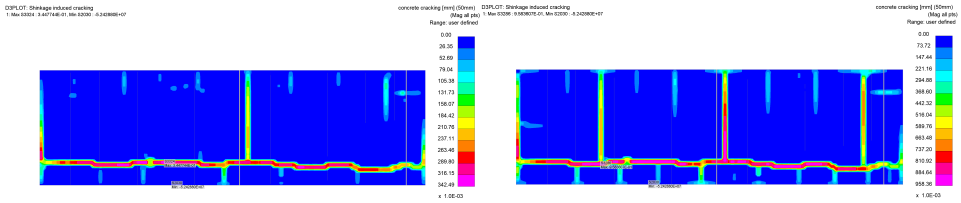

(a) Shrinkage cracks at t=3.13 **(b)** Shrinkage cracks at t=8.0

Figure E.25: Resultants from LS-Dyna for model with fibrereinforcement

F

Wind load model

F.1. Figures from rhino model

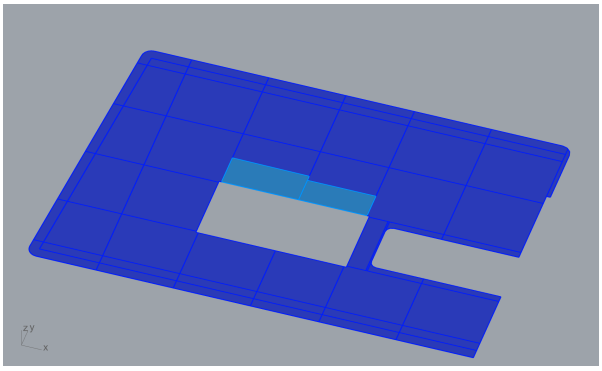

Figure F.1: Showcasing the rhino model of the floor slab studied in this chapter

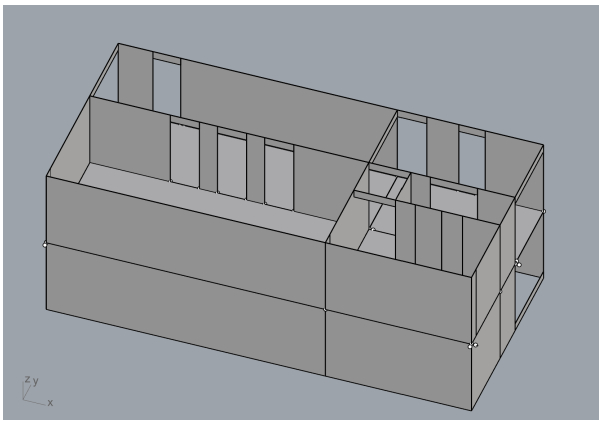

Figure F.2: Showcasing the rhino model of the core, for the slab studied in this chapter

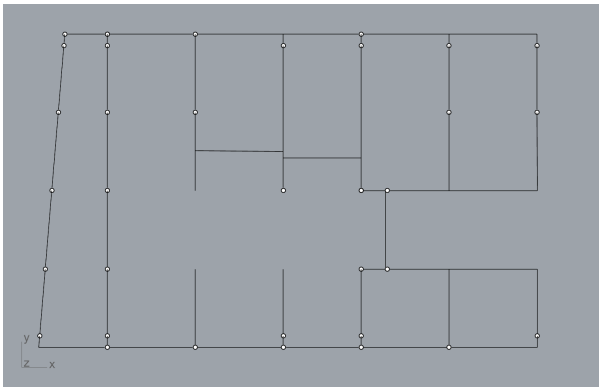

Figure F.3: Showcasing the rhino model of the beams, for the floor slab studied in this chapter

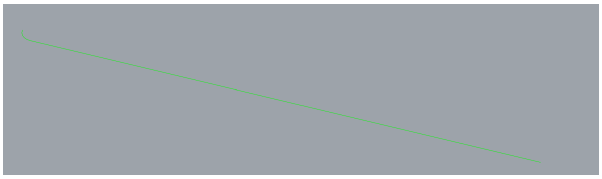

Figure F.4: Showcasing the rhino model of the edge beam under subjected to windloads, for the floor slab studied in this chapter